IFMBE Proceedings

Alicia El Haj · Dan Bader (Eds.)

Volume 30

8th International Conference on Cell & Stem Cell Engineering (ICCE)

June 11–12, 2010
Ireland

Springer

Series Editor: R. Magjarevic

The International Federation for Medical and Biological Engineering, IFMBE, is a federation of national and transnational organizations representing internationally the interests of medical and biological engineering and sciences. The IFMBE is a non-profit organization fostering the creation, dissemination and application of medical and biological engineering knowledge and the management of technology for improved health and quality of life. Its activities include participation in the formulation of public policy and the dissemination of information through publications and forums. Within the field of medical, clinical, and biological engineering, IFMBE's aims are to encourage research and the application of knowledge, and to disseminate information and promote collaboration. The objectives of the IFMBE are scientific, technological, literary, and educational.

The IFMBE is a WHO accredited NGO covering the full range of biomedical and clinical engineering, healthcare, healthcare technology and management. It is representing through its 60 member societies some 120.000 professionals involved in the various issues of improved health and health care delivery.

Previous Editions:

IFMBE Proceedings, "8th International Conference on Cell & Stem Cell Engineering",
Vol. 30, 2010, Ireland

IFMBE Proceedings BIOMAG2010, "17th International Conference on Biomagnetism Advances in Biomagnetism – Biomag2010",
Vol. 28, 2010, Dubrovnik, Croatia, CD

IFMBE Proceedings ICDBME 2010, "The Third International Conference on the Development of Biomedical Engineering in Vietnam", Vol. 27, 2010, Ho Chi Minh City, Vietnam, CD

IFMBE Proceedings MEDITECH 2009, "International Conference on Advancements of Medicine and Health Care through Technology", Vol. 26, 2009, Cluj-Napoca, Romania, CD

IFMBE Proceedings WC 2009, "World Congress on Medical Physics and Biomedical Engineering",
Vol. 25, 2009, Munich, Germany, CD

IFMBE Proceedings SBEC 2009, "25th Southern Biomedical Engineering Conference 2009",
Vol. 24, 2009, Miami, FL, USA, CD

IFMBE Proceedings ICBME 2008, "13th International Conference on Biomedical Engineering"
Vol. 23, 2008, Singapore, CD

IFMBE Proceedings ECIFMBE 2008 "4th European Conference of the International Federation for Medical and Biological Engineering", Vol. 22, 2008, Antwerp, Belgium, CD

IFMBE Proceedings BIOMED 2008 "4th Kuala Lumpur International Conference on Biomedical Engineering",
Vol. 21, 2008, Kuala Lumpur, Malaysia, CD

IFMBE Proceedings NBC 2008 "14th Nordic-Baltic Conference on Biomedical Engineering and Medical Physics",
Vol. 20, 2008, Riga, Latvia, CD

IFMBE Proceedings APCMBE 2008 "7th Asian-Pacific Conference on Medical and Biological Engineering",
Vol. 19, 2008, Beijing, China, CD

IFMBE Proceedings CLAIB 2007 "IV Latin American Congress on Biomedical Engineering 2007, Bioengineering Solution for Latin America Health", Vol. 18, 2007, Margarita Island, Venezuela, CD

IFMBE Proceedings ICEBI 2007 "13th International Conference on Electrical Bioimpedance and the 8th Conference on Electrical Impedance Tomography", Vol. 17, 2007, Graz, Austria, CD

IFMBE Proceedings MEDICON 2007 "11th Mediterranean Conference on Medical and Biological Engineering and Computing 2007", Vol. 16, 2007, Ljubljana, Slovenia, CD

IFMBE Proceedings BIOMED 2006 "Kuala Lumpur International Conference on Biomedical Engineering",
Vol. 15, 2004, Kuala Lumpur, Malaysia, CD

IFMBE Proceedings WC 2006 "World Congress on Medical Physics and Biomedical Engineering",
Vol. 14, 2006, Seoul, Korea, DVD

IFMBE Proceedings BSN 2007 "4th International Workshop on Wearable and Implantable Body Sensor Networks",
Vol. 13, 2006, Aachen, Germany

IFMBE Proceedings Vol. 30
Alicia El Haj and Dan Bader (Eds.)

8th International Conference on Cell & Stem Cell Engineering (ICCE)

June 11–12, 2010
Ireland

Springer

Editors

Alicia El Haj
Keele University
Inst. for Science & Technology in
Medicine
Thornburrow Drive
Hartshill
United Kingdom
Email: a.j.el.haj@bemp.keele.ac.uk

Dan Bader
University of London
School of Engineering and Mat.
Science
Mile End Road
E1 4NS London
United Kingdom
Email: d.l.bader@qmul.ac.uk

ISSN 1680-0737
ISBN 978-3-642-19043-8 e-ISBN 978-3-642-19044-5

DOI 10.1007/978-3-642-19044-5

Library of Congress Control Number: Applied for

The IFMBE Proceedings is an Official Publication of the International Federation for Medical and Biological Engineering (IFMBE)

Typesetting & Cover Design: Scientific Publishing Services Pvt. Ltd., Chennai, India.

Printed on acid-free paper

9 8 7 6 5 4 3 2 1

springer.com

Preface

The International Society for Cell and Stem Cell Engineering is a Working Group of the International Federation of Medical and Biological Engineering (IFMBE) currently chaired by Professor Gerhard Artmann. The Working group was formed in 1993 and has held meetings at intervals around the world. Our international meetings commenced in 1993 at Keele University, U.K. Followed by conferences in 1995 at San Diego, U.S.A., in 1997 at San Remo, Italy, in 1999 at Nara, Japan and in 2001 in Aachen, Germany. The 6th Conference took place in 2003 in Sydney, Australia and the 7th conference was held in Seoul, South Korea.

The 8th International Conference on Cell & Stem Cell Engineering was held in the Trinity College Dublin, Ireland on the 11th and 12th of June 2010. The local organizing committee, whose members were Professor Alicia El Haj from Keele University, UK; Professor Dan Bader and Professor David Lee from Queen Mary London, UK; and last but not least Dr. Danny Kelly from Trinity College Dublin, Ireland, did an excellent and professional job in organizing this meeting over the period of two days.

The meeting was the first one to include the area of stem cells as part of the overall cell engineering topic. This recognised the major expansion of the field of cell and tissue engineering as related to regenerative medicine. Theme titles for sessions included: Cell Matrix Interactions, Cell Bio-Mechanics, Cell Processing, EXPERTISSUES, Computational Modelling, Cell Network, Stem Cell Niche and Cell Regulation and Assembly.

There were 70-100 participants to the meeting with invited plenary speakers from the USA, Europe, Asia and Australia. The forum was cross disciplinary and embraced the many backgrounds of the participants from engineering, maths, physics and biology.

A subset of the abstracts presented at the meeting has been included in this volume as accepted symposium proceedings. These abstracts reflect the breadth of topics covered at the meeting. The conference was a great success with the Irish hospitality and charm contributing to the enjoyment of the participants. The next meeting is being planned as part of the 5th European Conference of IFMBE in Budapest, Hungary in September 2011.

Best regards,

Alicia El Haj
Professor of Cell Engineering
Editor of Conference Proceedings and Chair of Conference Organising Committee

Organizing Committee

Professor Alicia El Haj Professor of Cell Engineering	Keele University	Institute for Science & Technology in Medicine, Thornburrow Drive, Hartshill, Stoke-on-Trent, UK
Professor Dan Bader Professor of Medical Engineering	Queen Mary London	Mile End, Eng, 214, UK
Professor David Lee Professor of Cell and Tissue Engineering	Queen Mary London	Mile End, Eng, 338, UK
Dr. Danny Kelly Lecturer in Mechanical Engineering (Bioengineering)	Trinity College Dublin	Trinity Centre for Bioengineering, Parsons Building, Dublin 2, Ireland

Table of Contents

Online Monitoring the Mechanical Remodeling of Hydrogels by Corneal Fibroblasts

M. Ahearne[1], Alicia J. El Haj[1], S. Rauz[2], and Ying Yang[1]

[1] Institute of Science and Technology in Medicine, Keele University, Stoke-on-Trent, United Kingdom
[2] Academic Unit of Ophthalmology, School of Immunity and Infection, University of Birmingham, Birmingham, United Kingdom

Abstract— **Cell seeded hydrogels provide a useful model for examining cell behavior and matrix remodeling in-vitro. Fibroblasts are capable of manipulating the mechanical behavior of tissues by attaching to their surroundings matrix and applying strain. Any resulting change in the mechanical properties of the matrix can in turn affect the cells behavior. In this study, a non-destructive spherical indentation technique was used to examine the change in mechanical properties of collagen hydrogels seeded with either human corneal fibroblasts or human keratocytes over prolonged culture periods. Cell seeded hydrogels were clamped between two transparent circular rings and a sphere was placed on top of them, causing them to deform. The deformation displacement was measured using a CCD camera system and applied to a theoretical model to calculate the mechanical properties of each hydrogel. The non-destructive on-line nature of this technique enables repeated measurements the same hydrogels at several different time-points thus enabling the change in mechanical behavior of the hydrogels resulting from corneal fibroblasts remodeling to be examined. In this particular study, the effect of different culture medium on the cell behavior was investigated. The spherical indentation technique has also been used to examine the effect that different drugs and chemicals have on the cells ability to remodel of the hydrogels including MMP and actin inhibitors.**

Keywords— **Collagen, Tissue engineering, Cornea, Modulus, Fibroblast.**

I. Introduction

Cell seeded collagen hydrogels have become popular for in vitro modeling of three-dimensional tissues. One of the most interesting applications for these hydrogels is to model wound healing behavior. In the cornea, keratocytes are known undergo phenotypic changes in response to injury. Keratocytes become fibroblastic leading to an increase in extracellular matrix production and matrix contraction. Identifying and understanding these changes has many applications including in examining the corneas response to surgical procedures, injury and disease. It is also important in development treatments to reduce scar formation which can impede vision.

We have developed a spherical indentation system for examining the mechanical characteristics of cell seeded hydrogels over prolonged culture periods [1]. This system allows non-destructive online measurement of the mechanical properties of hydrogels without risk of contamination to the sample or damage to the instrument. To date this system has been used to monitor the change in mechanical properties of collagen hydrogels seeded with human corneal fibroblasts which have undergone UVA-riboflavin treatment [2], been subjected to MMP inhibitors [3] and been manufactured using different collagen and cell concentrations [4]. Here the effect of different culture condition will be investigated to try and determine role cell phenotype plays in matrix remodeling and to investigate if there is a difference in the mechanical characteristics of collagen hydrogels seeded with corneal fibroblasts and those seeded with corneal keratocytes.

II. Materials and methods

A. Materials Preparation

All chemicals used were from Sigma-Aldrich unless otherwise stated. Human corneal tissue was obtained and used to extract corneal fibroblasts. The epithelial and endothelial layers of the cornea were physically removed using tweezers. The remaining corneal stromal tissue was placed into culture flasks from which cells were allowed to migrate onto the flask. Once a confluent layer of the cells was formed, these cells could be used. Collagen hydrogels were produced from rat-tail collagen type-1 (BD Bioscience, Erembodegem, Belgium) using as previously described [2, 3]. Human corneal fibroblasts were suspended inside the collagen hydrogel solution prior to gelation at a concentration of $5x10^5$ cells per hydrogel. Hydrogels without cells were used as a control. The hydrogels were cultured in six-well plates in one of two types of culture media. The first type of culture media promoted a fibroblastic phenotype and consisted of low glucose Dulbecco's Modified Eagles Medium (DMEM) supplemented by 10% fetal calf serum, 1% L-glutamine and 1% antibiotic-antimycotic solution. Alternatively culture media which promoted a keratocyte phenotype [5] which consisted of DMEM/Ham F-12 supplemented with 1mM ascorbic acid, 0.1% insulin and 1% antibiotic-antimycotic solution was also used. The media was changed every 3 to 4 days. This research has received approval from Black Country Research Ethics Committee (06/Q2702/44).

A. El Haj and D. Bader (Eds.): 8th International Conference on Cell & Stem Cell Engineering, IFMBE Proceedings 30, pp. 1–4, 2011.
www.springerlink.com

B. Instrumentation

A sample holder was constructed to suspend the hydrogels during measurement (Fig. 1A). Each hydrogels were clamped between two transparent plastic circular rings of inner diameter 20 mm. The rings were held in place using the stainless steel samples holder shown. Three hydrogels could be held in each sample holder at any one time. Each sample holders was assembled in phosphate buffered saline (PBS) within a large rectangular Petri dish in a Class II laminar flow hood. A PTFE sphere (Insley, Berks, UK) of diameter 4 mm was placed onto the centre of each hydrogel. The weight of the sphere caused the hydrogel to deform. The Petri dish was then placed into an incubator at 37ºC. A multi-LED lamp was placed in the incubator to illuminate the sample.

The resulting deformation on the hydrogel was captured using a home built image acquisition system which consisted of a long-working-distance objective microscope (Edmund Industrial Optics, York, UK) connected to a computer-linked CCD camera (XC-ST50CE, Sony, Japan) which we have previously described in more details [1]. The camera was linked to an image acquisition card (National Instruments, USA) which was used to acquire and process the images. LABView (National Instruments, USA) was used to write a program to acquire images from the camera. An example of a hydrogel deformation image acquired by this system is shown (Fig. 1B). This system allowed images to be recorded of the deformation profile of the hydrogel from outside the incubator through a glass window. The magnification of the system was calibrated with the computer-acquired images of a stage micrometer. Images of the spherically deformed hydrogels were recorded 10 minutes after the sphere was initially placed onto the hydrogel. This was to allow time-dependent deformation to reach equilibrium. The elastic modulus was measured one day after hydrogel formation and every 3 to 4 days subsequently for up to 24 days.

A home-built optical coherence tomography (OCT) system was used to examine the cross-sectional thickness of each specimen at the same examining frequency as the modulus measurement. OCT is a low coherence interferometric technique which measures backscattered light after the light source has passed through a material [6]. This technique allowed non-destructive imaging of the hydrogels cross-sectional thickness to be measured under sterile conditions [7]. A superluminescent diode with a central wavelength of 1310 nm and bandwidth of 52 nm was used as the source of the OCT. The system has an axial resolution of 14 μm in free space and penetration depth up to 2 mm.

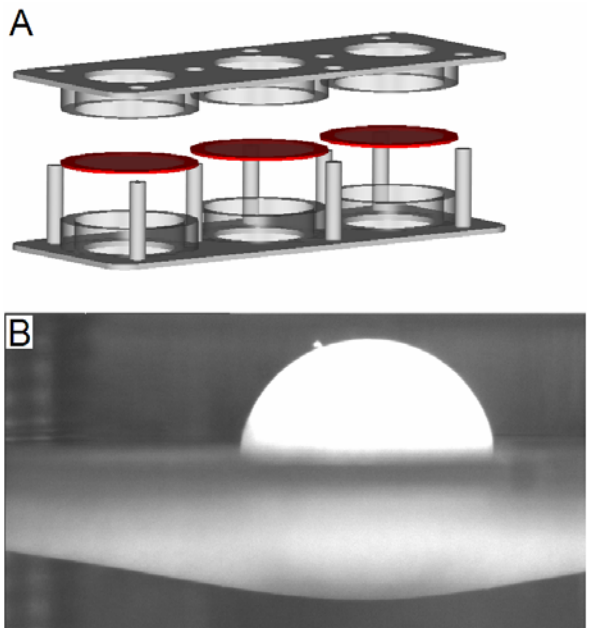

Fig. 1 (A) sample holder and hydrogels; (B) hydrogel deformed by PTFE sphere

C. Theoretical Modeling

The elastic modulus of the hydrogels was calculated from the images using a large deformation model [8]. From the acquired images, the central deformation (δ) of the hydrogel was calculated and substituted into equation 1 to find the elastic modulus (E);

$$6wr = Eh\,(0.075\delta^2 + 0.78r\delta) \quad (1)$$

where h is the hydrogel thickness, r is the radius of the sphere and w is the weight of the sphere. This equation is applicable when the ratio of $a/r = 5$ and $\delta/r \leq 1.7$, where a is the radius of the clamped portion of the hydrogel. This model also assumes that the ratio of thickness to the radius is low and the deformation is large, hence stretching of the membrane dominates over bending.

D. Immunofluorescent Staining

Cell viability was assessed using a live-dead cell double staining kit. The kit contained Calcein-AM and Propidium Iodide which fluorescently stain live cells green and dead cells red respectively. The presence of alpha smooth muscle actin in the cells was assessed using αSMA antibodies conjugated to FITC. The cells were examined using a FV300 confocal microscope (Olympus, Japan)

III. Results

The elastic modulus was measured over a 24 day culture period (Fig. 2). Hydrogels seeded with cells cultured in fibroblast media increased in modulus over the culture period. We have previously found this phenomena which is the result of contraction, remodeling and intrinsic strain applied by cells. Hydrogels seeded with cells cultured in keratocyte media showed little change in modulus over the culture period. Keratocytes have a quiescent phenotype in vivo which our results appear to mimic.

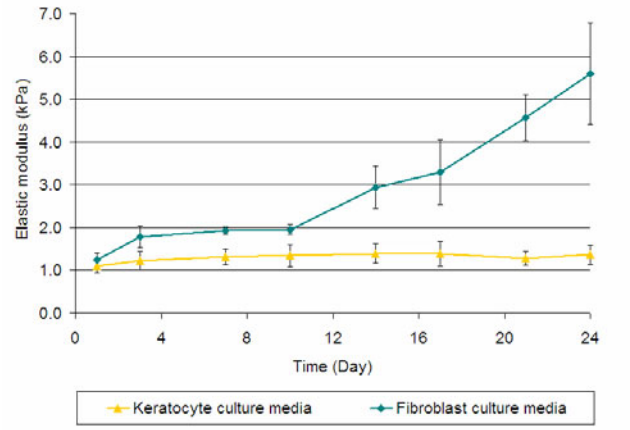

Fig. 2 Change in elastic modulus of cell seeded collagen hydrogels over a 24 day culture period

The change in thickness of the hydrogels was recorded using optical coherence tomography (Fig. 3). Cells in fibroblast media contracted the hydrogel making it thinner while those in the keratocyte media showed little or no change in thickness.

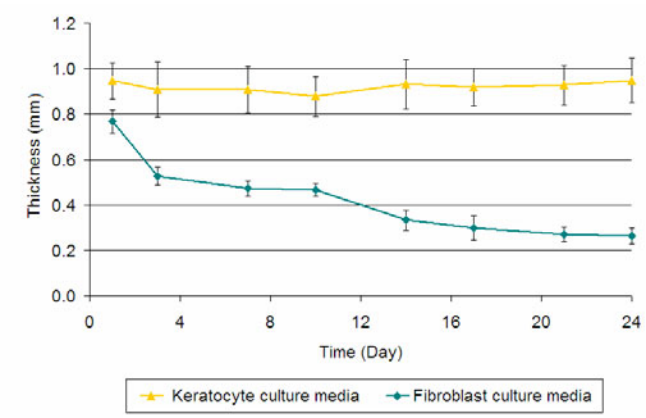

Fig. 3 Change in thickness of cell seeded collagen hydrogels over a 24 day culture period

To test the phenotype of the cells, they were stained for the presence of αSMA which has previously been shown to appear in corneal fibroblasts but not in keratocytes [9]. It can be seen that there was substantially more cells staining positive for αSMA in the hydrogels with fibroblast media compared to those with keratocyte (Fig. 4). This would appear to suggest that the culture media was able to dictate the cell phenotype.

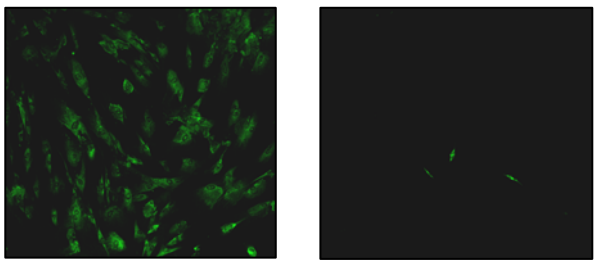

Fig. 4 Images of cells hydrogels cultured in fibroblast (left) and keratocyte (right) media and fluorescently stained for the presence of αSMA

IV. Discussion

It has been shown that altering the culture media in which corneal fibroblasts grow can affect the cell behavior. Cells in the fibroblast media displayed characteristics normally found in the cornea during wound healing such as matrix contraction and remodeling. These characteristics were removed when the cells were grown in keratocyte media. These cells are normally quiescent, which appears to correspond with our findings. The reduction in smooth muscle actin also appears to verify the phenotype change back into a keratocyte phenotype. However keratocytes in-vivo have a dendritic morphology which was not present in our cells. This might suggest that the cells do not fully return to a keratocyte phenotype but maintain some keratocyte and fibroblast characteristics. The matrix environment could also play a role in determining the cell morphology.

Previous studies have shown that altering the media conditions for corneal fibroblasts can results in different cell behaviors. Beales et al., (1999) showed that corneal cells retain their keratocyte characteristics in serum free media [10]. Berryhill et al., (2002) found that bovine corneal cells could partially return to a keratocyte phenotype after being transformed in fibroblasts in vitro [11]. Lakshman et al., 2010 found that by using different culture media, they could induce keratocyte or fibroblast phenotypes from rabbit corneal cells which resulted in different morphologies and contractile behaviors [12]. These results show that cell phenotype can be dictated by culture media conditions.

V. Conclusions

We have demonstrated that corneal phenotype can dictate the mechanical remodeling behavior of corneal stromal cells in three-dimensional matrices. This in-vitro approach to examining cell activity could be useful in determining new methods of reducing or preventing the induction of keratocytes into fibroblast.

Acknowledgment

This research was funded by BBSRC (BB/F002866/1). Sample holders were manufactured by KMF Precision Sheet Metal Ltd (UK).

References

1. Ahearne M, Yang Y, El Haj AJ et al. (2005) Characterizing the viscoelastic properties of thin hydrogel-based constructs for tissue engineering applications. J R Soc Interface 2:455–463
2. Ahearne M, Yang Y, Then KY et al. (2008) Non-destructive mechanical characterization of UVA/riboflavin crosslinked collagen hydrogels. Br J Ophthalmol 92:268–271
3. Ahearne M, Liu KK, El Haj AJ et al. (2010) Online monitoring of the mechanical behaviour of collagen hydrogels: Influence of corneal fibroblasts on elastic modulus. Tissue Eng C 16:319-327
4. Ahearne M, Wilson S, Liu KK et al. (2009) Influence of cell number and collagen concentration on the mechanical behaviour of collagen hydrogel constructs. Euro Cells Mater J 18:21
5. Musselmann K (2006) Developing culture conditions to study keratocyte phenotypes in vitro. PhD Thesis.
6. Bagnaninchi PO, Yang Y, Zghoul N, et al. (2007) Chitosan microchannel scaffolds for tendon tissue engineering characterized using optical coherence tomography. Tissue Eng 13:323-331
7. Ahearne M, Bagnaninchi PO, Yang Y et al. (2008) Online monitoring of collagen fibre alignment in tissue-engineered tendon by PSOCT. J Tissue Eng Regen Med 2:521-524
8. Ju BF, Liu KK, (20020 Characterizing viscoelastic properties of thin elastomeric membrane. Mech Mater 34:485-491
9. Jester JV, Petroll WM, Barry PA, et al. (1995) Expression of α-smooth muscle (α-SM) actin during corneal stromal wound healing. Invest Ophthalmol Vis Sci 36:809-819
10. Beales MP, Funderburgh JL, Jester JV et al. (1999) Proteoglycan synthesis by bovine keratocytes and corneal fibroblasts: Maintenance of the keratocyte phenotype in culture. Invest Ophthalmol Vis Sci 40: 1658-1663
11. Berryhill BL, Kader R, Kane B et al. (2002) Partial restoration of the keratocyte phenotype to bovine keratocytes meda fibroblastic by serum. Invest Ophthalmol Vis Sci 43:3416-3421
12. Lakshman N, Kim A, Petroll MW (2010) Characterization of corneal keratocyte morphology and mechanical activity within 3-D collagen matrices. Exp Eye Res 90:350-359

Mark Ahearne
Keele University
Thornburrow Drive
Stoke-on-Trent
United Kingdom
m.j.ahearne@istm.keele.ac.uk

New Improved Technique of Plastic Compression of Collagen Using Upward Fluid Flow

T. Alekseeva[1], H. Jawad[1], M. Purser[2], and R.A. Brown[1]

[1] UCL, Institute of Orthopaedics-TREC, Stanmore Campus, London UK
[2] The Automation Partnership (Cambridge) Ltd, Royston, Hertfordshire, UK

Abstract— **Plastic compression (PC) of collagen facilitates the fabrication of dense, tissue-like constructs without the need for cell activity. The process involves rapid expulsion of water from cell-seeded collagen gels, normally in a single axis of flow and takes minutes to perform. However, there has been a need for an improvement in terms of scaling up and reproducibility. We have designed a modified technique to fabricate tissue constructs in a multi well format (currently 12 wells) in less than one hour with good reproducibility using upward fluid flow. It has been shown in our group that compression time directly correlates with the height of the initial gel, for a constant fluid leaving area (in our case 22 mm diameter), so in order to determine a range of PC times we have examined the dynamic of liquid loss for a range of gel heights. This included 5.3 mm (2 ml), 7.9 mm (3 ml), 9.2 mm (3.5 ml), 10.5 mm (4 ml) and 13 mm (5 ml). Liquid loss was calculated as percentage increase in paper roll weight relative to the initial weight of paper and was taken every 5 min until plateau. Based on our results we have determined times of compression as 5 min, 10 min, 15 min, 20 min and 35 min for gels in ascending order. Measurements of wet weight and thickness of constructs showed good reproducibility (SD: ±0.005g and ±1.2 μm respectively). Modification of the method has no effect on cell activity and gives opportunity to fabricate constructs with increased complexity through multilayering. We can conclude that the new modified method of plastic compression allows scaling up of the process, with dramatic savings on time and results in reproducible constructs that allow cell culture. Method also opens new research directions using multilayered constructs.**

Keywords— **collagen I, plastic compression, fluid-flow, multi-well compression.**

I. Introduction

Plastic compression is a new method of cell-free fabrication of dense collagen constructs. Fast and reliable, this method has been used for multiple research projects either *in vivo* or *in vitro* [2-7]. Process of PC involves uniaxial removal of liquid from hyper-hydrated collagen gels with or without resident cells. Standard procedure consists of following steps: neutralizing of collagen solution, mixing with cells, setting in a mould, transfer on to the blotting elements and compression under a uniform load [1]. Preparation of one construct will thus take less than an hour (approx. 45 min), which is much faster than compaction of matrix by cell-remodeling that can take days with severe limits on final density. However, we found that there is a need for scaling up of the process without compromising reproducibility or cell viability. The aim of this study was to develop a method that will use the same principles but allow for simultaneous production of large number of uniform constructs, ideally using standard laboratory equipment, for example multi-well culture plates. We have shown that compression time depends on the correlation between the height of original gel and the fluid leaving area. Here, we kept the latter constant, changing the height (volume) of the gel to determine range of compression times for future applications. Cell behavior in the collagen was assessed using human corneal fibroblasts. Also, the possibility of multilayering was investigated.

II. Materials and Methods

A. Collagen Gels

Acid-soluble rat-tail collagen type I (FirstLink, UK) was diluted with equal volumes of 10XMEM (Gibco) and DMEM (Sigma) and neutralized using 5M NaOH until change of colour. Neutralised solution was then left on ice to degas. Collagen mixture was poured in the wells of 12 well plates (Orange Scientific, well diam. 22 mm) and allowed to set at 37 °C for 30 min. Volume (height) range included 2ml (5.3 mm), 3ml (7.9 mm), 3.5ml (9.2 mm), 4 ml (10.5mm) and 5ml (13 mm). In this paper we will refer to volumetric description of the gels, bearing in mind constant fluid leaving area and different heights.

B. Multiple Plastic Compressions

Watman paper No1 was used as blotting component. Each gel in the multi-well plate was covered with disc of nylon mesh and two discs of blotting paper. Watman paper roll (4.0 cm x 100 m, Whatman, UK) was spiral wound

A. El Haj and D. Bader (Eds.): 8th International Conference on Cell & Stem Cell Engineering, IFMBE Proceedings 30, pp. 5–8, 2011.
www.springerlink.com

using custom made rolling machine (TAP) into a cylindrical paper plunger (4cmx125cmx21cm, average weight 4.2 g) so that it can fit into the well of the plate. Using guiding plate (custom made, TAP) 12 paper cylinders were inserted into the wells and weight deposited on top. The weight change of the paper roll was taken as indicator of fluid leaving from the collagen gel and was used for further analysis as percentage change relative to the initial weight of paper roll. Weight increase of paper roll was monitored every 5 minutes for all volumes and constructs were deemed compressed when weight reached plateau. Resulting constructs were fixed in 10% neutral buffered formaldehyde and weighted before wax embedding. Samples were then sectioned in transverse plane and stained using routine hematoxiline and eosin method to determine thickness.

C. Cellular Collagen Constructs

Human corneal fibroblasts (gift from Dr. Hanna Lewis, UCL, Institute of Ophthalmology, UK) were used to determine cell behavior. Cells suspension in DMEM (500.000 cells per constructs) was mixed with neutralized collagen solution and 4 ml collagen gels were set in the 12 well-plate, compressed as described above and cultured for 2 weeks. Constructs were fixed and processed for routine histology.

D. Multilayering of PC Collagen

Neutralized collagen solution (2 ml) was allowed to set and compressed as described above. Fresh layer of neutralized collagen was poured on top of compressed layer and procedure repeated. Same volume of collagen solution was used for each layer. For the purpose of this study three and 6 layered constructs were fixed and processed as before for histology.

E. Histological Analysis

All constructs were treated in the same manner. Following fixation in 10% neutral buffered formaldehyde, samples were embedded in paraffin, blocked to give sections in transverse plane and sectioned using Leitz microtome (sections 7 μm thick). Sections were them mounted on glass slides and allowed to dry before rehydration and staining using standard H&E protocol. Sections were then viewed under light microscope (Olympus BH-2) and microphotographs taken with digital camera (Olympus).

F. Data Analysis

Data are presented as mean ± SD. For thickness and weight measurements we looked at group measurements as well as general SD to give indication of method reproducibility. For each group at least three separate experiments were carried out with n=6 for each group, multilayered constructs – n=2.

III. Results

A. Compression Times and Reproducibility

Based on the data of percentage fluid loss during compression of a range of collagen gel volumes (heights) we were able to determine necessary compression times as 5 min for 2ml, 10 min for 3ml, 15 min for 3.5ml, 20 min for 4 ml and 35 min for 5ml (Fig.1)

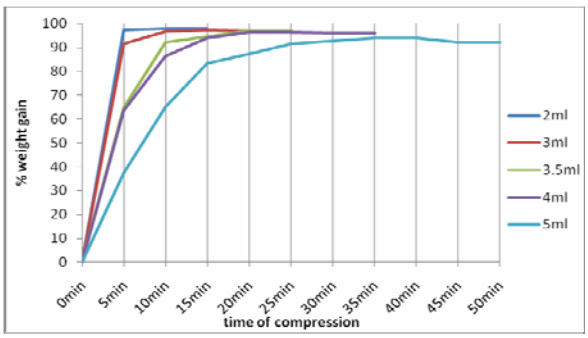

Fig. 1 Dynamic of weight change due to liquid absorbed in the paper roll for a range of collagen gel volumes in percent. Initial weight of the paper roll was set as 0% and collagen gel as a 100%. During compression liquid from the gel was transferred into the paper thus increasing its weight. Paper rolls were weighted every 5 min and compression was complete when no change in weight was observed

This data confirms our previous observation that given set fluid leaving surface area time of compression depends on the height of the gel.

Measurements of the weight of fixed compressed constructs gave as good reproducible results with the SDs in the range of ±0.005g. Thickness of the constructs ranged from 61.5 ± 1.3 μm for 2 ml gels to 151.75 ± 1.5 for 5 ml gels wit.

B. Cellular Constructs

Constructs seeded with human corneal fibroblasts were cultured for two weeks prior to fixation and processing for routine histology h average SDs±1.2 μm.

Histological sections showed signs of cellular activity and matrix remodeling that corresponds with the standard PC process (Fig.2).

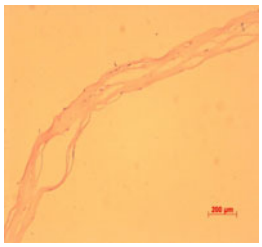

Fig. 2 Section of the PC construct seeded with HCF and compressed using modified method after two weeks in culture. Cells had remodeled the matrix, giving it characteristic 'lacy' appearance

C. Multilayering of PC Collagen

Modified method of plastic compression allows fabrication of complex, multilayered constructs. For this study we prepared three (Fig. 3a) and 6 (Fig. 3b) layered constructs that were fixed immediately after assembly and used for histological examination.

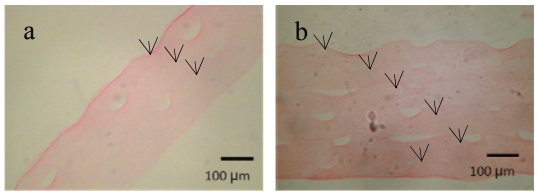

Fig. 3 Micrographs of multilayered PC constructs consisting of 3 (a) and 6 (b) layers with initial gel volume of 2 ml for each layer. Constructs were prepared by consecutive compression of collagen gels. Arrows indicate individual layers

Constructs were easy to handle and confirm the possibility of introducing cells between layers in as well as the collagen matrix.

IV. Conclusions

Method of plastic compression of collagen type I was introduced by Brown et al in 2005 [1] and had been used for various tissue engineering purposes. It has been proposed for engineering of bone [2], skin [3], bladder [4] and a model for monitoring oxygen perfusion [5]. Dense, tissue-like constructs are fabricated cell-independently by expulsion of liquid from hyper-hydrated collagen gels and does not significantly reduce cell viability. This study was aimed at scaling-up of the process using standard laboratory multi-well plates without losing the advantages of the original method. Using 12 well plate as a mould we modified the technique so that up to 12 constructs can be made simultaneously in semi-automated fashion using upward fluid absorption. It has been shown in our group that compression of collagen depends on the height of the gel and fluid leaving area. Having constant surface area (diameter of the well) we determined time, required for compression of a range of gel heights. Predictably, compression time was in direct correlation with gel height. Analysis of the resulting constructs (weight and thickness) showed good reproducibility.

Cell-seed constructs, cultured for 2 weeks exhibited the same morphological appearance as made by the conventional method. This method also minimizes handling of the constructs and hence risk of infection since constructs are made and cultured in the same plate. The latter is also beneficial for multi-layering. We have previously reported fabrication of double-layered hybrid collagen-Poly (lactic acid Co-caprolactone) construct using standard PC. Both gels were cast in to a mould with PLACL mesh sandwiched in between prior to compression [6]. Modified method uses consecutive compressions, where new layers of collagen are cast, set and compressed on top of the previous in a multi-well format, so far producing up to 6 layers and having no obvious limit.

New upward-flow method of plastic compression allows simultaneous fabrication of acellular or cellular ready-to-use collagen constructs in conventional tissue culture plastic ware with good reproducibility, opening possibility of rapid fabrication of complex, multi-layered constructs.

Acknowledgment

TSB-EPSRC for funding.

References

1. Brown, RA; Wiseman, M; Chuo, CB, et al. (2005) Ultrarapid engineering of biomimetic materials and tissues: Fabrication of nano- and microstructures by plastic compression. Advanced Functional Materials 15 (11): 1762-1770
2. Buxton PG, Bitar M, Gellynck K et al. (2008) Dense collagen matrix accelerates osteogenic differentiation and rescues the apoptotic response to MMP inhibition. Bone 43(2):377-85.
3. Hu K., Shi H., Zhu J. et al (2010) Compressed collagen gel as the scaffold for skin engineering. Biomed Microdevices DOI 10.1007/s10544-010-9415-4 2010
4. Engelhardt EM, Stegberg E, Brown RA et al. (2010) Compressed collagen gel: a novel scaffold for human bladder cells. J Tissue Eng Regen Med 4(2):123-30.
5. Cheema U, Brown RA, Alp B, MacRobert AJ. (2008) Spatially defined oxygen gradients and vascular endothelial growth factor expression in an engineered 3D cell model. Cell Mol Life Sci 65(1):177-86.
6. Ananta M, Aulin CE, Hilborn J et al. (2009) A poly(lactic acid-co-caprolactone)-collagen hybrid for tissue engineering applications. Tissue Eng Part A. Jul 15(7):1667-75.
7. Mudera V, Morgan M, Cheema U et al. (2007) Ultra-rapid engineered collagen constructs tested in an in vivo nursery site. J Tissue Eng Regen Med 1(3):192-8.

Author:
Institute: UCL, Institute of Orthopaedics
Street: Brockley Hill
City: Stanmore
Country: UK
Email: t.alekseeva@ucl.ac.uk

A Morphological Study of Cell Aggregations on Mineralization

Halil M. Aydin, Bin Hu, Swati Kesri, Alicia J. El Haj, and Ying Yang

Institute of Science and Technology in Medicine, School of Medicine, Keele University,
Stoke-on-Trent, ST4 7QB, UK

Abstract— **The key criteria for assessing the success of bone tissue engineering is the quality and quantity of the mineralization within scaffolds. It has been demonstrated that stem cells and isolated primary bone cells can be induced to generate minerals in in vitro culture when using osteogenesis medium. The accumulation of calcium ion and inorganic phosphate from culture medium serves as nucleating agents for the formation of hydroxyapatite, which is the main inorganic component of bone. Bone nodule formation is one of the hallmarks of mineralization in such culture. In this project, we understook a morphological study in which human bone marrow –derived mesenchymal stem cells (hMSCs) and osteoblast cell line have been cultured into cell aggregates under various culture conditions. We investigated the effect of the culture substrates on the capability of the formation of cell aggregates in terms of size and numbers, and the capability of the aggregates expansion and mineralization. It has been revealed that the nature of substrate affected the size and numbers of the cell aggregates. The number of bone nodules and the minerals generated from cell aggregates were higher than in monolayer cell culture.**

I. Introduction

In the past decades, tissue engineering of bone is an intensive studying area. It has prospected that tissue engineering bone can become a highly potential therapy for bone diseases caused by trauma or aging-related degeneration, such as osteoporosis. Many researchers including us have reported that primary osteoblastic cells and stem cells are capable of mineralization up to certain levels in vitro [1-2]. Bone nodule formation is one of the hallmarks of mineralization in such culture. Interestingly, it has been reported that embryoid body aggregates can generate higher minerals quantity in comparison to embryonic stem cells [3]. In this project, we undertook a morphological study in which human bone marrow–derived mesenchymal stem cells (hMSCs) and osteoblast cell line have been cultured into cell aggregates under various culture conditions. We investigated the effect of the culture substrates on the capability of the formation of cell aggregates in terms of size and numbers, and the capability of the aggregates expansion and mineralization. The aim of this study is to demonstrate whether culturing osteoblast aggregates will enhance mineralization and nodule formation.

II. Materials And Methods

A. Cells Sources

Two representative cell groups, human bone marrow-derived mesenchymal stem cells (hMSCs) and mouse osteoblastic cell line MLO-A5 were used to generate cell aggregates. hMSCs were purchased from Lonza (Passage 2) and expanded in DMEM with 10% FCS, 1% Antibiotic-Antimycotic, 1% L-glutamine. MLO-A5 is kindly donated by Professor Lynda Bonewald, USA.

B. Treatment of Substrates Surface

Three types of substrates were used to generate cell aggregates. The first type of substrate was commercial suspension culture flask (Sarstedt). The type two and third substrates were PEO (F127 F127 Pluronic, BASF) coated Sarstedt 24-well suspension cell culture plate with different coating concentration. Two types of culture medium were used in the aggregate formation period. They were undifferentiated media, α-MEM supplemented with 5% SFBS + 5% BCS, and 1% antibiotic-antimycotic solution, and osteogenesis media in which α-MEM was supplemented with 10% FCS, 1% L-glutamine, 1% ascorbic acid, 1% dexamethasone, 1% glycerophosphate and 1% antibiotic-antimycotic solution for mouse cell culture.

C. Aggregate Formation

In the 24 well plates, 100,000 cells, either hMSC or MLA-O5 were seeded and cultured for 40 hours under 37°C and 5% CO_2. The variation of culture conditions and substrates are summarized in Table 1.

D. Bone Nodules Formation

After 40 hour growth in the suspension culture plates, the cell aggregates were transferred to normal 6-well cell culture plates (cell adhesive) for further cell proliferation and mineralization. The osteogenesis medium was used for the further culture.

A. El Haj and D. Bader (Eds.): 8th International Conference on Cell & Stem Cell Engineering, IFMBE Proceedings 30, pp. 9–12, 2011.
www.springerlink.com

Table 1 The culture conditions of nodule formation

Group	Media	Sources of cell aggregates
1A	Normal	Non-adhesive suspension cell culture flask
1B	Osteogenic	Non-adhesive suspension cell culture flask
2A	Normal	PEO (Pluronic F 127) coating substrate 10 mg/ml
2B	Osteogenic	PEO (Pluronic F 127) coating substrate 10 mg/ml
3A	Normal	PEO (Pluronic F 127) coating substrate 20 mg/ml
3B	Osteogenic	PEO (Pluronic F 127) coating substrate 20 mg/ml

E. Characterisation of Aggregates and Minerals

The formation and outgrowth of aggregates were examined at given culture interval under a light microscope. After 10 days further culture, some cell wells were fixed with 10% formalin for Alizarin red staining and other quantitative and qualitative analysis for minerals including XRD and spectroscopy following Gregory method [4]. Some wells were trypinsed for cell counting.

III. Results

Both hMSC and osteoblasts cells have formed cell aggregates on both suspension and PEO coated culture plates. However, the numbers and size of the cell aggregates varied. Within 40 hour culture, hMSCs and osteoblasts generated high and homogeneous cell aggregates on commercial suspension plates with average aggregate size of 100 μm; whilst osteoblasts generated few but much bigger cell aggregates in PEO coated culture flasks regardless of original type of flask used for the coating. The average size of the big aggregates was 200-300 μm. With the same seeding density, the aggregates number generated in commercial suspension plate was about 50 to 100; whilst only average 5 big aggregates plus small number of aggregates found in PEO coated plates. The aggregates size increased with culture time (Figure 1). However, up to 60 hour or longer, the aggregates became unhealthy and dying at 100 hour (data not shown).

After transferring the cell aggregates into cell adhesive culture plate, all cell aggregates showed high rate of cell outgrowth. The cell outgrowth initiated from the aggregates' centre and displays a radial and symmetric cell population pattern (sun flower pattern). The proliferation of cells from aggregates continued along culture time, as demonstrated in Figure 2. Interestingly, after cell outgrowth, the aggregates remained thick and lump in the centre, which formed macroscopic visuable nodules.

The control specimens in which cells were seeded in cell adhesive plate (both hMSC and osteoblasts) straightly produced a homogenous cell growth with less visible nodule formation when the cells became confluent within the plates (Figure 3).

Alizarin red staining of both monolayer cell population and the cell population from aggregates demonstrated that the cell population from aggregates showed stronger red color than monolayer culture (Figure 4), indicating the higher mineral production. The preliminary XRD analysis of mouse cells after aggregates outgrowth confirms the presence of hydroxyapatite crystal and the minerals quantity was much higher in the specimens in which aggregates grew from PEO coated substrate in comparison to monolayer culture. A qualification analysis of minerals formation from hMSC cells from XRD is summarized in Table 2. The more quantitative analysis is being undertaken.

IV. Discussion And Conclusion

As far as we are aware that this is the first report on how hMSCs and osteoblasts can form cell aggregates and induce enhanced mineral formation. Our studies reveal that hMSCs and osteoblasts can form cell aggregates. These cell aggregates acted as embroyic body from embroyic stem cells and displayed higher potential for mineral formation. It is hypothesesed that the aggregates provide a more similar growth microenvironment as found in body, perhaps the aggregates contain high extrcellular matrix and can syntheses more organic matrix required for osteoid generation.

In conclusion, the two step cell culture process, i.e. formation of cell aggregates first and then mineralization through cell aggregates has a potential to enhance mineralization in the quantity and quality of minerals. Both hMSC and osteoblast cell line can generate high yield cell aggregates under appropriated substrate conditions.

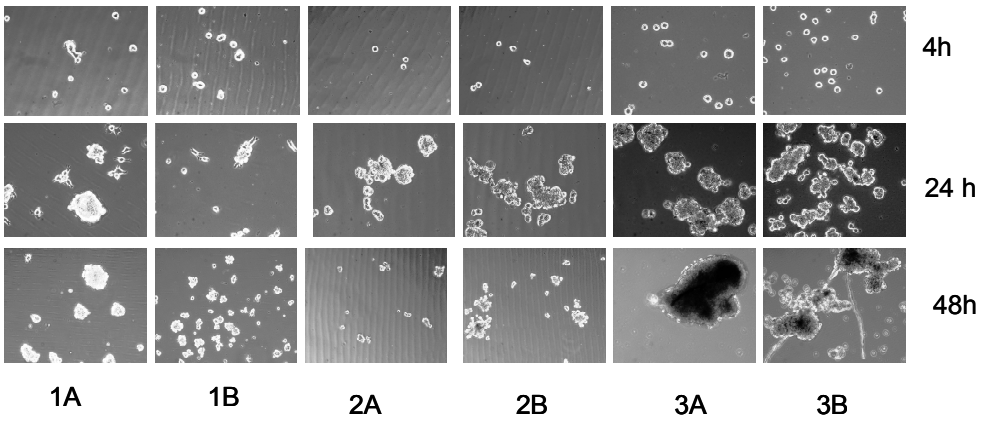

Fig. 1 The cell aggregates grew in different substrates and in different culture period. The original magnification is 100X

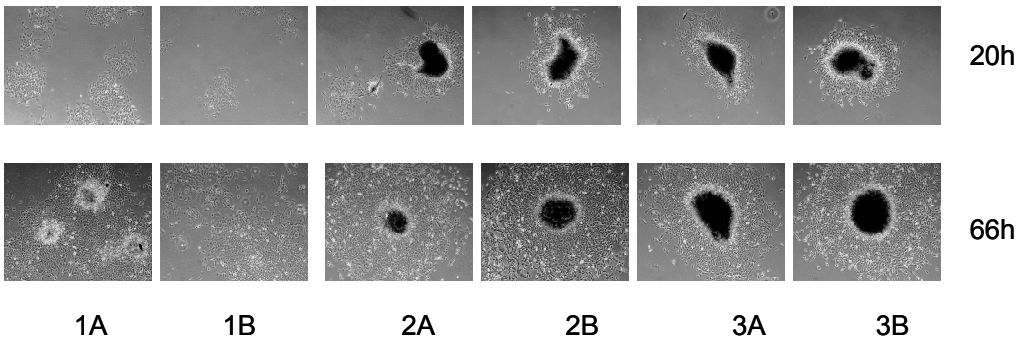

Fig. 2 The cell aggregates outgrew in cell adhesive culture plates under different culture period. The original magnification is 40X.

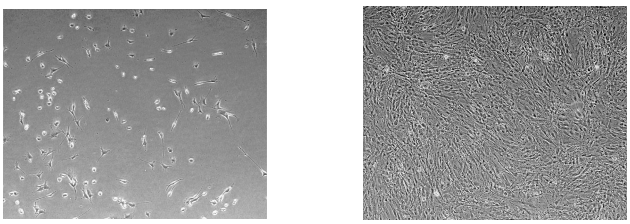

Fig. 3 The cells grew in adhesive culture plates: left: mouse cells; right: hMSCs

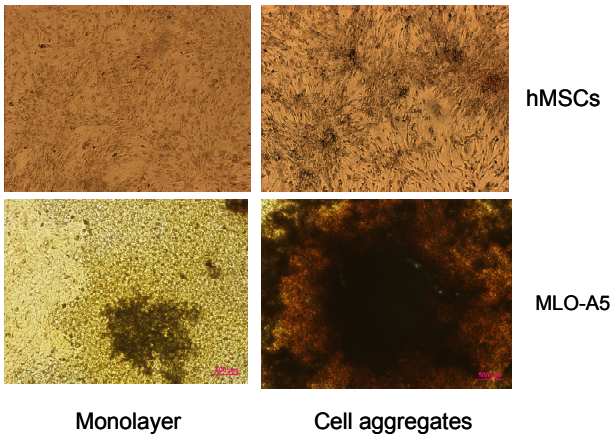

Fig. 4 Typical alizarin red staining after 10 days culture in hMSC and mouse cells

Table 2 The qualitative results from XRD analysis for the nodules

Group	XRD Evaluation
Control	No proper measurement due to insufficient specimen
1A	Amorphous phase is dominant. Crystallinity is better than 1B.
1B	Amorphous phase is dominant. Crystallinity is minimal.
2A	The best/highest crystalline phase Minimum amorphous structure
2B	Little amorphous structure Very high crystallinity ratio
3A	Crystallinity ratio high Less amorphous structure
3B	Crystallinity ratio high; less amorphous structure. Amorphous phase is less than 3A.

Acknowledgments

FP7 IEF Marie Curie action (PIEF-GA-2009-237762).

References

1. Shin M, Yoshimoto H, Vacanti JP. In vivo bone tissue engineering using mesenchymal stem cells on a novel electrospun nanofibrous scaffold. Tissue Eng. 2004;10(1-2):33-41.
2. Yang Y, Magnay J, Cooling L, Cooper JJ, El Haj AJ. Effects of substrate characteristics on bone cell response to the mechanical environment. Medical and Biological Engineering and Computing, 2004, 42(1), 22-29.
3. Kärner E, Bäckesjö CM, Cedervall J, Sugars RV, Ahrlund-Richter L, Wendel M. Dynamics of gene expression during bone matrix formation in osteogenic cultures derived from human embryonic stem cells in vitro. Biochim Biophys Acta. 2009;1790(2):110-8.
4. Gregory CA, Gunn WG, Peister A, Prockop DJ. An Alizarin red-based assay of mineralization by adherent cells in culture: comparison with cetylpyridinium chloride extraction. Anal Biochem. 2004, 329(1):77-84.

O_2 Diffusion through Collagen Scaffolds at Defined Densities: Implications for Cell Survival and Angiogenic Signalling in Tissue Models

U. Cheema[1], A.J. MacRobert[2], Z. Rong[3], T. Alekseeva[1], O. Kirresh[1], P. Vadgama[3], and R.A. Brown[1]

[1] Tissue Repair & Engineering Centre, Institute of Orthopaedics and Musculoskeletal Sciences and [2] National Medical Laser Centre, UCL Division of Surgery & Interventional Science University College London, London, UK. [3] IRC in Biomedical Materials, Queen Mary University of London, UK.

Abstract— **The success of any biomaterial for tissue engineering is dominated by its mechanical properties and ability to support nutrient diffusion. Collagen scaffolds are ideal candidates due to their ability to immerse cells in a biomimetic nano-fibrous matrix. We have established O_2 diffusion coefficients through native, dense collagen scaffolds at two tissue-like densities, with and without photo-chemical crosslinking, by adapting an optical fibre-based system for real-time core O_2 monitoring deep within collagen constructs. The high diffusion coefficients of these collagen scaffolds, as well as their material properties, render them viable tissue engineering matrices for tissue replacement. Due to this O_2 diffusion through cell-seeded collagen type I scaffolds, natural gradients of O_2 form and cells in different locations are subject to varying levels of O_2. These gradients were controlled by varying cell density, as it was found that cell consumption of O_2 played a greater role compared to material diffusion in formation of such O_2 gradients. Potent angiogenic signaling molecules were upregulated at both the gene and protein level, particularly within the core of 3D scaffolds, where O_2 was low, but remained within physiological hypoxia. By incorporating phosphate-based dissolving glass fibres into collagen constructs, as they are produced, it was possible to introduce channels throughout the construct in a gradual manner. Where channeled architecture was introduced to the 3D constructs, thus delivery of sustained O_2 to all cells even within the core, this upregulation of angiogenic factors was abolished. We can now engineer collagen type I scaffolds with varying density, varying degrees of crosslinking and various architectural features to control delivery of O_2 to all cells embedded within the construct.**

Keywords— **Collagen Scaffold, Biomimetic, Oxygen Diffusion, Oxygen permeability, Photo-chemical crosslinking, Phosphate-based dissolving glass fibres, Angiogenic Factors, Tissue-Constructs**.

I. Introduction

Within the fields of Tissue Engineering and Tissue Modelling, the formation of 3D cell-seeded constructs poses multiple problems of O_2, nutrient and lactate permeability both into and out of the 3D structure [1]. Given the nature of an engineered cell scaffold, a native vasculature does not exist, and therefore perfusive properties of the material are critical to take into consideration, especially with regards to the viability of cells within the core of 3D constructs. Development of synthetic polymer scaffolds have an advantage, whereby the architecture of a scaffold can be pre-determined, and porosity can be controlled to aid free-circulating culture media to supply cells throughout the 3D structure. However, synthetic scaffolds cannot mimic the mechanical and protein properties of native scaffolds. Collagen type I is an ideal biomimetic scaffold for engineering living tissues, as it is the predominant extracellular matrix protein within the body. It is difficult to control the architecture of this protein, as we do not manufacture it, instead we rely upon extraction of collagen from animal tissues, and then re-constitute it- or build it back up into a 3D tissue.

Due to the lack of vasculature, in a 3D cell-seeded constructs, natural gradients of O_2 exist from the surface to the core dependent upon perfusion of the O_2 and cell consumption of O_2 [2]. Therefore by manipulation of cell density or architecture of the collagen, these gradients can be manipulated, and in some experimental cases, provide good models of diffusion and varying effects of O_2 on cell behaviour. However, for the survival of a 3D tissue engineered model, an adequate, even and continuous supply of O_2 is critical viability of the core cells.

Here we describe a method to measure and model the diffusion of O_2 through collagen type I scaffolds at varying densities, with and without photo-chemical cross-linking. Once established we incorporated phosphate-based dissolving glass fibres into the structure, which dissolved over 24 hours to leave channels running through the 3D construct. We compare cell viability in constructs with and without channels, as well as regulation of angiogenic signals in constructs with and without channels. Our main hypothesis was that with that the incorporation of dissolving fibres increases supply of O_2 to core cells, and prevents them for up-regulating potent angiogenic signals, which are found when core cells are placed under defined levels of physiological and pathological hypoxia.

The aim being to produce 2 types of construct, the first where natural gradients of O_2 exist to control cell behaviour

A. El Haj and D. Bader (Eds.): 8th International Conference on Cell & Stem Cell Engineering, IFMBE Proceedings 30, pp. 13–16, 2011.
www.springerlink.com

in a specific locations within the 3D construct, and the second, to created channeled structures to supply all cells within a scaffold with the same O_2.

II. Experimental Set-Up

Collagen Scaffold Preparation:

0.5 ml of 10X Eagles MEM solution (Gibco, Paisley, UK) was added to 4ml of rat-tail type I collagen (First Link) in 0.1M acetic acid, protein concentration = 2.035 mg/ml, and then neutralized with 5M NaOH, using the indicator colour changes from yellow to cirrus pink. Following setting and incubation, gels were routinely compacted by a combination of compression and blotting using layers of mesh and paper sheets [3,4].

O2 Diffusion Measure:

O_2 diffusion through acellular plastic compressed (PC) scaffolds was measured using fibre-optic oxygen probes in conjunction with an OxyLab pO_2 E^{TM} (Oxford Optronix, Oxford, UK). Constructs were submerged in solutions of Phosphate Buffered Saline (PBS) exposed to atmospheric air at 37^{0}C, giving a background O_2 level between 140-160mmHg. To measure de-oxygenation rates, the same construct was submerged into a different solution of PBS, which had Nitrogen gas bubbled through continuously to displace any O_2 in the system. All experiments were carried out in a 37^{0}C incubator. The oxygen diffusion coefficient has been established using the Ficks Law model [5].

Channelling:

Phosphate-based dissolving glass fibres were incorporated into the collagen scaffold. These dissolved over a period of 24 hours to leave channels which ran through the entire construct.

Cell Viability:

Quantitative cell viability was assessed using Live/Dead reduced biohazard viability/cytotoxity kit (Molecular Probes, L-7013) according to the manufacturer's protocol. SYTO® 10, a green fluorescent nucleic acid stain and dead Red (ethidium homodimer-2) and after capturing images, live/dead nuclei were counted to ascertain percentage viability. 5 random areas within constructs were visualized with confocal microscopy, and live/dead cell percentages determined (BioRad Radiance 2100, Carl Zeiss Ltd, Hertfordshire, UK).

Scanning Electron Microscopy:

Constructs were fixed in 4% paraformaldehyde (in 0.1M sodium cacodylate buffer) for 1 hour, then fixed in 1% tannic acid (in 0.05M sodium cacodylate buffer) for a further 1 hour. Samples were then dehydrated through an alcohol series to hexamethyldisilazane (HMDS) with air drying. Samples were then cut in various planes and gold-palladium sputter-coated, then viewed using a JEOL 5500LV SEM.

III. Results

Constructs were assembled by rolling the compressed collagen sheets to give 3D spiral configuration (figure 1). O_2 probes were inserted into the core of 3D spiralled collagen constructs to monitor the core levels as the O_2 tension of the external media was dropped from 21% to 0% (O_2 was displaced by bubbling with N_2).

The resulting O_2-time plot (figure 2) was used for mass transport modelling. It is clear from this figure that O_2 diffusion across the full thickness (1.1mm) of the construct was measurable and the collagen construct equilibrated to the O_2 tension of the external media. O_2 concentration changes were derived from a model based on the solution to Fick's second law, and matched to observational findings using 2 collagen matrix densities, with and without photo-chemical cross-linking. O_2 diffusion rates were high in single compressed (11%) native collagen construct, at 4.5 x 10^{-6} cm^2/s^{-1}. Increasing matrix density by approximately 3-fold (from 11 to 34% collagen) produced a fall in O_2 diffusion by ~62% to 1.7 x 10^{-6} cm^2/s^{-1} (Table 1). These data were charted alongside data previously published for cell viability in identical scaffolds (Table 1). A clear relationship between increased O_2 diffusion and increased cell viability can be seen in figure 5. This provides a good correlation of scaffold properties, density and diffusion coefficient with 24 hour cell viability.

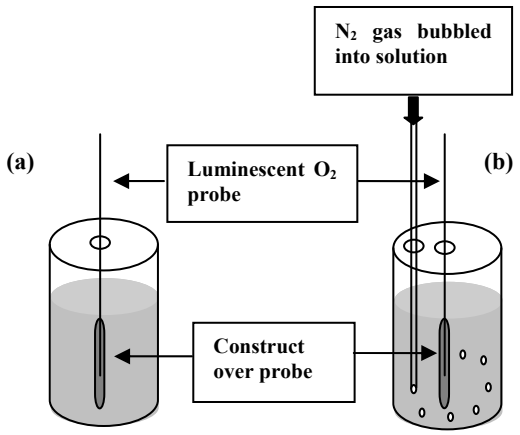

Fig. 1 **Diagrammatic representation of set-up for testing (a) oxygenation and (b) de-oxygenation of constructs.** The set-up was maintained at 37^{0}C, with constructs sealed at both end. N_2 was bubbled through the 0% O_2 solution for 30 minutes prior to testing

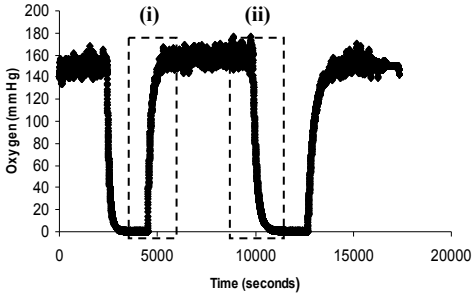

Fig. 2 A graph showing the oxygenation and de-oxygenation of a single compressed construct in either (i) normal PBS solution (140-160mmHg range), or (ii) PBS where N_2 is bubbled through (0mmHg)

Where PBDGF's were incorporated into cell-seeded scaffolds, after 24 hours, levels of O_2 increased in the core (fig. 3b). Resultant channels provided a means by which to deliver O_2 to the entire construct, even to cells within the core.

Table 1 **O_2 Diffusion coefficients of collagen materials at 2 densities.** The cell viability values denote the percentage of cell survival after 24 hours within such collagen constructs with standard deviation (*cell viability values for single compressed taken from: Cheema et al. 2008 [2])

Collagen type	Diffusion Coefficient	Cell viability (% viability at 24 hrs)
Single compressed- 11%	**$4.5 \times 10^{-6} \pm 2.1\%$ cm^2/s**	**90 ± 2.4% ***
Double compressed- 34%	**$1.7 \times 10^{-6} \pm 2.5\%$ cm^2/s**	**67 ± 4.1%**

IV. Discussion

The diffusion coefficient of O_2 through dense collagen scaffolds varies dependent upon density, however at 11% density collagen, the diffusion coefficient falls within the range of some native tissues, including small intestinal submucosa [6]. The O_2 monitoring system allows the diffusion coefficient of materials to be established due to the non-consumption of O_2 at the site of reading. These values are important to consider for survival of cells in scaffolds at early time points. It is clear then, that cell O_2 consumption gradients, which will develop as the cells/tissue grows, will play an increasingly important role in limiting effective delivery of nutrients to the core. The O_2 consumption by cells seeded within the 3D collagen scaffold results in the formation of O_2 gradients, where levels of O_2 are low within the core of 3D constructs.

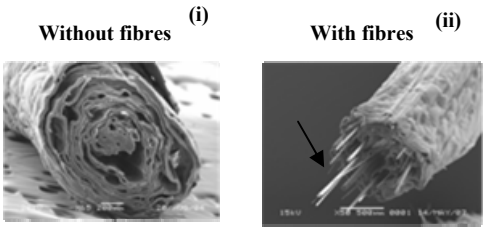

Figure 3a

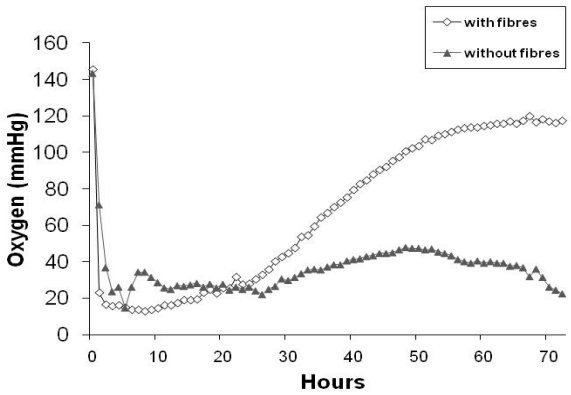

Figure 3b

Fig. 3 **(a) (i) SEM micrographs** of collagen constructs with and without glass fibres. **(ii)** Construct containing dissolving glass fibres, as the fibre dissolves continuous channels are left. . Arrow indicates fibre**(b) O_2 levels in the core of a cellular collagen construct with and without dissolving PBDGF.** By 24 hrs the fibres have completely dissolved, and levels of O_2 increase in the core, compared to control constructs without fibres, up to 3 days, n=1

It is well known that exposed to levels of physiological hypoxia can result in the upregulation of cell-generated angiogenic signaling [2], and that by the introduction of phosphate-based dissolving glass fibres, a channeled architecture can be introduced into the 3D scaffold. As O_2 is delivered to cells within the core, it is hypothesized that this signaling will be switched off.

For engineering of cell-rich tissues, the introduction of channeled features will help maintain a greater density of cells as nutrient limitations and O_2 limitation will not occur. Compared to matrix-rich tissues, i.e. tendon tissue

engineering, where the density of cells is much lower, such channeled features may not be necessary.

References

[1] Karande, T.S. Ong, J.L. Agrawal, C.M. (2004) 'Diffusion in muscloskeletal tissue engineering scaffolds: design issues related to porosity, permeability, architecture, and nutrient mixing'. *Ann. Biomed. Eng*. 32(12): 1728-1743.

[2] Cheema, U. Brown, R.A. Alp, B. MacRobert, A.J. (2008) 'Spatially defined oxygen gradients and VEGF expression in an engineered 3D cell model.' *Cell. Mol. Life Sci.* 65(1): 177-186.

[3] Brown, R.A. Wiseman, M. Chuo, C.B. Cheema, U. Nazhat, S.N. (2005) 'Ultrarapid Engineering of Biomimetic Materials and Tissues: Fabrication of Nano- and Microstructures by Plastic Compression.' *Adv. Funct. Mater*. 15 (11): 1762-1770

[4] Abou-Neel, E.A. Cheema, U. Knowles, J.C. Brown, R.A. Nazhat, S.N. (2006) 'Use of multiple unconfined compression for fine control of collagen gel scaffold density and mechanical properties.' *Soft Matter*. 2:986-992.

[5] Rong, Z. Cheema, U. Vadgama, P. (2006) 'Needle enzyme electrode based glucose diffusive transport measurement in a collagen gel and validation of a simulation model'. *Analyst.* 131(7): 816 – 821

[6] Androjna, C. Gatica, J.E. Belovich, J.M. Derwin, K.A. (2008) 'Oxygen diffusion through natural extracellular matrices: Implications for estimating "critical thickness" values in tendon tissue engineering'. Tissue Eng. Part A 14(4): 559-569.

Finite Element Modeling of Cell Deformation When Chondrocyte Seeded Agarose Is Subjected to Compression

Jinju Chen, D.L. Bader, D.A. Lee, and M.M. Knight

School of Engineering & Materials Science, Queen Mary University of London, London, UK

Abstract— **Dynamic loading is known to be essential in the biosynthesis and maintenance of healthy matabolism in articular cartilage and chondrocyte-seeded hydrogels. This is thought to be a result of a range of factors, including cell deformation. However, the nature of this deformation remains elusive. This study utilises the well-characterized chondrocyte seeded agarose model and finite element analysis based on a viscoelastic model to demonstrate the cell deformation during-both static and dynamic compression in the stage of initial culture. The prony series viscoelastic models were adopted to model agarose and chondrocyte which have been implemented in finite element analysis. The findings suggest that cell strain during loaded phase and unloaded phase strongly depends on the frequency and number of cycles, both of which have been implicated in various mechanotransduction pathway. Due to the mechanical properties mismatch between the cell and agarose construct, the cell strain is amplified through-out the cyclic compression.**

Keywords— **Chondrocyte, agarose, cell deformation, viscoelastic model, finite element analysis.**

I. Introduction

The experimental model system involving isolated chondrocytes seeded in hydrogel, such as agarose, PEG and alginate [1-7], has proved popular due to its ability to maintain phenotype, express both aggrecan and collagen type II characteristic of articular cartilage. Using this model system, dynamic mechanical compression has been shown to stimulate the production of a cartilage matrix [1-2]. Many factors such as cell deformation, dynamic fluid flow, osmotic pressure and electrical streaming potentials have been implicated in the associated mechanotransduction pathways. Although cell deformation has been claimed to be a secondary effect on biosynthesis during dynamic compression [5], it generally refers to a residual deformation after many compression cycles. It is proposed that the instantaneous cell deformation and the stress state are important in controlling signalling pathways. However, the temporal profile of this deformation is difficult to acquire from experimental data due to practical limitations, such as the resolution of the camera, geometric factors and refractive index mismatch. Due to the complex stress state during dynamic contacts and the history-dependent viscoelastic behaviour, an analytical solution is almost impossible to achieve. Accordingly, the present study employs finite element (FE) analysis to predict chondrocyte deformation during cyclic compression regimes. Three prescribed physiological frequencies were examined (i.e. 0.1 Hz, 0.3Hz and 1Hz), each of which have been reported to be significant in chondrocyte response to compression [1-2, 7].

II. Methods

Both agarose (3% type VII) and chondrocyte exhibit time dependency. At relatively high loading rates, linear viscoelastic models are reasonable approximations to capture their time-dependent behaviour. In this study, the linear viscoelastic model defined by a Prony series expansion of the dimensionless relaxation modulus g_R was used:

$$g_R(t) = 1 - \sum_{i=1}^{N} g_i \left(1 - e^{-t/\tau_i}\right) \quad (1)$$

Where g_i and τ_i are material constants.

The viscoelastic parameters of agarose were obtained from stress relaxation tests in the host laboratory, which gives g_1=0.643, τ_1=14.4s, g_2=0.264, τ_2=198.9s, equilibrium Young's modulus E_{equ}=12.6kPa. To investigate the sensitivity of the viscoelastic parameters on the cell deformation, various combinations of viscoelastic parameters of chondrocyte were used (see Table 1), from which the g_i and τ_i could be determined.

Table 1 Viscoelastic parameters of chondrocyte

Set	Viscoelastic parameters			
	k_1(kPa)	k_2 (kPa)	μ (kPas)	E_{equ} kPa)
A1: Tricky *et al* [8]	0.24	0.16	3.0	0.36
A2	0.24	0.16	30	0.36
A3	0.24	0.16	0.3	0.36
B1: Leipzig et al [9]	1.48	0.99	1.92	2.22
B2	1.48	0.99	19.2	2.22
C1: Freeman et al [10], Ofek et al [11]	2.67	1.78	1.92	4
C2	2.67	1.78	19.2	4

The viscoelastic parameters in Set A1 was taken from pipette aspiration tests [8], with fixed values of the two spring constants k_1, k_2 and varying viscocity values for μ. Values for data set B1 were taken from cytocompression creep tests [9].

A. El Haj and D. Bader (Eds.): 8th International Conference on Cell & Stem Cell Engineering, IFMBE Proceedings 30, pp. 17–20, 2011.
www.springerlink.com

Values for data set C were taken from equilibrium modulus of compression of chondrocyte-seeded agarose constructs [10] and cytocompression [11] where the values of k_1/k_2 and μ were assumed to be equivalent to Set B. Similar values were assumed for dynamic properties of chondrocytes, although no experimental evidence was available.

In this study, the chondrocytes were assumed to maintain constant volume during cyclic compression in a hydrated condition [3, 11]. In addition, the cell strain determined from the experimentally measured cell deformation index was based on volume conservation [2]. The axial cell strain can be determined by

$$\varepsilon_y = \left(\frac{y}{x}\right)^{\frac{2}{3}} - 1 \qquad (2)$$

where y is the dimension of the cell at the axial direction of the applied load, x is the lateral cell diameter, the ratio of y/x is so-called cell deformation index. The agarose was assumed to be nearly incompressible [12].

The chondrocyte was assumed to be initially spherical with a representative diameter of 12μm [3]. The 2D axisymmetric FE model was implemented using ABAQUS 6.8. Fig.1. displays the mesh used in this study, where a fine mesh is required in the cell. In the initial culture period, there is no pericellular matrix associated with the individual cells, and thus no adhesion was assumed at the chondrocyte-agarose interface. Frictionless contact was assumed in the two contact interfaces, i.e. the plate-agarose and agarose-cell. In the first simulation, a static compression up to 15% strain was followed by a 20min stress relaxation period and a subsequent 10mins of unloading. A dynamic compression strain (0-15%) was applied in a trapezoidal waveform to cell seeded agarose constructs. The strain rate was fixed at 60%/s which was equivalent to the experimental protocol [2]. This simulation spans 160 cycles at each frequency, again reflecting the experimental data. On the other hand, it avoids the complexity induced by the fatigue of the agarose, which could occur during prolonged cyclic loading at a high strain rate.

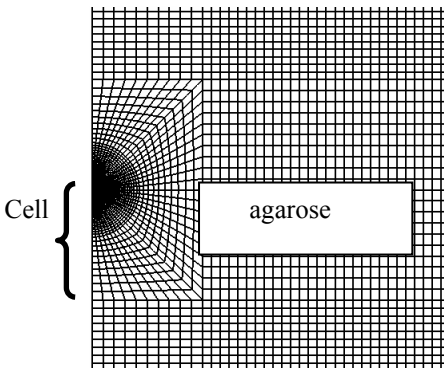

Fig. 1 The finite element mesh used to represent a chondrocyte encapsulated in agarose

III. Results

The results has shown that the mechanical response of the agarose subjected to static compression and dynamic loading can be reasonably well described by the model presented here (Fig.2).

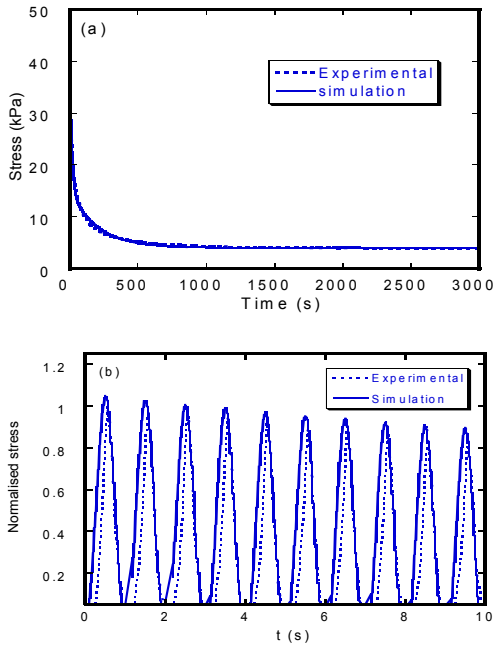

Fig. 2 The mechanical response of agarose during (a) the static and (b) dynamic compression

A sensitivity analysis was performed to examine the effects of viscosity on the simulated data. Results indicated that variations of 1-2 orders of magnitude of the viscocity-had negligible effect on cell strain (data not shown).

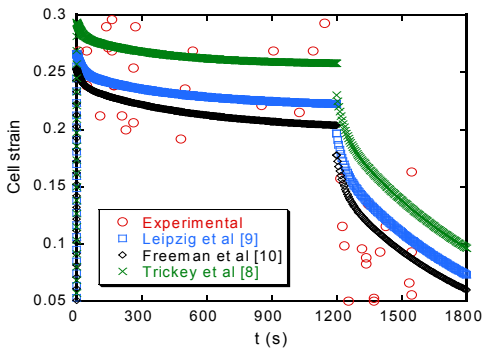

Fig. 3 The axial cell strain changes with time for the static compression. Where the viscoelastic parameters were based on data set taken from [8-11]

Fig.3 displays the cell strain with the viscoelastic paramters in Sets A1, B1, C1 (Table 1) for the static loading/ unloading time profile. Close examination of the data reveals that the model based on Set B1 best represents the experimental measurement [2]. Accordingly, this data set was used to examine cell strain in agarose constructs subjected to dynamic compression.

In each case, strain was estimated from the deformation at the end of both loading and unloading phases for each cycle. Fig.4 indicates that the initial cell strain in the loaded phase is almost the same for all frequencies as the loading rates were identical. The maximum cell strain decreases with the number of cycles, in association with the stress relaxation in the agarose. This effect was less pronounced at the highest frequency of 1Hz, where both the agarose and cell have less time to relax. It is interesting to note that over 160 cycles, the rate of decrease in cell strain is more constant at 0.3Hz than at 0.1 Hz. The former frequency corresponds to a unit cycle period of 3.3s which is very similar to the time constant estimated for chondrocytes [9]. The corresponding contribution from the agarose is not significant, because there is little change in the deformation of agarose at these two frequencies (data not shown).

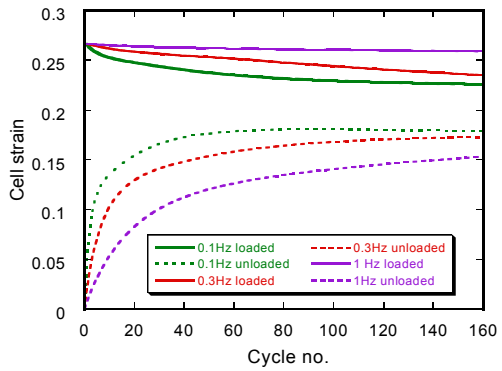

Fig. 4 The axial cellular strains at loaded and unloaded phases for chondrocytes with viscoelastic parameters given by Set B1 (Table 1) under cyclic compression for the three prescribed frequencies

The residual strain in the unloaded phases increases with number of cycles due to an increase in the stored energy (Fig.4). In the initial 10 cycles, the residual cell strain increases most significantly at 0.1 Hz. Beyond that, the residual strain achieves a value of approximately 15%. This is equivalent to that reported for chondrocytes seeded in PEG under 0.3 Hz compression [5].

The micromechanical environment of the cell is also critical when considering its response. This can be represented by the parameter cell strain amplification, e.g. the ratio of the cell strain to the gross strain in the matrix [13]. This is depicted in Fig.5 over the first 10 cycles. It is clear that this parameter is both larger at the higher frequency and decreases with the cycle number. It is interesting to note that the peak cell strain amplification in the first few cycles occurs in the unloading phase for both 0.3Hz and 1Hz. Furthermore, it was found that the cell strain amplification can exceed 2 in the first 3 cycles at 1Hz.

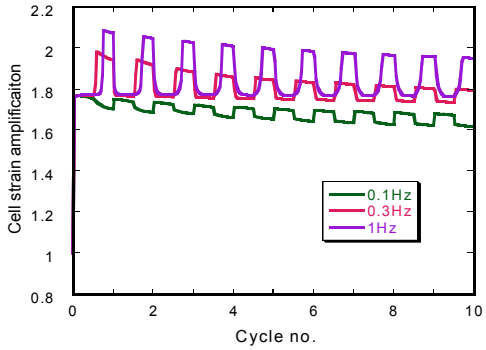

Fig. 5 The cell strain amplification during the cyclic compression for the three prescribed frequencies

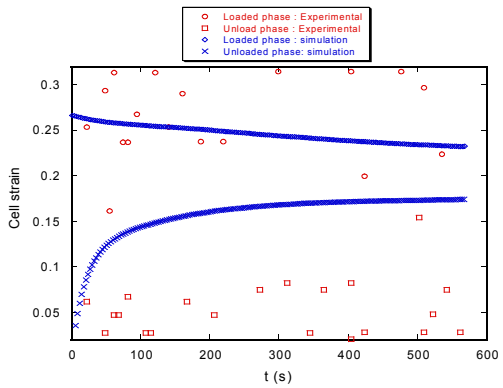

Fig. 6 The comparison of axial cellular strain in chondrocyte for loaded and unloaded phase determined by simulation and experimental measurements for a 0.3Hz trapezoidal compression regime

Fig. 6 indicates the axial cell strain for chondrocytes determined by simulation and experimental measurement for 0.3Hz [2]. The simulation fairly well represents the cell strain during the loaded phase. By contrast, the model deviates from the experimental data in the unloaded phase, overestimating the residual strain. However, it is important to mention how the latter data was acquired. Rather than track single cells, the preferred method, a cell deformation index of different sub-populations were estimated before and after compression. This practical method can, however,

cause uncertainty particularly for small cell deformation in restricted cell populations.

IV. Discussion

The computational approach was designed to examine the temporal profile of chondrocyte strain in agarose constructs subjected to both static and dynamic compression. Certain assumptions were made to simulate the conditions at an early stage of culture under mechanical stimulation. Viscoelastic parameters for both the agarose and the chondrocyte were selected, based on experimental data. Indeed, changes in viscocity of 1-2 orders of magnitude in static compression did not significantly affect cell deformation. This finding could be attributed to the fact that the instantaneous cell strain reaches an asymptotic value, when the instantaneous moduli mismatch between agarose and cell is sufficiently large. For dynamic compression, frequency affects the effective cell strain magnitude (Fig.4). For example, the difference between the maximum cell strain and residual cell strain is highest at 1Hz. This may have implications in the activation of strain-triggered signaling pathways, which are frequency dependent [1]. The discrepancy of the residual cell strain determined from experimental measurement and computational simulation can be due to limitations in both the experimental measurement and the model assumptions and its associated parameters. The micro-fracture in agarose at high strain rate compression is also possible.

The model also offers the potential of monitoring stress evolution and demonstrates both frequency and cycle number dependent behaviour (data not shown). This is currently being expanded to account for membrane effects and internal cell properties.

The living cell can dynamically remodel itself, which may violate the simple viscoelastic model. Thus, more sophisticated models are required for further examination of the frequency and cyclic number dependent mechanical response of cell.

V. Conclusion

The model well represents the mechanical response of agarose during static and dynamic compression. This study demonstrates that an FE model permits the in-situ monitoring of cell deformation and the micromechanical environment of the cell. This may provide important insight into cell mechanics and mechanotransduction during cyclic compression.

Acknowledgment

This work was supported by The Engineering and Physical Sciences Research Council (EPSRC) Platform Grant entitled "Multiscale Mechanobiology for Tissue Engineering".

References

1. Lee DA, Bader DL. (1997) Compressive strains at physiological frequencies influence the metabolism of chondrocytes seeded in agarose, Journal of Orthopaedic Research 15: 181-188.
2. Knight MM, Ghori SA, Lee DA, Bader DL. (1998) Measurement of the deformation of isolated chondrocytes in agarose subjected to cyclic compression. Medical Engineering & Physics 20: 684-688.
3. Knight M M, Bravenboer J, Lee DA, van Osch G, Weinans H, Bader DL. (2002) Cell and nucleus deformation in compressed chondrocyte-alginate constructs: temporal changes and calculation of cell modulus. Biochimica et Biophysica Acta 1570:1-8.
4. Villanueva I, Hauschulz DS, Mejic D, Bryant SJ. (2008) Static and dynamic compressive strains influence nitric oxide production and chondrocyte bioactivity when encapsulated in PEG hydrogels of different crosslinking densities. Osteoarthritis and Cartilage 16: 909-918.
5. Villanueva I, Sara K. Gladem, Jeff Kessler, Bryant SJ (2010) Dynamic loading stimulates chondrocyte biosynthesis when encapsulated in charged hydrogels prepared from poly(ethylene glycol) and chondroitin sulfate,Matrix Biology 29: 51-62
6. Buschmann MD, Gluzband YA, Grodzinsky AJ, and Hunziker EB. (1995) Mechanical Compression Modulates Matrix Biosynthesis in Chondrocyte Agarose Culture. Journal of Cell Science. 108:1497-1508.
7. Chowdhury TT, Bader DL, Lee DA. (2006) Dynamic compression counteracts IL-1 beta induced iNOS and COX-2 activity by human chondrocytes cultured in agarose constructs. Biorheology. 43: 413-429.
8. Trickey WR, Lee GM, Guilak F. (2000) Viscoelastic properties of chondrocytes from normal and osteoarthritic human cartilage. Journal of Orthopaedic Research: 18: 891-898.
9. Leipzig ND, Athanasiou KA. (2005) Unconfined creep compression of chondrocytes. Journal of Biomechanics. 38:77-85.
10. Freeman PM, Natarajan RN, Kimura JH, Andriacchi TP. (1994) Chondrocyte Cells Respond Mechanically to Compressive Loads. Journal of Orthopaedic Research. 12: 311-320.
11. Ofek G, Natoli RM, Athanasiou KA. (2009) In situ mechanical properties of the chondrocyte cytoplasm and nucleus. Journal of Biomechanics. 42: 873-877.
12. Normand V, Lootens DL, Amici E, Plucknett, KP, Aymard P. (2000) New insight into agarose gel mechanical properties. Biomacromolecules 1: 730-738.
13. Guilak F, and Mow VC. (2000) The mechanical environment of the chondrocyte: a biphasic finite element model of cell-matrix interactions in articular cartilage, Journal of Biomechanics 33:1663-1673.

Corresponding author: Dr. Jinju Chen
Institute: Queen Mary University of London
Street: Mile End Road
City: London
Country: UK
Email: v.chen@qmul.ac.uk

Matrix Elasticity Directs Stem Cell Fates – How Deeply Can Cells Feel?

D.E. Discher[1], I. Ivanovska[2], and A. Buxboim[1]

[1] University of Pennsylvania, Philadelphia, PA, USA

Abstract— **Cells make a number of key decisions by actively applying forces to the objects that they 'touch'. Naive mesenchymal stem cells (MSCs) from human bone marrow will be shown to specify lineage and commit to phenotypes with extreme sensitivity to tissue level elasticity. Soft matrices that mimic brain appear neurogenic, stiffer matrices that mimic muscle are myogenic, and comparatively rigid matrices that mimic collagenous bone prove osteogenic. Inhibition of the motor protein myosin blocks all elasticity directed lineage specification. While the results have significant implications for understanding physical effects of the in vivo microenvironment around cells and also for use of materials in biological studies and therapeutic applications of stem cells, they raise additional questions such as how far cells can feel. This question is addressed with MSCs and a series of gels of controlled thickness, with the results showing that cells probe microns into matrix.**

Keywords— **stem cells, matrix, elasticity, forces, differentiation.**

I. Introduction

Cellular organization within a multicellular organism requires a cell to assess its relative location, taking in multiple cues from its microenvironment. Given that extracellular matrix (ECM) consists of the most abundant proteins in animals and contributes structure and elasticity to tissues, ECM scaffolds likely provide key physical cues to tissue cells extending to processes such as stem cell differentiation [1]. In vivo, fibrous characteristics of ECM may be less prominent and less important than cell-scale elasticity: a cell engages ECM and actively probes it, sensing in deformation the elastic resistance that seems to characterize different tissues. Deformations propagate into the ECM and nearby cells but like the proverbial princess who feels a pea placed many mattresses below, the cell possesses feedback and recognition mechanisms that also establish how far a cell can feel. Initial experiments and computational modeling of cell and matrix mechanics lend insight into the sub-cellular sensitivity, propagating into the deformable nucleus [2] and manifested in molecular transitions detected by novel Mass Spectrometry methods [3]. Continuity of deformation from matrix into the cell and further into the cytoskeleton-caged and linked nucleus suggests mechanisms to directly modeulate processes such as differentiation of stem cells.

II. Methods and results

Cells feel their physical environment by applying traction stresses to matrix and then sensing mechanical response(s) at the cell-matrix interface. The propagation of deformations into elastic and homogeneous media is relatively long range, decaying as the inverse of the distance from the force source, but cells might not be very sensitive to much of the displacement field that they genereate. For thin gel substrates affixed to an underlying rigid substrate, the long range propagation of displacements will be affected. If the cells feel matrix displacements, then one would predict very different responses for cells on thin versus thick substrates.

The spread area of a cell is a simple morphological metric of cell state and can be used to identify the critical thickness of a compliant matrix at which cells start to feel a rigid substrate that is hidden beneath the cell. In general, cells spread more and generate more stress (prestress or tension) on matrices with higher E. A thin gel matrix on rigid glass is expected to be effectively stiffer than a thick version of the same matrix. The first study that aimed to assess how deep cells feel showed that smooth muscle cells do not change spread area when plated on either 5 μm or 70 μm thick polyacrylamide gels [2], but subsequent work with MSCs showed that cell spreading on matrices softer than $E \sim 5$ kPa is larger on sub-micron thin gels than on thicker substrate [1]. Differences in cell morphology extend into the cell to the nucleus, with increasingly distinctive nuclear changes with soft substrates thinner than a few microns. Ongoing transcript profiling studies are beginning to correlate changes in the expression of nuclear envelope and cytoskeletal genes with nuclear morphology, suggesting mechanical linkage and transduction processes.

III. Conclusions

The experimental results to date thus show that mechanosensitivity – at least in depth perception by cells – is limited to sub-cellular length scales. Ultimately, even if one's cells are not of royal descent, they seem to feel the difference not only between stiff or soft but also thick or thin matrix surroundings.

A. El Haj and D. Bader (Eds.): 8th International Conference on Cell & Stem Cell Engineering, IFMBE Proceedings 30, pp. 21–22, 2011.
www.springerlink.com

ACKNOWLEDGMENT

Support from the NIH, NSF, and HFSP is gratefully acknowledged.

REFERENCES

1. A. Engler, S. Sen, H.L. Sweeney, and D.E. Discher. Matrix elasticity directs stem cell lineage specification. ***Cell*** 126: 677-689 (2006).
2. J.D. Pajerowski, K.N. Dahl, F.L. Zhong, P.J. Sammak, and D.E. Discher. Physical plasticity of the nucleus in stem cell differentiation. ***Proceedings of the National Academy of Science – USA*** 104: 15619-15624 (2007).
3. C.P. Johnson, H-Y. Tang, C. Carag, D.W. Speicher, and D.E. Discher. Forced unfolding of proteins within cells. ***Science*** 317: 663-666 (2007).
4. Engler, A.J., L. Richert, J.Y. Wong, C. Picart, and D.E. Discher. 2004c. Surface probe measurements of the elasticity of sectioned tissue, thin gels and polyelectrolyte multilayer films: Correlations between substrate stiffness and cell adhesion. *Surface Science*. 570:142-154.
5. D.E. Discher, D.M. Mooney, P. Zandstra. Growth factors, matrices, and forces combine and control stem cells. ***Science*** 324: 1673-1677 (2009).

Mechanical Conditioning Using Magnetic Nanoparticles Bound to PDGF Receptors on HBMSCs Promotes the Smooth Muscle Alpha Actin (SMA) Expression

Bin Hu, Ying Yang, J.P. Dobson, and Alicia J. El Haj

Institute of Science and Technology in Medicine, School of Medicine, Keele University, Stoke-on-Trent, ST4 7QB, UK

Abstract— **Mechanotransduction is believe to have the potential to guide the cell fate by coupling mechanical cycles to biochemical signaling. This study investigated the possibility of controlling cell differentiation by mechanical stimulation of cell membrane surface receptor. Magnetic nanoparticle anchored multivalent ligands targeting platelet-derived growth factor receptor α and β (PDGFR α and β) of human bone marrow stromal cells were mechanically stimulated via a Lab-designed magnetic bioreactor. Smooth muscle α actin (SMA) expression was shown to be enhanced by immunofluorescence staining. Quantitative RT-PCR revealed that after 3 hrs magnetic stimulation via PDGFR α conjugated magnetic nanoparticles (MNPs), smooth muscle α actin mRNA expression levels were significantly upregulated both in 3 hrs and 24 hrs further culture groups.**

Keywords— **Magnetic conditioning, Mechanoresponsive, smooth muscle α actin.**

I. Introduction

Mechanical force has been shown to open ion channels, activate phosphorylation, and expose binding sites for other proteins [1]. Mechanical stimulation via magnetic particles has been employed in our group and succeeded in remote control of ion channels activation [2]. Platelet-derived growth factor receptor is known to be mechanoresponsive in vascular progenitor cells [3, 4]. PDGFR-α activation on HBMSC was demonstrated to upregulate smooth muscle cell α-actin (SMA) expression, whereas PDGFR-β activation stimulating SMA depolymerization [5]. The objective of this work is to identify whether magnetic fields applied to magnetic nanoparticle bound PDGF receptors can promote SMA up-regulation in HMBSC.

II. Materials and Methods

Cell Culture

Human bone marrow stromal cells (HBMSCs) were purchased from Lonza. Anti-human PDGFR-α and β antibodies (R&D Systems) were conjugated to the surface of 250 nm magnetic particles (Micromod) after the particles were functionalized with the Fc-specific secondary antibody (Sigma-Aldrich) according to the manufacturer's protocol.

After 48 hrs in serum free medium (DMEM, 1% L-glutamine, 1% antibiotic - antimyotic), HBMSCs (passage 4-6) were coated with antibody-immobilized magnetic particles (MP). Magnetic bioreactor described previously in our group (Fig 1) was used to apply translational force to receptors bound magnetic particles. Cells without magnetic conditioning were used as controls.

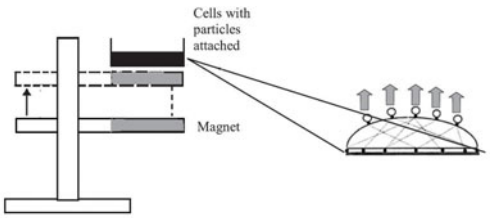

Fig. 1 Diagram of magnetic force bioreactor

Immunofluoresecnce Analysis

After 3 hrs and 24 hrs following culture, cells were washed with phosphate-buffered saline (PBS) and fixed in 95% ethanol for 10 min at room temperature. After washing with PBS, 3% Bovine serum albumin (BSA) in PBS was used to incubator cells for blocking non-specific binding. Then cells were incubated with a monoclonal mouse anti-human primary antibody (Dako) to smooth muscle α-actin clone 1A4. After washing with PBS, goat anti-mouse FITC-conjugated secondary antibody was incubated for 1hr at room temperature, then cells washed and stained nuclear with propidium iodide. Cell numbers were counted and expression levels quantified using confocal microscopy.

Quantitative Real Time RT-PCR

mRNA was isolated from 3 hrs and 24 hrs further cultured cells respectively using solution D, then using isopropanol to purify. mRNA (1 μg) was reverse transcriptted into cDNA using QuantiTect Reverse Transcription Kit (Qiagen). The efficiency-corrected relative quantitation method of relative quantification real-time PCR was performed using Applied Biosystems reagents in 25 μl reactions containing 50 ng cDNA, 12.5 μl 2 x Taqman Universal PCR Master Mix, 1.25 μl Probes and Primer Mix (SMA: Hs00909449_m1; 18s:

A. El Haj and D. Bader (Eds.): 8th International Conference on Cell & Stem Cell Engineering, IFMBE Proceedings 30, pp. 23–25, 2011.
www.springerlink.com

Hs99999901_m1;) and STRATGENE Mx3005P QPCR system was used. The cycle condition is set according to the manufacturer's protocol.

Statistical Analysis

One way ANOVA was used for results statistics analysis. A value of $P < 0.05$ was considered significant.

III. Results and Analysis

A. Immnuofluorescence Staining Images

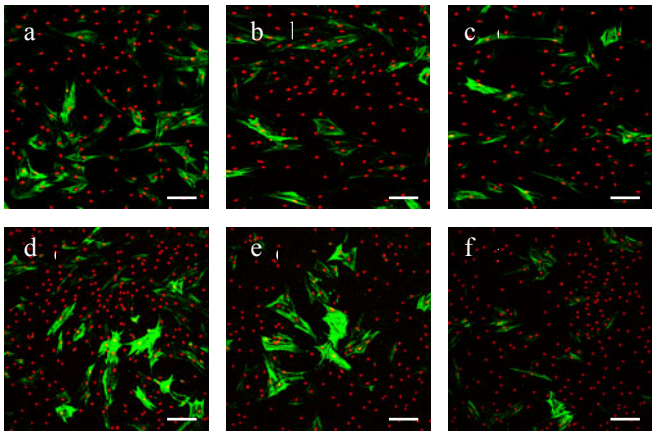

Fig. 2 Smooth muscle α-actin expression of HBMSCs. a: cells after 3hrs loading via PDGFRα conjugated MNPs and 3 hrs further culture; b: upper middle: cells after 3hrs loading via PDGFRβ conjugated MNPs and 3 hrs further culture; c: control cells without treatment; d: cells after 3hrs loading via PDGFRα conjugated MNPs and 24 hrs further culture; e: bottom middle: cells after 3hrs loading via PDGFRβ conjugated MNPs and 24 hrs further culture; f: control cells without treatment. Scale bar: 200 μm

B. Semi-quantification of SMA Expression

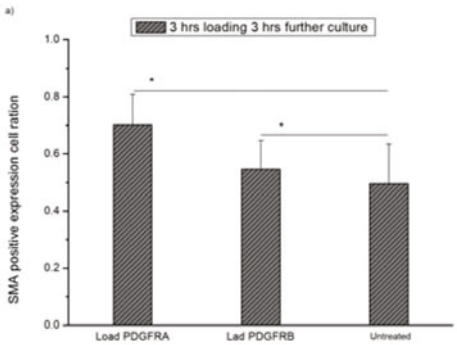

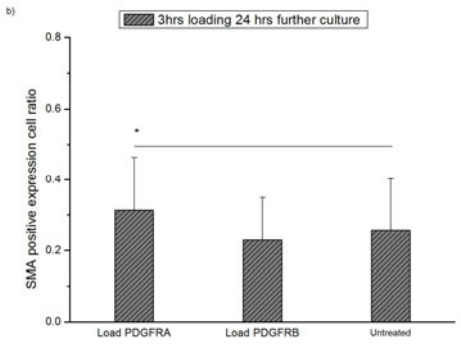

Fig. 3 a) SMA expression significantly changed after 3 hrs magnetic stimulation and 3 hrs further culture (n=5, *p<0.05). b) SMA expression significantly changed after 3 hrs magnetic stimulation and 24 hrs further culture (n=5, *p<0.05)

C. Real Time RT-PCR

Compared with untreated cells, after 3 hrs further culture, mRNA of cells stimulated via PDGFRα conjugated MNPs were upregulated; after 24 hrs further culture, mRNA of cells stimulated via both PDGFRα and PDGFRβ conjugated MNPs were upregulated.

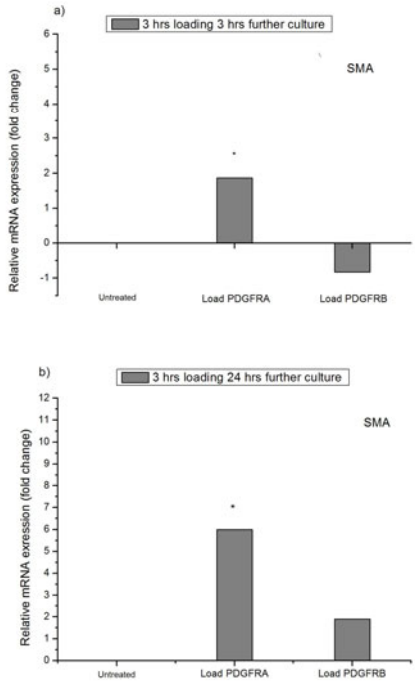

Fig. 4 Relative mRNA expression of SMA in HBMSCs at untreated control group and magnetic stimulated groups, all data have been normalized to 18s and to 0 for control cells without treatment (ANOVA, n=4, *p<0.05)

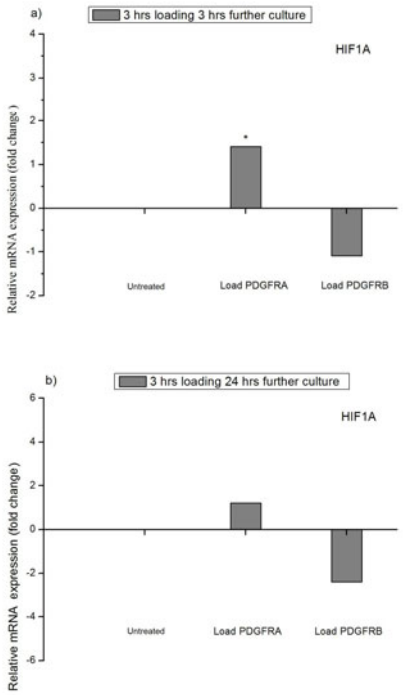

Fig. 5 Relative mRNA expression of HIF1A in HBMSCs at untreated control group and magnetic stimulated groups, all data have been normalized to 18s and to 0 for control cells without treatment (ANOVA, n=4, *p<0.05)

IV. Conclusions

Our results demonstrated that magnetic stimulation could activate cell membrane surface receptors and holds the promise to be a potential tool for remote control of stem cells differentiation.

Acknowledgment

EXPERTISSUES.

References

1. Vogel V, Sheetz MP (2009) Cell fate regulation by coupling mechanical cycles to biochemical signaling pathways. Curr Opin Cell Biol 21:38-46.
2. Hughes S, McBain S, Dobson J, El Haj AJ (2008) Selective activation of mechanosensitive ion channels using magnetic particles. J R Soc Interface 5: 855-863.
3. Shimizu N, Yamamoto K, Obi S et al. (2008) Cyclic stain induces mouse embryonic stem cell differentiation into vascular smooth muscle cells by activating PDGFR β. J Appl Physiol 104:766-772.
4. Lin YC, Grinnell F. (1993) Decreased level of PDGF-stimulated receptor autophosphorylation by fibroblasts in mechanically relaxed collagen matrices. J Cell Biology 122:663-672.
5. Ball SG, Shuttleworth CA, Kielty CM (2007) Platelet-derived growth factor receptor-α is a key determinant of smooth muscle α-actin filaments in bone marrow-derived mesenchymal stem cells. Int J Biochem Cell Biol 39: 379-391.

Introducing Microchannels into Chondrocyte-Seeded Agarose Hydrogels Influences Matrix Accumulation in Response to Dynamic Compression and TGF-β3 Stimulation

T. Mesallati, C.T. Buckley, T. Nagel, and D.J. Kelly

Trinity Centre for Bioengineering, School of Engineering, Trinity College Dublin, Ireland

Abstract— **Tissue engineering technologies combining cells with scaffolds are promising strategies for cartilage repair. A recurring problem with scaffold-based therapies is the formation of superior peripheral tissue, resulting in an inhomogeneous tissue construct. Nutrient transfer limitations to the centre of the construct are believed to be responsible for the phenomena. The introductions of channels into a scaffold or hydrogel, or using mechanical loading to improve nutrient transfer, are two potential approaches to overcome this limitation. If both approaches are combined, the mechanical environment within dynamically compressed hydrogels will be modified by the introduction of microchannels into the construct. The objective of this study was to investigate how chondrocytes will respond to this altered mechanical environment.**

Isolated porcine chondrocytes were suspended in 2% agarose. Microchanneled and solid construct cylinders (Ø 6 x 4 mm) were fabricated and maintained in supplemented media containing TGF-β3 (10ηg/ml). Loaded solid and channeled constructs were subjected to a compressive strain amplitude of 10%, for 2 hours/day, 5 days/week, for a duration of 6 weeks.

In the presence of TGF-β3, dynamic compressive loading in solid constructs resulted in an increase in sulphated glycosaminoglycan (sGAG) accumulation. There was a trend towards greater sGAG synthesis in microchanneled constructs; however sGAG accumulation was lower in these groups. While the introduction of microchannels alone may not result in the development of engineered tissue suitable for implantation, it does represent a unique model to investigate chondrocyte mechanobiology.

Keywords— **Dynamic compression, agarose hydrogel, chondrocytes, channeled constructs, TGF-β3.**

I. Introduction

Tissue engineering strategies aim to repair cartilaginous defects through the use of porous scaffold or hydrogel based systems which provide a 3D environment allowing cells to maintain their differentiated phenotype and deposit extracellular matrix (ECM). Agarose hydrogels are commonly used for cartilage tissue engineering applications, as they have been found to support the chondrogenic phenotype and the synthesis of cartilage ECM (1-2). In addition they have been shown to provide a well characterized mechanical environment (3), suitable for investigating cellular responses to biophysical stimuli. The biosynthetic activity of chondrocytes during in vitro cultivation is known to depend on both the biochemical and biophysical stimuli experienced by the cells. Previous studies have shown that the application of dynamic compressive loading to chondrocyte-seeded agarose hydrogels enhances cartilage specific matrix synthesis (4-6).

However a recurring problem with these agarose constructs is the heterogeneous deposition of ECM within them, with typically greater matrix accumulation in the peripheral regions of the construct (7). Kelly et al. (8) reported a greater stiffness in the periphery of both free-swelling and dynamically loaded constructs. Ng et al. (9) also observed a heterogeneous development of material properties in free swelling chondrocyte-seeded agarose disks. It has been suggested that nutrient diffusion limitations are a possible reason for these heterogeneous constructs (10). Dynamic compression can enhance nutrient transport within agarose constructs (11). Altering the architecture of the constructs is another possible way to overcome nutrient transport limitations. Bian et al. (12) obtained a more homogeneous cartilaginous tissue upon the introduction of macroscopic channels throughout the depth of the construct. Buckley et al. (13) found that the introduction of microchannels, in addition to rotational culture, resulted in sGAG accumulation levels in the core similar to those measured in the periphery of solid constructs.

The objective of this study is to investigate the influence of construct architecture and dynamic loading on matrix accumulation within chondrocyte seeded agarose hydrogels. Channels were transversely introduced into cylindrical agarose gels, and constructs were subjected to dynamic loading over a 42 day period. In addition solid, non-channeled constructs were cultured in parallel. Our original hypothesis was that dynamic compressive loading of channeled constructs would enhance nutrient delivery and fluid flow, and therefore lead to a greater and more homogeneous deposition of matrix throughout the construct compared to solid gels or free swelling conditions.

II. Materials and Methods

A. Cell Isolation, Expansion and Hydrogel Encapsulation

Articular cartilage was aseptically harvested from the femoropatellar joints of two 4-month old porcine donors

A. El Haj and D. Bader (Eds.): 8th International Conference on Cell & Stem Cell Engineering, IFMBE Proceedings 30, pp. 26–30, 2011.
www.springerlink.com

(~50kg). Isolated chondrocytes were plated at a seeding density of 8.75×10^6 cells/cm^2 and expanded to passage one (P1).

Chondrocytes were then suspended in DMEM/F12 and mixed with 4% agarose (Type VII, Sigma-Aldrich, Arklow, Ireland) at ~40ºC, to yield a final gel concentration of 2% and a cell density of 15×10^6 cells/ml. The agarose/cell suspension was cast in a polytetrafluoroethylene (PTFE) mould, and solid construct cylinders were removed using a 6mm biopsy punch. An equal number of channeled construct cylinders were fabricated via a moulding process as previously described (13). Channels were of 500µm diameter, with a centre-centre spacing of 1mm. Constructs were maintained in 6-well plates in a chemically defined chondrogenic medium (CDM) consisting of DMEM GlutaMAX supplemented with penicillin (100U/ml)-streptomycin (100µg/ml) (all GIBCO, Biosciences, Ireland), 1.5 mg/ml bovine serum albumin (BSA), 100µg/ml sodium pyruvate, 40µg/ml L-proline, 4.7 µg/ml linoleic acid, 50 µg/ml L-ascorbic acid-2-phosphate, 1× insulin-transferrin-selenium, 2.5 µg/ml amphotericin B, and 100nM dexamethasone (all Sigma-Aldrich, Ireland). Media was also supplemented with 10ng/ml TGF-β3 (R&D Systems, Abingdon, UK). After cell encapsulation, constructs were left in free swelling conditions for 72 hours before the addition of TGF-β3, and the initiation of dynamic loading (Day 0). Medium was fully replaced twice a week, with 500µl samples taken from wells for each group (n=2-3) at each medium exchange.

B. Dynamic Compression Application

Intermittent dynamic compression (DC) was carried out in a custom pneumatic based compression bioreactor housed within an incubator as previously described (14). The compression protocol consisted of ~10% strain amplitude superimposed on a 0.01 N/construct preload at a frequency of 1Hz. Constructs were loaded each day for 2 consecutive hours, 5days/week over 42 days. Free swelling (FS) controls were maintained adjacent to the bioreactor during loading periods, in the same amount of medium. Both solid and microchanneled constructs were subjected to both culturing regimes, and constructs were assessed at 0, 21, and 42 days.

C. Biochemical Analysis

The biochemical content of constructs was assessed at each time point. All constructs were cored using a 3mm biopsy punch and separated from the annulus. The wet mass of both the core and annulus was recorded and all samples were subsequently frozen at -85ºC for later analyses. Samples were digested with papain (125µg/ml) in 0.1M sodium acetate, 5mM L-cysteine-HCL, 0.05 M EDTA, pH 6 (all Sigma-Aldrich, Ireland) under constant rotation at 60ºC for 18 hours. DNA content was quantified using the Hoechst Bisbenzimide 33258 dye assay. Proteoglycan content was estimated by quantifying the amount of sGAG in each hydrogel core/annulus using the dimethylmethylene blue dye binding assay (Blyscan, Biocolor Ltd., Northern Ireland), with a shark chondroitin sulphate standard. sGAG secreted to culture media was also analysed for each group, with total media volume accounted for. Total collagen content was determined by measuring the hydroxyproline content, using a hydroxyproline to collagen ratio of 1:7.69.

D. Histology and Immunohistochemistry

At each time point, two or more samples per group were formalin fixed, dehydrated, and embedded in paraffin. Sectioning at 5µm produced a cross section perpendicular to the disc face. Sections were stained with 1% alcian blue 8GX (Sigma-Aldrich, Arklow, Ireland) in 0.1M HCL for sGAG accumulation. Samples were stained with picro-sirius red for collagen deposition. Collagen type I and II deposition were identified by immunohistochemical analysis. A mouse monoclonal collagen type I antibody (1:200; 1.4 mg/ml; Abcam, UK) and mouse monoclonal anti-collagen type II antibody (1:80; 1mg/ml; Abcam) were used as primary antibodies for collagen types I and II respectively. An anti-mouse IgG biotin secondary antibody (1:200; 1mg/ml; Sigma-Aldrich) was used for the detection of both primary antibodies.

E. Statistical Analysis

Statistical analyses were performed using the software package MINITAB 15.1 (Minitab Ltd., Coventry, UK). Groups were analysed for significant differences using a general linear model for analysis of variance with factors of culture time, architecture, dynamic compression, and interactions between these factors examined. Tukey's test for multiple comparisons was used to compare conditions. Significance was accepted at a level of $p<0.05$. Numerical and graphical results are presented as mean ± SD (n=3-4 for each group at each time point).

III. Results

sGAG accumulation was observed to significantly increase in all experimental groups (Fig. 1A). By day 42 dynamically compressed solid groups (DCS) were found to have significantly greater sGAG content (534.7±38.7 µg) compared to all other groups. Dynamically compressed microchanneled groups (DCM) accumulated comparable levels of sGAG as

compared to free swelling microchanneled groups (FSM) (307.18±10.64 μg vs. 304.4±22.2 μg). We also noted that there was no significant difference in sGAG levels between the four groups at the final time point when normalized to DNA (Fig. 1D). DNA content was found to be significantly greater in DCS groups (11.029±1.135 μg), when compared to free swelling solid (FSS) groups (7.566±0.44 μg) after 42 days in culture (Fig. 1C).

We next compared core and annulus accumulation at day 42 (Fig. 3A). All groups were found to have significantly greater sGAG levels in the annulus compared to their corresponding core (μg). This is to be expected as the annulus represents a volume three times that of the core. When normalized to wet weight however (data not shown), each group produced significantly more sGAG in the core than their corresponding annulus. We also found that the FSS, FSM, and DCS groups produced significantly more sGAG in the core than their corresponding annulus at day 42 when normalized to DNA.

At day 42, DCM constructs were found to release the greatest amount of sGAG (1026.6±49.6 μg) to the media ($p<0.05$). We also found at this time point that DCS constructs released significantly more sGAG (921±37.5 μg) to the media than either FSM (812.7±24.4 μg) or FSS (654.08±8.02 μg) constructs ($p<0.05$). Taking into account sGAG both accumulated and released per construct over the 42 day culture period, we calculated that DCM constructs produced the greatest overall sGAG amounts when normalized to DNA (156.3743±15.97704 μg/μg) (Fig. 1F), although the differences were not statistically significant.

Collagen accumulation was observed to increase at each time point (Fig. 1B). DCS groups produced the highest levels of collagen (239.77±21.99 μg) at day 42 ($p<0.05$). Loading was also seen to enhance collagen accumulation in microchanneled groups. When collagen was normalized to DNA, we found no significant difference between groups at day 42 (Fig. 1E).

Construct sections from all experimental groups stained positively with Alcian blue (Fig. 2). DCS constructs exhibited slightly more intense staining for sGAG than FSS constructs, while staining was comparable between the DCM and FSM groups. Less intense staining was observed around the periphery of the constructs. This corresponded to our sGAG biochemical results (%w/w). We also observed that the staining seemed to decrease in intensity further into the core of the construct. A more homogeneous sGAG distribution was observed around DCM constructs. Immunohistochemistry for type II collagen revealed a more homogenous distribution in loaded constructs (Fig. 2).

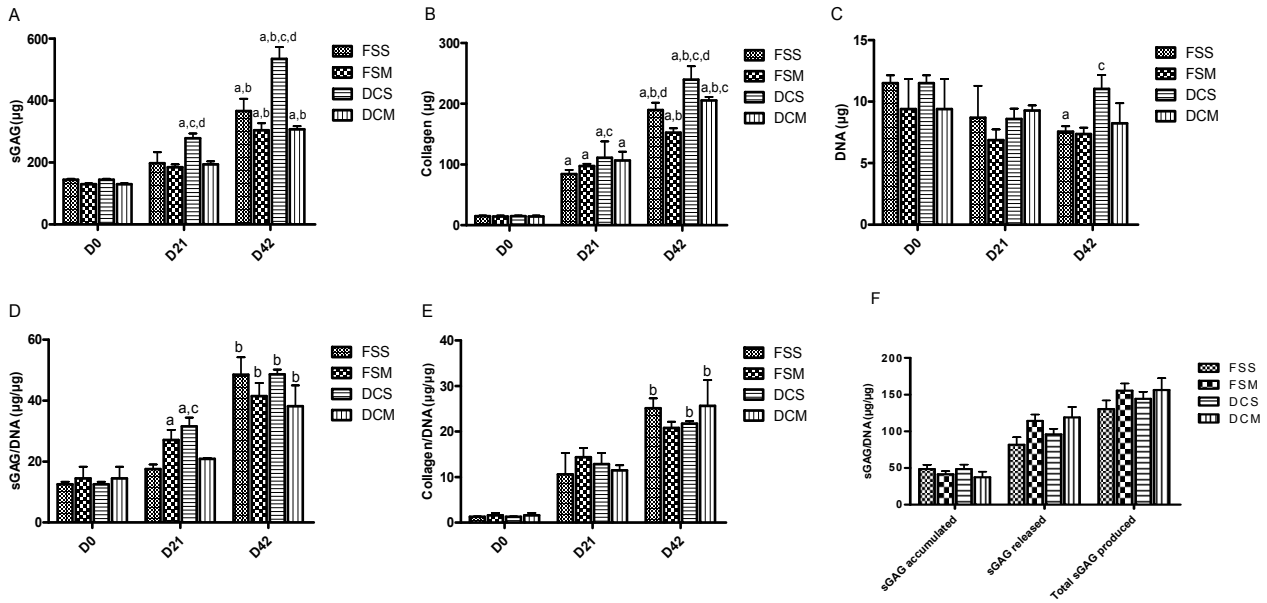

Fig. 1 Biochemical composition of constructs for FSS, FSM, DCS, and DCM groups. (A): sGAG content (μg); (B): Collagen content (μg); (C): DNA content (μg); (D) sGAG/DNA (μg/μg); (E) Collagen/DNA (μg/μg); (F): Total sGAG/DNA accumulated, released, and produced at day 42 (μg/μg). a: $p<0.05$ vs. Day 0; b: $p<0.05$ vs. Day 21; c: $p<0.05$ vs. different culturing conditions with same architecture at same time point; d: $p<0.05$ vs. different architecture with same culturing conditions at same time point.

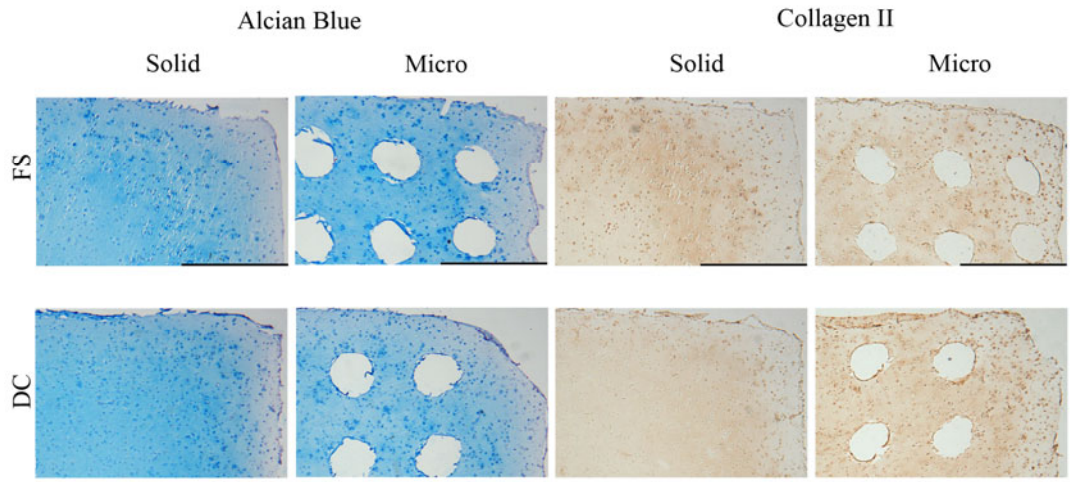

Fig. 2 Alcian Blue staining and type II collagen immunohistochemistry staining of solid and microchanneled constructs subjected to dynamic compression (DC) and free swelling (FS) conditions. Scale bar 1mm. Sections are representative of ¼ of a construct

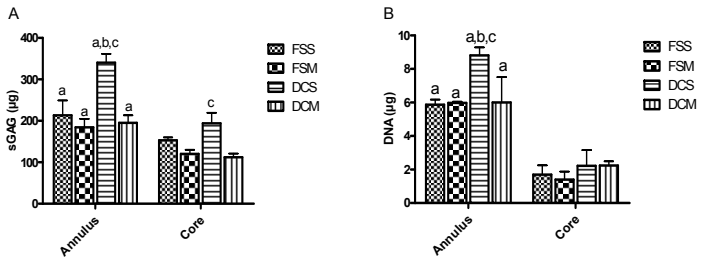

Fig. 3 Biochemical composition of core and annular regions for FSS, FSM, DCS, and DCM groups at D42. (A): sGAG content (µg); (B): DNA content (µg). a: $p<0.05$ vs. core; b: $p<0.05$ vs. different culturing conditions with same architecture in same region; c: $p<0.05$ vs. different architecture with same culturing conditions in same region

IV. Discussion

The purpose of this study was to investigate the influence of dynamic compressive loading and modified construct architecture on the in vitro development of engineered cartilage tissue. It has been previously shown that the biosynthetic activity of chondrocytes depends on the biophysical stimuli experienced by the cells (5). We also observed greater sGAG accumulation in loaded solid constructs compared to all other groups, but we did not find that loading enhanced matrix accumulation in DCM groups. It was seen that loading enhanced cell proliferation in solid gels at day 42, when compared to FSS constructs (Fig. 1C). Comparable sGAG synthesis rates (sGAG/DNA) between all groups at this time point (Fig. 1D) indicate that this superior sGAG accumulation in DCS constructs was due to a higher cell number. The fact that loading maintains cell viability and/or promotes proliferation in solid constructs and not in microchannel constructs may be due to higher levels of fluid flow in loaded channeled constructs. From previous finite element biphasic models for solid and channeled constructs, we predicted high levels of strain and fluid flow at the edges of channels, with pore pressure greatest in the radial spaces separating the channels.

A more homogeneous distribution of sGAG was observed throughout DCM and FSM hydrogels (Fig. 2), suggesting that a modified scaffold architecture can result in a more homogeneous construct. This corresponded to our biochemical results (%w/w), with the DCM and FSM groups presenting the least heterogeneous spatial distribution of sGAG (data not shown). From our histological sections we can see that a significant amount of sGAG is diffusing out into the media, with poor staining around the periphery of the constructs. The fact that both solid and microchannel constructs are releasing sGAG in this manner, for both culturing conditions indicates that agarose may not be an efficient scaffold for retaining ECM. A high oxygen environment at the periphery of the constructs could also be

inhibiting chondrogenesis. We also observed that staining seemed to decrease in intensity the further into the core of the solid construct we passed, once we proceeded past the initial peripheral region, indicating that there may be some nutrient transport limitations towards the core.

Greater sGAG release to the media was observed in loaded constructs, with DCM constructs releasing the greatest amount of sGAG (µg). This can be explained by the microchannels providing a conduit for the diffusion of ECM components into the surrounding media. Taking into account sGAG both accumulated and released per construct over the 42 day culture period (Fig. 1F), we observe a trend towards greater sGAG synthesis in microchanneled constructs, when normalized to DNA. However total sGAG accumulation was lower in this group. This indicates that while the introduction of microchannels may lead to greater ECM synthesis in constructs, the additional ECM components seem to be lost to the surrounding media and not retained by the constructs. Overall the total sGAG accumulation in the construct is reduced by the introduction of channels.

In conclusion this study presents an approach to modifying the local mechanical environment of chondrocytes, in order to understand their basic cellular mechanobiology and engineer cartilaginous tissues. Although a modified architecture may increase the total production of ECM, it does not lead to a greater overall retention in the engineered construct. Further work must look to develop novel approaches to retain sGAG within the developing tissue.

Acknowledgements

Funding was provided by IRCSET, and the President of Ireland Young Researcher Award (08/Y15/B1336).

References

1. Benya P, Shaffer J (1982) Dedifferentiated chondrocytes reexpress the differentiated collagen phenotype when cultured in agarose gels. Cell 30: 215-224
2. Buschmann M, Gluzband Y, Grodzinsky A et al. (1992) Chondrocytes in agarose culture synthesize a mechanically functional extracellular matrix. Journal of Orthopaedic Research 10: 745-758
3. Buckley C, Thorpe S, O'Brien F et al. (2009) The effect of concentration, thermal history and cell seeding density on the initial mechanical properties of agarose hydrogels. Journal of the Mechanical Behavior of Biomedical Materials 2: 512-521
4. Mauck R, Soltz M, Wang C et al. (2000) Functional tissue engineering of articular cartilage through dynamic loading of chondrocyte-seeded agarose gels. Journal of Biomechanical Engineering 122: 252-260
5. Buschmann D, Gluzband Y, Grodzinsky A et al. (1995) Mechanical compression modulates matrix biosynthesis in chondrocyte/agarose culture. Journal of Cell Science 108: 1497-1508
6. Mauck R, Seyhan S, Ateshian G et al. (2002) Influence of seeding density and dynamic deformational loading on the developing structure/function relationships of chondrocyte-seeded agarose hydrogels. Annals of Biomedical Engineering 30: 1046-1056
7. Kelly T, Ng K, Ateshian G et al. (2009) Analysis of radial variations in material properties and matrix composition of chondrocyte-seeded agarose hydrogel constructs. Osteoarthritis and Cartilage 17: 73-82
8. Kelly T, Ng K, Wang C et al. (2006) Spatial and temporal development of chondrocyte-seeded agarose constructs in free-swelling and dynamically loaded cultures. Journal of Biomechanics 39: 1489-1497
9. Ng K, Wang C, Mauck R et al. (2005) A layered agarose approach to fabricate depth-dependent inhomogeneity in chondrocyte-seeded constructs. Journal of Orthopaedic Research 23: 134-141
10. Martin I, Wendt D, Heberer M (2004) The role of bioreactors in tissue engineering. Trends in Biotechnology 22: 80-86
11. Albro M, Li R, Banerjee R et al. (in press, 2010) Validation of theoretical framework explaining active solute uptake in dynamically loaded porous media. Journal of Biomechanics
12. Bian L, Angione S, Ng K et al. (2009) Influence of decreasing nutrient path length on the development of engineered cartilage. Osteoarthritis and Cartilage 17: 677-685
13. Buckley C, Thorpe S, Kelly D (2009) Engineering of large cartilaginous tissues through the use of microchanneled hydrogels and rotational culture. Tissue Engineering - Part A 15: 3213-3220
14. Thorpe S, Buckley C, Vinardell T et al. (in press, 2010) The Response of Bone Marrow-Derived Mesenchymal Stem Cells to Dynamic Compression Following TGF-β3 Induced Chondrogenic Differentiation. Annals of Biomedical Engineering: 1-14

Author: Daniel J. Kelly
Institute: Trinity Centre for Bioengineering, Trinity College Dublin
Street: College Green
City: Dublin
Country: Ireland
Email: kellyd9@tcd.ie

Dirty Surface – Cleaner Cells? Some Observations with Bio-assembled Extracellular Matrices

Y. Peng[1], F.C. Loe[2], A. Blocki[2], and M. Raghunath[1,3]

[1] National University of Singapore/Division of Bioengineering, Faculty of Engineering Singapore
[2] National University of Singapore/NUS Graduate School of Integrative Science and Engineering, Singapore
[3] National University of Singapore/Department of Biochemistry, Yong Loo Lin School of Medicine, Singapore

Abstract— **Conventional propagation of mesenchymal stem cell (MSC) on tissue culture polystyrene (TCPS) decreases their self-renewal capacity and drives them into senescence. Human embryonic stem cells (hESC) cannot be propagated on TCPS at all and require feeder layers or Matrigel™, both of which introduce a xenogenic threat. Obviously, these platforms do not emulate the physiological stem cell microenvironment, consisting of soluble factors, neighbouring cells and a complex extracellular matrix (ECM).**

We directed ECM deposition by human fibroblasts through application of macromolecular crowding followed by detergent lysis to achieve a cell-free matrix. Long-term propagation of MSCs for 58 days on these bioassembled matrices increased their population doublings by 79% compared to TCPS controls. In addition, these MSCs showed a better retention of adipogenic differentiation capability.

HESCs cultured on these matrix in combination with a chemically defined medium for more than 13 passages and showed 40% more population doublings compared to Matrigel™ cultures. Matrix-propagated hESCs maintained a desirable morphology and growth pattern and retained the expression of pluripotency markers. These cells were able to form teratomas in SCID mice, while exhibiting normal karyotypes.

The application of macromolecular crowding to create bioassembled human matrices shows great promise in the propagation of MSCs or hESCs.

Keywords— **Stem Cells, Extracellular Matrix, Pluripotent, Macromolecular Crowding.**

I. Introduction

Standard culture of MSCs on TCPS ages the cells fast and decrease their self renewal [1, 2]. As therapeutically high numbers of MSCs need to be grown from a limited number of cells that can be harvested from tissue, there is an unmet need to increase the expansion efficiency of MSCs in a critical time window. Aging poses a smaller problem in hESCs, however, they tend to differentiate fast and uncontrollably under suboptimal culture conditions and lose their potential rapidly. To maintain their pluripotency ESCs must be grown on feeder cells (murine or human fibroblasts) [3, 4]. This is technically difficult and impedes downstream analysis and applications. In the quest for feeder-free culture systems, coating of culture plates with isolated matrix components like laminin or fibronectin has been tried, but the current gold standard is to grow HESC on Matrigel in conditioned medium [5]. Matrigel is a complex matrix isolated from mouse sarcoma [5, 6]. The xenogenic origin of these matrices facilitates immunogen expression in hESCs, and hampers their application in transplantation [7].

TCPS obviously differs from the native ECM microenvironment of a stem cell, characterized by a complex mix of various glycoproteins and proteoglycans. The ECM does not only provide an anchoring substrate for cells [8], they also interact and store growth factors such as FGF-2 and TGF-β [9, 10, 11].

In vitro, such an ECM can be bio-assembled by mesenchymal cells, such as fibroblasts. However, the highly dilute aquaeous culture conditions prevent an efficient matrix deposition. We have previously remedied this by adding negatively charged macromolecules, which drives the conversion of procollagen to collagen and thus enhances collagen deposition dramatically [12, 13]. We have taken this technology further by decellularising these bioassembled matrices to create cell-free supports that allows for increased population doubling rate and better retention of differentiation capacity in MSCs and hESCs.

II. Materials and methods

A. Cell Culture

Matrices: Wi38 fetal lung fibroblasts were grown in high glucose Dulbecco's modified Eagle's medium as previously described [12, 13]. For enhanced matrix deposition cells were switched to 0.5% FBS supplemented with 100μg/ml dextran sulfate on the following day for 3 days. Cell layers were then lysed with 0.5% sodium deoxycholate to obtain cell-free Matrix-A (3 washes) or Matrix B (6 washes).

*MSCs (*Cambrex, passage 2) were cultured in low glucose Dulbecco's modified Eagle's medium (Gibco) and 10% FBS. Cells were maintained at subconfluency prior to being passaged 1:4 using TrypLE™ Express (Gibco).

A. El Haj and D. Bader (Eds.): 8th International Conference on Cell & Stem Cell Engineering, IFMBE Proceedings 30, pp. 31–34, 2011.
www.springerlink.com

hESCs: H9 (WiCell, WA09) at passage 33 were passaged using collagenase IV equally onto Matrigel (BD, hESC-qualified) and Matrix-B and cultured using defined medium mTeSR-1 (StemCell Technologies). Culture medium was changed daily and subculture was done every 5-7 days.

B. Characterization of Matrices

Decellularised matrices were immunofluorescently analysed with an array of antibodies (from Invitrogen, unless stated differently): mouse anti PDI, Alexa-Fluor 594 phalloidin, mouse anti collagen I (Sigma, C2456), rabbit anti fibronectin (Dako, A0245), mouse anti heparan sulfate (Seikagaku, 370255), mouse anti fibrillin (Chemicon, MAB 2499), rabbit anti decorin and rb anti biglycan (gift from Dr Larry Fisher), rb anti LTBP-1 (gift from Dr Carl Heldin, AB39). Detection was with Alexa Fluor 594 goat anti ms Alexa Fluor 488 chicken anti rabbit and DAPI.

C. Analysis of MSCs

Population Doubling Curve: Representative cultures were fixed and stained with DAPI. Nuclei were counted via automatic adherent cytometry at each passage.

Adipogenic Induction: MSCs were seeded at an initial density of $3.5x10^4$cells/well in 24-well plates (Cellstar, Greiner-bio-one). Adipogenic differentiation was achieved using standard protocols [14].

Flow Cytometry to assess percentage of differentiated cells: Cells were brought into suspension were stained with Nile Red, fixed with formaldehyde (FA) and subjecte to flow cytometry was performed using CyAn (Dako).

D. Analysis of hESCs

Population Doubling Curve: Representative cultures were harvested for cell counting using a hemocytometer.

Immunofluorescence of pluripotent markers: hESCs were formaldehyde-fixed, labelled with goat anti Oct 4 (Santa Cruz, sc-8628), mouse anti SSEA-4 (Chemicon, MAB 4304), and visualised with Alexa Fluor 488 donkey anti goat , Alexa Fluor 594 goat anti mouse, and DAPI .

Flow Cytometry: hESCs were brought into single cell suspension with TrypLE, fixed with formaldehyde, and labelled with goat anti Oct 4, ms anti TRA-1-61 (Chemicon, MAB 4360), mouse anti TRA-1-81 (Chemicon, MAB 4381), rat anti SSEA-3 (Chemicon, MAB 4303), mouse anti SSEA-4 (Chemicon, MAB 4304). Detection was with Alexa Fluor 488 donkey anti goat, Alexa Fluor 488 chicken anti mouse A21200 and Alexa Fluor 488 goat anti rat.

Teratoma formation: hESCs cultured on Matrigel or Matrix-B were injected into SCID by Toh Wei Seong and Prof Cao Tong, Department of Dentistry.

Induced neural differentiation: The protocol for neural differentiation was adapted from WiCell Research Institute, National Stem Cell Bank.

Karyotype: This was performed at KK Women's and Children Hospital.

III. Results and Discussion

A. Characterization of Matrices A and B

Removal of intracellular structures: After deposition of a collagen-rich matrix under macromolecular crowding with dextran sulfate [12, 13], cells were removed by either lysis procedure A or B resulting in Matrix-A and Matrix-B, respectively. The absence of typical intracellular structures such as nuclei, endoplasmic reticulum and actin filaments was confirmed in both matrices (not shown).

Presence of glycoproteins: Immunofluorescence analysis of matrix A revealed collagen I, fibronectin, decorin, biglycan, heparan sulfate, LTBP-1 and fibrillin. Collagen was markedly reduced in Matrix B while fibrillin was not detectable (not shown). The presence of heparan sulfate indicates potential binding partners for FGF-2 [9], an important growth factor for the undifferentiated proliferation of MSCs and hESCs [15, 16]. In addition, fibrillin and fibronectin both bind LTBP-1. LTBP-1 is associated with latency-associated protein [10], which in turn, binds TGFβ in its latent form [11]. TGFβ prevents embryonic stem cells differentiation [17].

B. MSCs Cultured on Matrix-A

Population doubling: MSCs were cultured on Matrix-A for 6 passages (58 days), with control MSCs cultured on TCPS for 5 passages. By the passage 2, the population doubling rate was higher in matrix-cultured MSCs (Fig 1A), and by passage 6, it exceeded that control by 79%. As a result, passaging had to be more frequent on matrix-cultured MSCs to prevent overconfluency. Despite the marked increased in population doubling rate, matrix cultured MSCs retained a more spindly morphology compared to those on TCPS, which had a flattened morphology which are usually seen in older cultures that have lost their multipotency.

Retention of adipogenic differentiation potential: Matrix cultured MSC harvested after passage 4 and adipogenically induced showed twice as much lipid droplet content as with TCPS culture (Fig 2B, C). Hence, despite the extensive propagation, matrix-cultured MSCs retained adipogenic differentiation potential at a higher level than with TCPS.

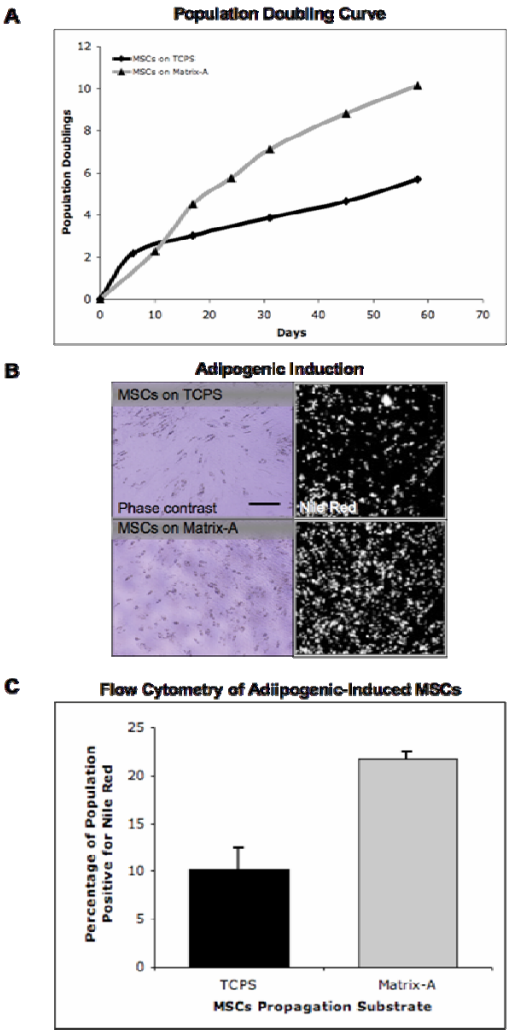

Fig. 1 A. Population doublings of MSCs cultured on Matrix-B exceeded by far the TCPS control. B: MSCs that underwent long-term propagation on Matrix-B or TCPS were induced into adipogenic differentation. Phase contrast and Nile Red fluorescence showed an increase in oil droplets in adipogenic induced differentiation of the Matrix-B-MSCs, showing the retention of differentiation capacity after long term culture. Bar 200µm. C: MSCs pre-propagated on Matrix-A showed a doubling of the percentage of population positive for adipogenic marker, Nile Red

C. hESCs Cultured on Matrix-B

Population doubling: In the first eight passages, population doublings were similar in both hESCs cultures, the dip in population doubling in the second passage could be due to adaptation of the hESCs cells to the matrices. From passage 9 onwards, population doublings of matrix-cultured hESCs surpassed Matrigel-cultured hESCs. By the 13th passage, hESCs cultured on Matrix-B showed a 43% higher population doublings in comparison to the control (Fig 2A).

Morphology of hESCs: Despite the increased population doubling rate, matrix-cultured hESCs retained a pluripotent morphology, namely small, tight, rounded colonies, with clear defined edges, and a high nuclear to cytoplasm ratio (Fig 2B) throughout the 13 passages. In contrast, Matrigel colonies were larger, albeit with defined margins, but with more areas of spontaneous differentiation.

Pluripotency markers: On both supports, hESCs showed colonies positive for Oct-4 and SSEA-4 in adherent immunofluorescence, while flow data showed across a panel of five pluripotency markers comparable expression, meaning an undiminished expression of pluripotency markers despite greater proliferation in matrix-cultured HESc.

In Vivo induced differentiation of hESCs: matrix-cultured hESCs were, after 18 passages, able to form histologically confirmed teratomas in SCID mice (not shown). In contrast, Matrigel culture hESCs did not elicit tumors, suggesting a loss of pluripotency on Matrigel.

In Vitro induced neural differentiation of hESCs: Accordingly, after 13 passages, matrix-cultured hESCs seeded on non-adherent TCPS formed embryoid bodies. Transfer to laminin-coated plates in neural induction medium resulted in neuronal extensions that stained positive for beta III tubulin (not shown).

Karyotype: On both supports, hESCs retained a normal female karyotype (not shown).

IV. Conclusions

Decellularised bioassembled fibroblast matrices created under macromolecular crowding represent a promising platform to promote the undifferentiated proliferation of both MSCs and HESC's, whilst retaining their differentiation potential.

Acknowledgment

YP is a President's Graduate Fellow, FL an NGS scholar. The work was funded by the Life Science Institute (NUS-Baden-Wuerttemberg) and the Faculty Research Committee. The support of the NUS Tissue Engineering Program is gratefully acknowledged.

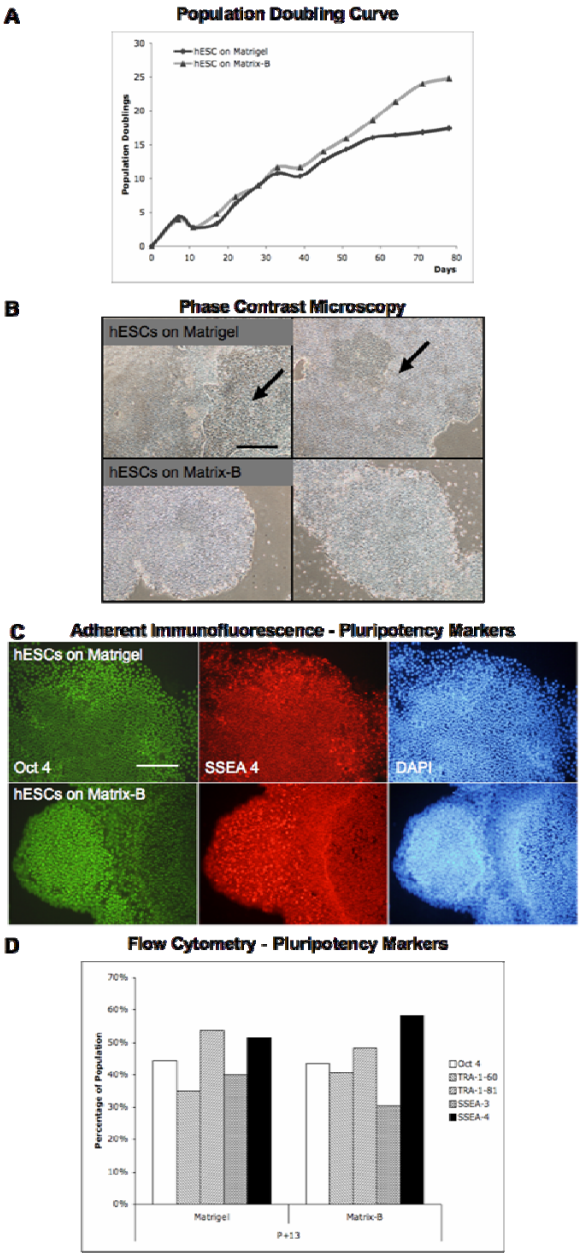

Fig. 2 Analysis of hESCs after 13 passages. A: hESCs cultured on Matrix showed increased population doublings compared to hESCs cultured on Matrigel. B: hESCs cultured on either Matrigel or Matrix showed defined colony edges and high cytoplasm to nucleus ratio. The latter hESCs grew in smaller colonies than the former. Arrows indicate examples of spontaneous differentiation. Bar 500um. C: hESCs cultured on either Matrigel or Matrix were stained for various pluripotency markers and the positive percentage of population were plotted, showing no obvious difference in pluripotency levels. D: Immunofluorescence for pluripotency markers, TRA-1-60 and SSEA-3, showed hESCs cultured on Matrigel grew in pluripotent colonies but lost pluripotency at the colony fringes. hESCs cultured on Matrix grew in tighter colonies and with better retention of pluripotency at colony fringes. Bar 100µm

References

1. Banfi A, Muraglia A, Dozin B, et al. (2000) Proliferation kinetics and differentiation potential of ex vivo expanded human bone marrow stromal cells: Implications for their use in cell therapy. Exp Hematol. 28:707-771
2. DiGirolamo CM, Stokes D, Colter D et al. (1999) Propagation and senescence of human marrow stromal cells in culture: A simple colony-forming assay identifies samples with the greatest potential to propagate and differentiate. Br. J. Haematol. 107:275–281
3. Thomson JA, Itskovitz-Eldor J, Shapiro S, Waknitz MA, Sweir-giel JJ, Marshall VS, et al. (1998). Embryonic stem cell lines derived from human blastocysts. Science, 282:1145–1147
4. Richards M, Tan S, Fong CY, Biswas A, Chan WK, Bongso A. (2003) Comparative evaluation of various human feeders for prolonged undifferentiated growth of human embryonic stem cells. Stem Cell 21:546-556
5. Xu C, Inokuma MS, Denham J, Golds K, Kundu P, Gold JD, Carpenter MK. (2001) Feeder-free growth of undifferentiated human embryonic stem cells. Nat Biotechnol 19:971-974
6. Amit M, Shariki C, Margulets V, Itskovitz-Eldor J. (2004) Feeder layer- and serum-free cultured of human embryonic stem cells. Biol Reprod 70: 837-845
7. Martin MJ, Muotri A, Gage F, Varki A. (2005) Human embryonic stem cells express am immunogenic nonhuman sialic acid. Nat Med 11(2):228-232
8. Miranti CK and Brugge JS. (2002) Sensing the environment: a historical perspective on integrin signal transduction. Nat Cell Biol 4:83-90
9. Saksela O, Moscatelli D, Sommer A, Rifkin DB. (1988) Endothelial cell-derived heparin sulfate binds basic fibroblast growth factor and protects it from proteolytic degradation. J Cell Biol 107:743-751
10. Raghunath M, Unsold C, Kubitscheck U, Bruckner-Tuderman L, Peters R, Meuli M. (1998) The cutaneous microfibrillar apparatus contains latent transforming growth factor-β binding protein-1 and is a repository for latent TGFβ1. Soc Invest Dermatol 111(4):559-564
11. Chong H, Vodovotz Y, Cox GW, Barcellos-Hoff MH. (1999) Immunocytochemical localization of latent transforming growth factor-β1 activation by stimulated macrophages. J Cellular Physiology 178:275-283
12. Lareu RR, Arsianti I, Subramhanya KH, Peng YX, Raghunath M. (2007a) In vitro enhancement of collagen matrix formation and crosslinking for applications in tissue engineering –a preliminary study. Tissue Eng. 13:385–391
13. Lareu RR, Subramhanya KH, Peng Y, Benny P, Chen C, Wang Z, Rajagopalan R, Raghunath M. (2007b) Collagen matrix deposition is dramatically enhanced in vitro when crowded with charged macromolecules: the biological relevance of the excluded volume effect. FEBS Lett. 581:2709-2714
14. Pittenger MF, Mackay AM (1999) Multilineage Potential of Adult Human Mesenchymal. Stem Cells Science 284:143-147
15. van den Bos C, Mosca JD, Winkles J et al. (1997) Human mesenchymal stem cells respond to fibroblast growth factors. Hum Cell 10:45–50
16. Xu RH, Peck RM, Dong SL, Feng X, Ludwig T, Thomson JA. (2005) Basic FGF and suppression of BMP signaling sustain undifferentiated proliferation of human ES cells. Nat Methods 2(3):185-190

Bendall SC, Stewart MH, Menendez P, George D, Vijayaragavan K, Werbowetski-Ogilvie T, Ramos-Mejia V, Rouleau A, Yang J, Bosse M, Lajoie G, Bhatia M. (2007) IGF and FGF cooperatively establish the regulatory stem cell niche of pluripotent human cells in vitro. Nature 448(7157):1015-1021

Acute Stimulation of Dissociated Cortical Neurons of Newborn Rats with Orexin A: Effect on the Network Activity

I.I. Stoyanova*, J. le Feber, and W.L.C. Rutten

University of Twente, Faculty of Electrical Engineering, Mathematics and Computer Sciences, Neurotechnology group, Enschede, the Netherlands

Abstract— **Orexin A (OXA) and B are hypothalamic neuropeptides with recognized importance in the physiological regulation of various brain activities, including sleep/wakefulness, learning and memory, locomotion, autonomic control. Orexin activity is mediated by two types of receptors; OR1 binds OXA with higher affinity, while OR2 binds both ligands equally. There is a growing interest in OXA role in neurodegenerative diseases with respect to the non-motor symptoms such as sleep and attention disorders. Recent studies in Parkinson's patients found 40% lower concentration of OXA in the frontal cortex and 25% reduction in the cerebrospinal fluid. Both the number of orexinergic neurons in the hypothalamus and the levels of orexin in the cerebrospinal fluid are reduced by 72% in the end-stage in mouse model of Huntington's disease. Despite the extensive information about OXA expression and function in the nervous system of adults, data about the orexin system and its role in the functioning of developing neuronal networks are still insufficient. Neuronal cell cultures are often used as a model for brain inquiries; therefore, we undertook our study to investigate immunocytochemically the expression of OR1 in dissociated cortical neurons at various ages, and the acute effect of OXA application on the network activity of neurons, cultured on multi electrode arrays. Initially, control recordings were made after refreshing 50% (300 microliters) of the culture medium. After 2 hours, 300 microliters of medium were replaced again either with medium containing OXA (0.5-2 micromolar, n=8) or plain medium (n=5). Paired t-tests indicated a significant increase in the network activity after acute OXA application ($p<0.003$), but not after plain medium treatment ($p>0.32$), supporting the hypothesis that OXA stimulates neuronal activity in the cortex. These results indicate that potential drugs, based on OXA are attractive candidates for prevention and treatment of disorders associated with neuronal activity decline.**

Keywords— **orexin A, orexin receptor 1, neuronal network activity, multielectrode array, rat cortex.**

I. Introduction

Orexin A (OXA) and orexin B (OXB) are specific hypothalamic neuropeptides with recognized importance in the physiological regulation of various brain activities, including sleep/wakefulness, learning and memory, locomotion, autonomic control [1,2,3]. They have recently been implicated in neurodegeneration associated with narcolepsy, impaired learning and decreased memory abilities [4]. Recent studies in Parkinson's patients found 40% lower concentration of OXA in the frontal cortex and 25% reduction in the cerebrospinal fluid [5]. Both the number of orexinergic neurons in the hypothalamus and the levels of orexin in the cerebrospinal fluid are reduced by 72% in the end-stage in mouse model of Huntington's disease [6].

Orexin activity is mediated by two types of G-protein-coupled receptors which bind both orexins with varying selectivity; OR1 binds OXA with higher affinity, while OR2 binds both ligands equally [7].

Despite the extensive information about OXA expression and function in the nervous system of adults, data about the orexin system and its role in the functioning of developing neuronal networks are still insufficient.

Neuronal cell cultures are often used as a model for brain inquiries. We undertook our study to investigate immunocytochemically the expression of OR1 in dissociated cortical neurons at various ages, and the acute effect of OXA application on the network activity of neurons, cultured on multi electrode arrays.

II. Material and methods

A. Dissociated Cell Cultures

Cortical neurons were obtained from newborn Wistar rats. Under sterile conditions, the whole brain was removed and placed in a Petri dish with a RPMI-medium supplemented with extra glucose to a final concentration of 6.5 mg/ml. The meninges of the cortices were removed, and the striatum and the hippocampus were prepared free. The remaining cortices were collected in a tube with chemically defined R12 culture medium and trypsin for chemical dissociation. After removal of trypsin, 150 µl of soybean trypsin inhibitor and 125 ml of DNAse I (20.000 units, Life Technology) were added. It was followed by mechanical dissociation of the neurons into the solution, and the suspension was centrifuged at 1200 rpm for 5 minutes. The supernatant was removed and the pallet of neurons was resuspended. The obtained neurons were plated and cultured on glass

A. El Haj and D. Bader (Eds.): 8th International Conference on Cell & Stem Cell Engineering, IFMBE Proceedings 30, pp. 35–38, 2011.
www.springerlink.com

cover slips pre-coated with 20mg/ml poly-ethylene-imine (Fluka, Buchs, Switserland) for enhancement of the cell adhesion. Cells were kept in serum-free R12 medium under standard conditions of 37°C and 5% CO2 in air. An initial cell density approximately 3000 cells/mm^2 was used in all experiments. After one- or two-week incubation, cultures for detection of OR1 were fixed in 4% paraformaldehyde in 0.1 M PBS, pH 7.4, and processed immunocytochemically.

B. Electrophysiological Experiments

For the experiments, testing the acute effect of OXA on the network activity, neurons were cultured on multi electrode arrays. These are glass culture chambers with 60 electrodes (diameter of 10 or 30 μm) incorporated in the bottom. In all experiments, cultures were moved to the measurement set up one hour prior to recording to adapt to the conditions and we recorded baseline activity. Then we replaced 300 μl of the medium by 300 μl of fresh medium as a control for the effect of administration of an equal amount of OXA containing medium. After 2 hours recording, 300 microliters of medium were replaced again either with medium containing OXA (0.5-2 micromolar, n=8) or plain medium (n=5). We tested the differences in activity for statistical significance using a paired t-test. $P<0.05$ was considered significant.

C. Immunocytochemistry

The immunohistochemical staining procedure was performed according to the ABC (avidin-biotin-horseradish peroxidase) method. Briefly, a hydrogen peroxide (0.3% in absolute methanol for 30 min) was used to inactivate endogenous peroxidase. Appropriate washes in PBS followed this and subsequent treatments. Incubation in primary antibody goat anti-orexin receptor-1 IgG (AbD Serotec, Oxford, dilution 1:200) lasted for 20 h at room temperature and was followed by 2 h biotinilated donkey anti-goat IgG (1:500; Jackson ImmunoResearch, West in ABC complex (1:500; Vector Labs, Burlingame, CA, USA). Following rinsing, peroxidase activity was visualized using 2.4% SG substrate kit for peroxidase (Vector) in PBS for 5 min, at room temperature. Finally, the cultures were dehydrated in a graded series of alcohols, cleared in xylene, and coverslipped with Entellan (Merck, Darmstadt, Germany). Negative controls included incubation after antigen-antibody preabsorption with the native antigen, at 4 ^{o}C for 24 h. After immunostaining, the cultures were photographed with AxioCam MRC digital camera linked to a Zeiss Axioplan 2 research microscope. All digital images were matched for brightness and contrast in Adobe Photoshop 7.0 software.

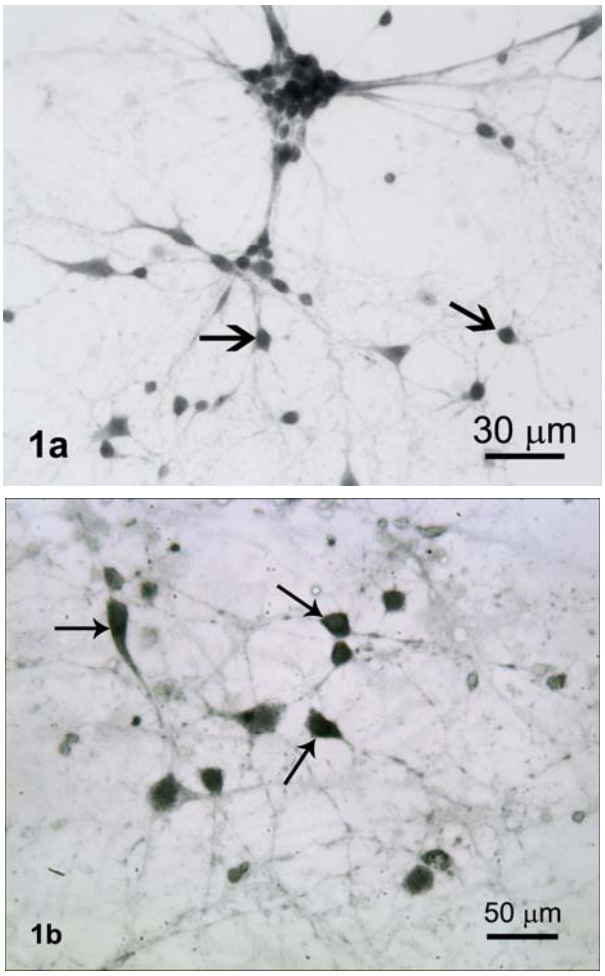

Fig. 1 Dark gray staining of OR1-immunoreactive neurons (arrows) in one-week (a) and two-week-old culture (b)

III. Results

No immunoreactivity for OR1 was detected in the cultures when the primary or secondary antibody was replaced with normal serum. The immunoreactivity was readily discernible at the light microscopic level by the presence of a dark-gray immunoreactive product. Neuronal structures were considered to be immunopositive when their staining was clearly stronger than that in the background.

Five cortical cultures for each incubating period were used for demonstration of OR1. Immunocytochemical labeling revealed that most of the neurons in one-week-old cultures were OR1-immunoreactive (IR). The reaction product was evenly distributed on the cellular surface and along neuronal outgrowth (Fig. 1a, b). This OR1-expressing popu-

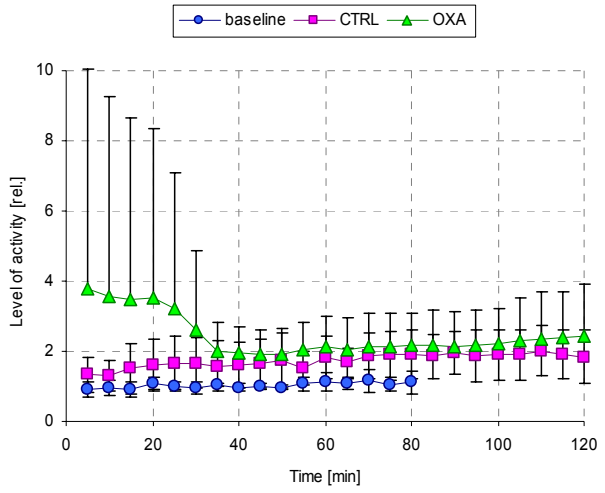

Fig. 2 Chart illustrating the significant increase in the network activity after OXA administration compared to the baseline and control experiment with plain medium

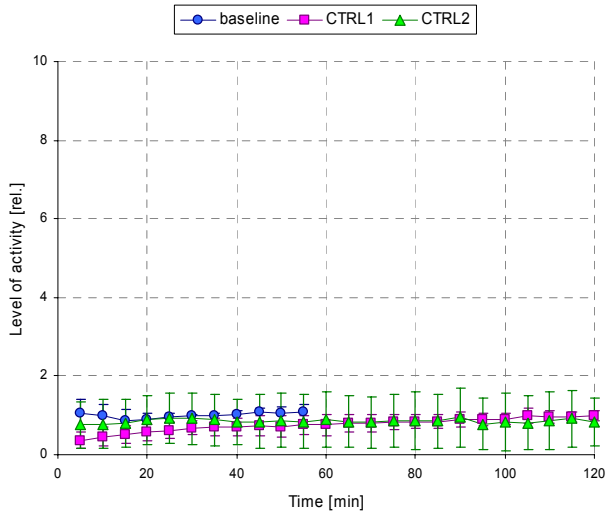

Fig. 3 Double control demonstrating a lack of significant change in the neuronal activity after two consecutive treatments of the culture with a plain medium

lation consisted of two types of cells: bipolar neurons with two major neurites arising from opposite poles of the cell body, and multipolar neurons with several major neurites emerging from a stellate-shaped soma. A fairly high density of OR1-IR neurons was observed in cultures incubated for two weeks.

In 13 experiments we evaluated the effect of acute OXA administration on electrical network activity. As a control, we first changed 300 µl of the medium with 300 µl fresh medium which did not have a significant effect on the activity. Then, we replaced 300 µl of the medium with a similar volume containing orexin. After both manipulations we recorded activity in the culture for 2 hours. Figure 2 compares the activity after OXA administration to that after control. OXA increased the network activity particularly during the first half an hour. Figure 3 demonstrates that there was no significant change in the network activity after two consecutive administrations of a plain medium.

Paired t-tests indicated a significant increase in the network activity after acute OXA application ($p<0.003$), but not after plain medium treatment ($p>0.32$), supporting the hypothesis that OXA stimulates neuronal activity in the cortex.

IV. Discussion

Our study clearly demonstrates that dissociated cortical neurons are well equipped with OR1 and the acute application of the neurotransmitter OXA enhances their electrical activity. Analogous effect was shown with recent *in vivo* studies on genetically modulated animal models, where the loss of orexinergic neurons led to similar behavioral characteristics as humans with neurodegenerative diseases [8]. In addition, replacement of orexin in those animal models reversed some, if not most of the deficits observed [9]. Moreover, the permanent ischemia after brain injury dramatically increases the OR1 mRNA and protein expression, suggesting that orexins, and particularly OXA, play a role in neuronal survival/death [10]. This is in consent with our finding that in culturing conditions neurons express OR1 at early stages of development and OXA stimulation significantly increases neuronal activity.

V. Conclusions

Dissociated cortical neurons of the newborn rats express OR1 and the acute application of OXA significantly increases the network activity. These results indicate that potential drugs, based on OXA are attractive candidates for prevention and treatment of disorders associated with neuronal activity decline.

Acknowledgment

We thank Karin Groot Jebbink and Bettie Klomphaar for their assistance in cell culturing. This study is part of the EU research project NEURoVERS-it. It was supported by grant MRTN-CT-2005-019247.

References

1. Lin L, Faraco J, Li R, Kadotani H et al. (1999) The sleep disorder canine narcolepsy is caused by mutation in the hypocretin (orexin) receptor 2 gene. Cell 98:365-376
2. Fadel J, Bubser M, Deutch AY (2002) Differential activation of orexin neurons by antipsychotic drugs associated with weight gain. J. Neurosci. 22:6742-6746
3. Samson WK, Bagley SL, Ferguson AV et al. (2010) Orexin receptor subtype activation and locomotor behaviour in the rat. Acta Physiologica 198: 313-32
4. Lock I, Jerov M, Scovith S (2003) Future of modeling and simulation, IFMBE Proc. vol. 4, World Congress on Med. Phys. & Biomed. Eng., Sydney, Australia, 2003, pp 789–792
5. Fronczek R, Overeem S, Lee SYY et al. (2007) Hypocretin (orexin) loss in Parkinson's disease. Brain 130:1577-1585
6. Petersen A, Gil J, Maat-Schieman MLC et al. (2005) Orexin loss in Huntington's disease. Hum Mol Genet 14:39-47
7. Sakurai T, Ameliya A, Isgii M et al. (1998) Orexins and orexin receptors: A family of hypothalamic neuropeptides and G protein-coupled receptors that regulate feeding behavior. Cell 92:573-585
8. Zhang S, Lin L, Thankchan S et al. (2010) The development of hypocretin (orexin) deficiency in hypocretin/ataxin-3-transgenic rats. Neuroscience 148:34-43
9. Mieda M, Willie JT, Hara J et al. (2004) Orexin peptide prevent cataplexy and improve wakefulness in an orexin neuron-ablated model in mice. PNAS 101:4649-4654
10. Irving EA, Harrison DC, Babbs AJ et al. (2002) Increased cortical expression of the orexin-1 receptor following permanent middle cerebral artery acclusion in the rat. Neurosci Lett 324:53-56

Address of the corresponding author*:

Author: Irina Stoyanova
Institute: UT
Street: P. O. Box 217, 7500 AE
City: Enschede
Country: the Netherlands
Email: stoyanovai@yahoo.co.uk

Atomistic Simulations of Collagen Fibrils

I. Streeter and N.H. de Leeuw

Institute of Orthopaedics and Musculoskeletal Science, University College London, UK
Department of Chemistry, University College London, UK

Abstract— **Computational molecular dynamics simulations are used to investigate the supramolecular structure of a collagen fibril at an atomistic scale of resolution. The simulations use a newly developed protocol that allows the overall fibrillar structure of collagen to be studied, rather than only providing data on individual, fully solvated proteins. The data generated provide new information regarding the arrangement of collagen proteins and water molecules within a fibril, and the nature of the inter-protein attractions that are responsible for the process of fibrillogenesis. It is anticipated that this new approach to modelling a fibril will lead to a better understanding of how collagen's material properties depend on the dynamic behaviour of the underlying proteins and water molecules.**

Keywords— **collagen, molecular dynamics, simulation, fibril, structure.**

I. Introduction

Collagen is used in the field of tissue engineering as a material for building scaffolds that have the potential to direct cells into forming new tissue. It has an advantage over any synthetic material as it is naturally the principal protein component of the extracellular matrix, and so it is biocompatible and has low immunogenicity. Collagen is a highly complex material: the underlying proteins have a very long, non-repeating amino acid sequence, and they aggregate in combination with water to form fibrils with a specific supramolecular arrangement. This complexity in structure makes collagen correspondingly complex to handle as a material. A typical protocol for making a collagen scaffold might involve stimulating a solution of the proteins to gel into fibrils, compressing the gel to remove excess water, and then using cells to slowly resorb and remodel the collagen into the micro-architecture of a natural tissue [1].

Generally, when manipulating a material for a given function, it is advantageous to understand how its underlying structure contributes to its material properties. Molecular dynamics (MD) simulations provide an effective way of bridging between these atomistic-scale interactions and macroscopic observable properties [2]. In a typical MD simulation, a molecular system is first built on an atom by atom basis, and the system dynamics are then calculated by applying classical equations of motion to each atom. The atoms are allowed to interact with each other as they would in the real system, for example via covalent bonds, electrostatic interactions, or Van der Waals forces. The calculated trajectory represents a statistical ensemble of different atomic configurations accessible to the system, and so the material's bulk properties can be predicted by taking appropriate averages from this ensemble.

Although MD simulations have long been used in both the fields of protein science and materials science, simulations of collagen have so far remained fairly limited in terms of what they can tell us about collagen as a material, because most MD simulations to date have only modelled short segments of a collagen protein under conditions where they are fully solvated by water molecules [3-5]. Although this has given us insight into the nature of collagen's triple helix conformation, it does not tell us about the molecular organisation within a fibril, or how the dynamic behaviour of the proteins and water molecules are affected when they are packed together into a fibrillar environment. Extending these molecular dynamics simulations from a single molecule to an entire collagen fibril would ordinarily be problematic because such an increase in the system size would require prohibitively large computational resources.

We have developed a new protocol for modelling the structure of the full collagen fibril, including its constituent proteins and intrafibrillar water molecules, whilst retaining the detail of the system at the atomistic scale. This new approach works by modelling the system as a densely packed unit cell and then applying periodic boundary conditions in such a way that it generates the supramolecular structure inferred from x-ray diffraction experiments. The periodic unit cell is small compared to the size of an entire fibril, and so the computational requirements for this approach are relatively modest. This is an approach that would be more commonly associated with modelling crystalline solid materials, but we find that it can work for collagen even though there are many differences between a fibril and a genuine crystal, in that collagen proteins are large, flexible, disordered, and partially solvated.

A. El Haj and D. Bader (Eds.): 8th International Conference on Cell & Stem Cell Engineering, IFMBE Proceedings 30, pp. 39–42, 2011.
www.springerlink.com

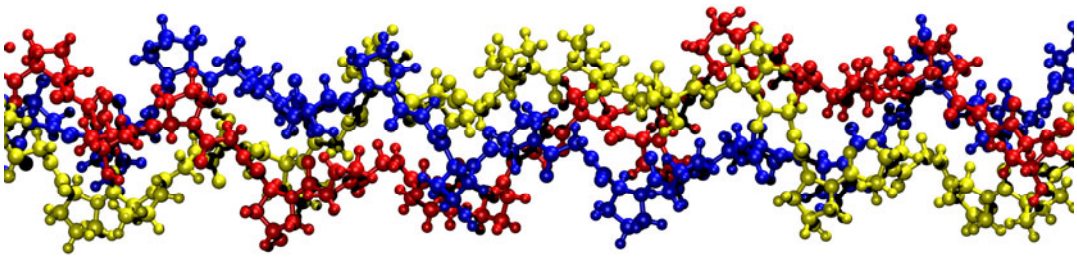

Fig. 1 Triple helical segment of a collagen protein showing atomistic resolution

II. Methods

The first stage in performing these simulations was to build the system with an appropriate starting conformation. The primary structure of the type I collagen protein was taken from the sequenced genes COL1A1 and COL1A2. The local conformation of collagen's triple helical structure is known from high resolution x-ray crystallography of collagen-mimetic peptides [6]. The supramolecular arrangement of collagen proteins is also known from x-ray diffraction of the fibril, but the spatial resolution of this latter experiment is a lot lower [7]. The initial system conformation was therefore inferred by combining these data: the local conformation was consistent with the high resolution data for collagen-mimetic peptides and the overall protein shape and topology was consistent with the low resolution data of the entire fibril. The programme THeBuScr was used to generate the local conformation of the helix [6], and then a python script written in-house was used to translate this into the correct supramolecular topology. Entry 1y0f in the online RCSB Protein Data Bank contains the crystallographic details of the supramolecular structure of collagen, including the orientation and position of the proteins in relation to the periodic unit cell [8].

Water molecules were placed in the unit cell to fill all the intrafibrillar spaces. For each collagen protein, 11980 waters were added, which equates to 0.75 g water / g collagen, and is therefore consistent with previous studies of fibrillar water content [9]. This quantity was selected using a trial and error approach: any more water caused the unit cell to expand beyond its crystallographic dimensions, but any less water led to a contraction.

This ratio of protein to water highlights the key difference between these simulations and standard simulations of proteins. Proteins are nearly always modelled by using a unit cell and by applying periodic boundary conditions, but normally an excess of water is used so that the unit cell is large to the extent that proteins from neighbouring cells do not directly interact with each other. Our simulations use relatively little water in such a way that the unit cells reflect the densely packed structure of the collagen fibril.

Molecular dynamics were performed using the software Amber 9, which is commercially available and is designed specifically for simulating large biomolecules [2]. A standard protocol was followed for the simulations: the system was first minimised to remove any bad contacts, and then heated and equilibrated at constant volume for 120 ps. Finally the trajectory was calculated under constant pressure conditions for 20 ns.

III. Results

The MD simulation of the collagen fibril ran successfully for 20 ns and the system was stable throughout. The tropocollagens flexed and gyrated within their positions due to thermal energy, but they remained in a triple helix conformation and the overall supramolecular arrangement of the proteins was preserved. Water molecules were more dynamic: they appeared to be fairly fluid as they flowed and rotated within the intrafibillar spaces left vacant by the proteins.

Figures 1-3 show various images of the system taken at the end of the 20 ns trajectory. Figure 1 shows a short segment of a tropocollagen with atomistic resolution. Each alpha chain is shown in a different colour, and it can be seen how they twist around each other in a triple helix conformation. Figures 2 and 3 show cross sectional slices of the fibril, taken perpendicular to and parallel to the fibril's long axis, respectively. For both figures, each protein is shown in a different colour, and it can be seen how they have a parallel allignment and are tightly packed to the extent that they interact directly with one another. Water molecules are also shown (red and white), and they fill all of the intrafibrillar spaces and are largely disordered in terms of their positions and orientation.

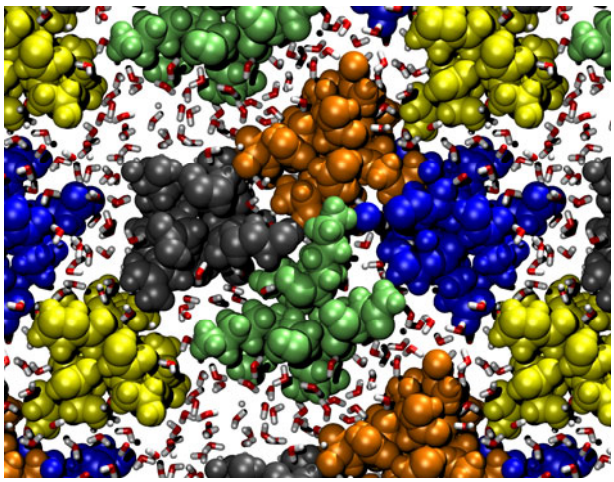

Fig. 2 Axial cross section of the fibril

The energy within the system decreased gradually for the first 8 ns, indicating that the molecules were slowly relaxing during this period to find more stable positions and to optimise intermolecular interactions. This is a fairly long time period for a relaxation, but it is no surprise given that the collagen molecules are so large, and that the starting conformation did not come directly from an experimental atomistic structure.

Although the system energy was stable after the initial 8 ns, the collagen proteins continued to gyrate and flex, and this was therefore interpreted as motion due to thermal energy rather than motion due to any relaxation process. The proteins were observed to be more flexible in the gap region of the fibril where the molecular packing is not as dense as in the overlap region. This can be quantified in terms of the root mean square fluctuation (rmsf) of the protein's alpha carbon atoms; that is the root mean square distance of each alpha carbon from its average position over the course of the simulation. In the densely packed overlap region, the average rmsf of alpha carbon atoms was 1.5 Å; the corresponding rmsf in the gap region was 2.7 Å. It is important to note that this increased flexibility in the gap region is manifested as the bulk movement of entire proteins, and not as any conformational change in the helix itself.

IV. Discussion

The simulations of the collagen fibril described here have a number of unusual features that are worth emphasising. Typically, MD simulations of proteins only ever consider a single protein in a fully solvated state, not in a densely packed environment as in a collagen fibril. Conversely, densely packed environments are often considered in computational studies of materials such as crystalline solids, but these studies rarely have to consider molecules as large as type I collagen, which is over 300 nm long. Our simulations have therefore combined techniques used by both of these branches of computational science to achieve a completely new approach to modelling the collagen fibril with atomistic resolution.

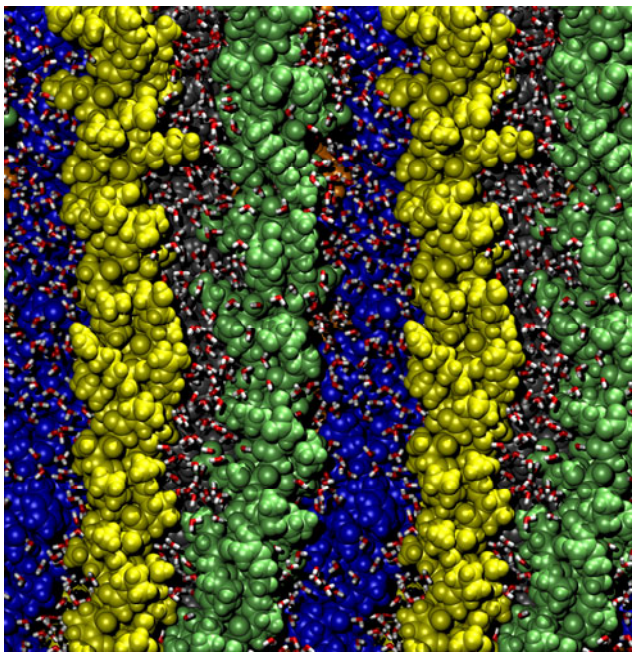

Fig. 3 Lateral slice through the fibril

The simulations reported here give a helpful insight into the nature of the collagen fibril. They give an impression of a fibril that is dynamic rather than static, with collagen proteins continually flexing and gyrating within their fibrillar positions, and with water molecules lubricating this motion by continually flowing and rotating in all of the intrafibrillar spaces. This flexibility of structure is particularly apparent in the gap region of the fibril, as indicated by the rmsf of the alpha carbon atoms in this region. The tropocollagens are less densely packed in this gap region, and there is a higher proportion of water molecules, which increases fluidity.

An important feature of this simulation method is that it allows a study of the manner in which the densely packed collagen proteins interact with each other. One type of important interaction is the inter-protein hydrogen bond, which could be an important factor for bringing strength to the collagen fibril and for driving the process of fibrillogenesis. Such inter-protein hydrogen bonds were observed to be a common feature in these simulations. They generally occurred either between two hydrophillic amino acid sidechains from two neighbouring tropocollagens, or between the protein backbone

of one protein and an amino acid side chain in its neighbour. Conversely, it was very rare to observe a hydrogen bond between two protein backbones in two neighbouring tropocollagens. All inter-protein hydrogen bonds were dynamic and transient; they were continually being broken and reformed due to the fluidity in the fibril structure. These observations provide new insight into the nature of protein-protein interactions, which would not have been possible had we only performed a more traditional MD simulation of a single fully solvated protein.

It is interesting to consider the role of intrafibrillar water molecules in the collagen fibril, as it is known from experiments that water is critical to collagen's material properties [10]. It can be seen from Figure 2 that water molecules surround all of the proteins, and in many places find themselves sandwiched between two neighbouring proteins. We find that on average 44.0% of all intrafibrillar water molecules are found within 3.2 Å of a protein, measured as the distance from the water's oxygen atom to the nearest protein non-hydrogen atom. This distance corresponds to the first hydration shell, and it demonstrates the high proportion of intrafibrillar water that is in direct contact with a protein. Water molecules in close association with proteins generally behave differently compared to the bulk liquid phase, and they have slower rates of translation and rotation. Previous computational studies have shown that collagen distorts the structure of water up to a distance of 6 Å away from its surface. We find that only 5.8% of intrafibrillar water molecules lie further than 6 Å away from their nearest protein in our simulations of a collagen fibril. This highlights a feature of collagen that is common to many biological systems in that the vast majority of the constituent water is very different in character to bulk water in the liquid phase. In the case of collagen, this is likely to be a pertinent point when considering mineralisation and the formation of apatite crystals, which are nucleated in the intrafibrillar spaces, and are likely to be sensitive to the nature and dynamics of their local environment.

V. Conclusions

The most important conclusion from this work is that it is now possible to simulate an entire collagen fibril whilst retaining atomistic resolution, provided one takes advantage of the periodic unit cell as revealed by x-ray diffraction. This is an important step forward that takes us away from modelling single collagen molecules, and brings us towards models that give us a better understanding of larger scale collagen structures. We acknowledge that the model described still cannot tell us everything about a collagen fibril. For example, because the simulations use an infinitely repeating unit cell, they tell us nothing about the outer surface of a collagen fibril. However, it is hoped that this new simulation protocol can be just the first in a series of steps towards achieving simulations that reveal the underlying interactions responsible for collagen's material properties.

The initial results from this simulation method have given an interesting description of the fibril. In particular, it has highlighted the dynamic and disordered nature of the proteins and water molecules at small length scales, even though the fibril has a fairly regular packing arrangement at larger length scales. It has told us new information regarding the positions of inter-protein hydrogen bonds, and it has demonstrated the close association of the water and protein phases, which emphasises that the water molecules are in a very different environment to a pure liquid phase and the proteins are in a very different environment to a fully solvated state.

References

1. Cheema U, Nazhat S, Alp Burçak et al. (2007) Fabricating tissues: an analysis of farming versus engineering strategies. Biotechnol Bioprocess Eng 12:9–14
2. Case D, Cheatham T, Darden T et al. (2005) The Amber biomolecular simulations programs. J Comput Chem 26:1668–1688
3. Klein T, Huan C (1999) Computational investigations of structural changes resulting from point mutations in a collagen-like peptide. Biopolymers 49:167–183
4. Ravikumar K, Hwang W (2008) Region-specific role of water in collagen unwinding and assembly. Proteins 72:3120–1332
5. Raman S, Parthasarathi R, Subramanian V et al. (2008) Role of length-dependent stability of collagen-like peptides. J Phys Chem B 112:1533–1539
6. Rainey J, Goh M (2004) An interactive triple-helical collagen builder. Bioinformatics 20:2485–2459
7. Orgel J, Irving T, Miller A (2006) Microfibrillar structure of type I collagen *in situ*. Proc Natl Acad Sci USA 103:9001–9005
8. RCSB Protein Data Bank at www.rcsb.org/pdb
9. Sivan S, Merkher Y, Wachtel E et al. (2006) Correlation of swelling pressure and intrafibrillar water in young and aged human intervertebral discs. J Orthop Res 24:1292–1298
10. Nomura S, Hiltner A, Lando J et al. (1977) Interaction of water with native collagen. Biopolymers 16:231–246

Corresponding author:

Ian Streeter
Institute of Orthopaedics and Muscoluskeletal Science
University College London
Brockley Hill
Stanmore HA7 4LP
UK
Email: i.streeter@ucl.ac.uk

Can Dynamic Compression in the Absence of Growth Factors Induce Chondrogenic Differentiation of Bone Marrow Derived MSCs Encapsulated in Agarose Hydrogels?

S.D. Thorpe, C.T. Buckley, and D.J. Kelly

Trinity Centre for Bioengineering, School of Engineering, Trinity College, Dublin, Ireland

Abstract— **The objectives of this study were twofold; to determine if cartilage specific matrix synthesis by mesenchymal stem cells (MSCs) is regulated by the magnitude and/or duration of dynamic compression in the absence of growth factors, and to investigate if expanding MSCs in the presence of both fibroblast growth factor-2 (FGF-2) and transforming growth factor β-3 (TGF-β3) would influence their subsequent response to dynamic compression following encapsulation in agarose hydrogels. Porcine bone marrow derived MSCs were suspended in agarose and cast to produce cylinders (Ø5×3mm). Constructs were maintained in a chemically defined medium. Dynamic compression was applied at 1 Hz at strain amplitudes of 5%, 10% and 5% superimposed upon a 5% pre-strain for durations of 1, 3 and 12 hours. MSCs were also expanded in the presence of FGF-2 and TGF-β3. The biochemical constituents of constructs were analyzed. Under strain magnitudes of 5% and 10% and durations of 1 and 3 hours small increases in sGAG accumulation relative to unloaded controls were observed. However this was orders of magnitude lower than that induced by TGF-β3 stimulation. Expansion in FGF-2 and TGF-β3 did not positively modulate chondrogenesis of MSCs in either unloaded or loaded culture.**

Keywords— **Tissue engineering, Cartilage, Mesenchymal stem cells, Mechanobiology, TGF-β3.**

I. Introduction

Chondrogenic differentiation of MSCs can be induced by members of the transforming growth factor-β (TGF-β) superfamily [1-3]. The differentiation pathway and biosynthetic activity of MSCs is also somewhat regulated by their biophysical environment [4,5]. MSCs have been cultured three-dimensionally *in vitro* in bioreactors designed to imitate joint loading, most commonly hydrostatic pressure and dynamic compression [6-8]. It has been demonstrated that dynamic compressive loading in the absence of TGF-β family members can increase chondrogenic gene expression [7-13] and accretion of cartilage specific ECM constituents [8,11,14]. Nevertheless some uncertainty remains as despite increases in gene expression, a number of studies have also demonstrated no positive effect of loading on glycosaminoglycan accumulation in the absence of chondrogenic cytokines [13,15].

Expansion conditions can influence the subsequent chondrogenic differentiation of MSCs. Monolayer expansion in the presence of fibroblast growth factor-2 (FGF-2) has been shown to enhance proliferation during expansion and the subsequent chondrogenic potential of MSCs [16-19]. The addition of growth factors including FGF-2 and TGF-β1 to chondrocyte expansion media has been shown to modulate the cells potential to re-differentiate and respond to regulatory molecules on transfer to a 3D environment [20,21]. Similarly, media including these growth factors added to fat pad and synovial cells during expansion resulted in enhanced sulfated glycosaminoglycan (sGAG) deposition and collagen type II gene expression [22]. It remains unclear what role MSC expansion conditions will have on the cells subsequent response to biophysical stimulation.

As outlined, there is significant variability in the reported responses of MSCs to mechanical loading. This can potentially be attributed to numerous factors, one of which could be that MSCs are sensitive to the magnitude and duration of loading they experience, as suggested by a number of computational studies [23,24]. It has previously been demonstrated that the frequency of dynamic compression modulates MSC viability and chondrogenic differentiation in the absence of growth factors [25]. The first objective of this study was to determine if cartilage specific matrix synthesis by MSCs is also regulated by the magnitude and/or duration of dynamic compression in the absence of growth factors. Related to this question, it is unclear what effect MSC expansion conditions will have on their subsequent response to dynamic compression. The second objective of this study is therefore to investigate if expanding MSCs in the presence of both FGF-2 and TGF-β3 will influence their response to dynamic compression following encapsulation in agarose hydrogels.

II. Materials and Methods

A. Experimental Design

This study comprised of two parts. The first involved MSC expansion in normal conditions (Norm) with constructs undergoing various magnitudes and daily durations of dynamic compression (DC) for 6 days in the absence of TGF-β3 as outlined in table 1. Unloaded free-swelling controls (FS) were kept both in the absence and presence of

A. El Haj and D. Bader (Eds.): 8th International Conference on Cell & Stem Cell Engineering, IFMBE Proceedings 30, pp. 43–46, 2011.
www.springerlink.com

TGF-β3. Constructs were taken for analysis at day 7 and day 28. The second study involved MSC expansion either in normal conditions (Norm) or with the addition of FGF-2 and TGF-β3 (FGF/TGF). Constructs from both conditions were kept in the absence or presence of 10 ng/mL TGF-β3 (CM- or CM+), and loaded to 10% strain for 2 hours/day, 5 days/week for 3 weeks. Each part of the study was preformed independently with separate porcine donors; *n*=4-6 constructs per condition.

Table 1 Loading conditions investigated in Study A

Strain amplitude	Duration	TGF-β3
0%	0 hrs	+/-
5%	1, 3 hrs	-
10%	1, 3, 12 hrs	-
5%(pre-strain) + 5%	1, 3, 12 hrs	-

B. Cell Isolation and Expansion

MSCs were isolated from the femora of two 4 month old porcine donors (~50 kg) within 3 hours of sacrifice as described [26]. Mono-nuclear cells were plated at a seeding density of 2.5×10^6 cells/10cm dish for colony forming unit fibroblast assay, or 10×10^6 cells/75cm^2 flask for expansion in high-glucose Dulbecco's modified eagles medium (4.5 mg/mL D-Glucose, 200mM L-Glutamine; hgDMEM) supplemented with 10% foetal bovine serum (FBS) and penicillin (100 U/mL)-streptomycin (100 µg/mL) (GIBCO, Biosciences, Dublin, Ireland) (Norm). FGF-2 (5 ng/mL) and TGF-β3 (0.5 ng/mL) (ProSpec-Tany TechnoGene Ltd., Israel) were added to a number of flasks from each animal (FGF/TGF) as described above. At the first passage colony's were stained with crystal violet (Sigma-Aldrich, Arklow, Ireland) and counted to obtain the colony-forming cell fraction. Cells were subsequently plated at 5×10^3 cells/cm^2 and expanded to passage two (18.5-20 population doublings) in a humidified atmosphere at 37°C and 5% CO_2.

C. Agarose Encapsulation and Dynamic Compression

MSCs from 2 donors were pooled, suspended in hgDMEM and mixed with 4% agarose (Type VII, Sigma-Aldrich) in phosphate buffered saline (PBS) at a ratio of 1:1 at ~40°C, to yield a final gel concentration of 2% and a cell density of either 30×10^6 cells/mL (Study A) or 15×10^6 cells/mL (Study B). The agarose-cell suspension was cast between two plates and cored to produce cylindrical constructs (Ø 5mm×3mm thickness). Intermittent dynamic compression was carried out as described previously [27]. The dynamic compression protocol consisted of strain amplitude and duration as described above at 1 Hz.

D. Biochemical Analysis

The biochemical content of constructs (*n*=3-4) was assessed at each time point as described previously [27]. Constructs were cored using a 3mm biopsy punch and digested with papain (125µg/ml; Sigma–Aldrich) at 60°C for 18 hours. This enabled spatial variations in biochemical content of the core and annulus of the construct to be determined. DNA content was quantified using the Hoechst Bisbenzimide 33258 dye assay [28]. Sulphated glycosaminoglycan (sGAG) was quantified using the dimethylmethylene blue dye-binding assay (Blyscan, Biocolor Ltd., Carrickfergus, UK). Total collagen content was determined through measurement of the hydroxyproline content [29] with a hydroxyproline-to-collagen ratio of 1:7.69 [30]. Samples of cell culture medium taken for analysis at each media exchange (*n*=3) were analyzed for sGAG and hydroxyproline secreted to the media.

E. Statistical Analysis

Statistics were preformed using MINITAB 15.1 software package (Minitab Ltd., Coventry, UK). Groups were analysed for significant differences using a general linear model for analysis of variance. Tukey's test for multiple comparisons was used to compare conditions. Significance was accepted at a level of $p\leq0.05$. Numerical and graphical results are presented as mean ± standard error.

III. Results

A. Study A: The Influence of Compression Magnitude and Duration

In the absence of TGF-β3 construct DNA content dropped with time in FS culture and was significantly less at day 28 than at either day 0 or day 7 ($p<0.05$). Conversely, with TGF-β3 addition, DNA content increased with time ($p<0.05$). FS controls in the presence of TGF-β3 demonstrated robust chondrogenesis, with sGAG accumulation of 1.03±0.05 %ww with TGF-β3 supplementation as opposed to 0.02±0.0003%ww in its absence. While increases in sGAG were slight, statistical increases were seen above FS controls in construct annuli for both 5% and 10% strain for durations of 1 and 3 hours ($p<0.05$; Fig. 1). Dynamic compression periods of 12 hours were detrimental to accumulation of both sGAG and collagen in construct cores. In the absence of TGF-β3, ECM accumulation was greatest in the annulus region ($p<0.0001$), while in its presence ECM accumulation was greatest in the core ($p=0.0003$).

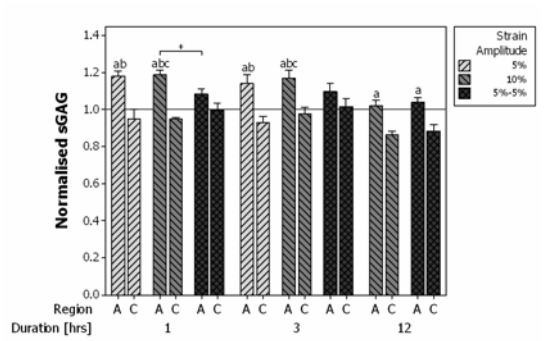

Fig. 1 Day 28 construct sGAG [%wet-weight] normalized to FS control. A: annulus, C: core. $p<0.05$, a vs. core; b vs. FS control; c vs. 12 hrs

B. Study B: Expansion Conditions

Greater consistency in colony forming units between donors was observed for cells expanded in the presence of FGF-2 and TGF-β3 (Fig 2). Colonies tended to be smaller and stained more intensely under FGF/TGF expansion than Norm conditions (Fig 2). On analysis of expansion media, FGF/TGF expanded MSCs were found to have secreted substantial quantities of sGAG while non-measurable levels were found in the Norm expansion media group.

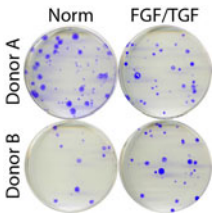

Fig. 2 Representative CFU-F assay plates

Dynamic compression in CM+ conditions inhibited matrix accumulation, although increases were seen over day 0 sGAG and collagen levels. In the absence of TGF-β3, loading had no effect on sGAG or collagen accumulation (Fig. 3). Overall, sGAG accumulation was greatest in the Norm expansion FS constructs; however this was not significantly different than under FGF/TGF expansion (Fig 3A). These same trends were also apparent for collagen accumulation (Fig. 3B). Despite low collagen accumulation levels under CM- conditions, a considerable quantity was secreted to the media (2.45±0.29 µg/construct accumulated vs. 56.79±2.62 µg/construct secreted; not shown). Significantly more collagen was secreted to the media than remained in the construct for all CM+ groups bar FS Norm expansion. A greater proportion of total collagen production was secreted to media for loaded constructs in comparison to FS (p=0.003), although levels remained lower than FS groups.

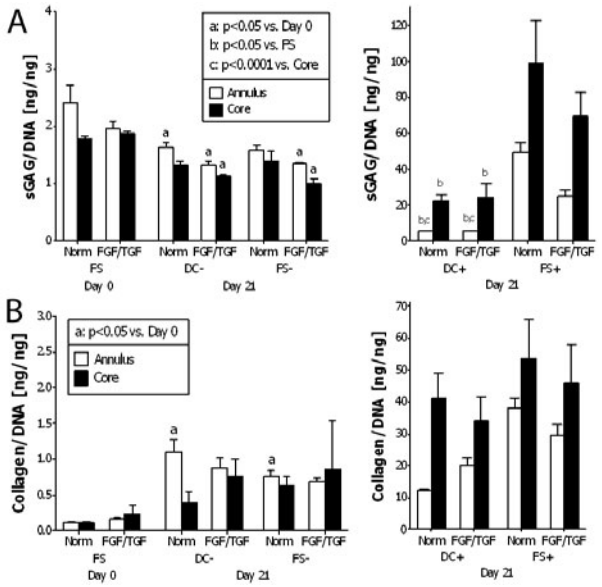

Fig. 3 A: sGAG/DNA. B: Collagen/DNA. Left: CM-, Right: CM+

IV. Discussion

Previously, Huang et al. showed that dynamic compression alone applied to rabbit MSCs in agarose induced similar levels of aggrecan and collagen type II gene expression as TGF-β1 stimulation [7]. Under certain magnitudes and durations we saw an increase in sGAG accumulation relative to FS controls. However this was orders of magnitude lower than that affected through TGF-β3 stimulation as seen here and elsewhere [8,14]. In the absence of growth factors, dynamic compression has been shown to increase chondrogenic gene expression without a consequent increase in accumulated extra cellular matrix (ECM) [13]. This may suggest a disparity between gene expression results and accumulated ECM.

MSC expansion conditions did not affect the subsequent response to loading. Expansion with FGF-2 and TGF-β3 reduced sGAG and collagen accumulation in unloaded culture in the presence of TGF-β3, although this was not significant. This result is in contrast with previous work where fat pad and synovium cells were treated with FGF-2 and TGF-β1 [22]. This may be due to different concentrations of TGF-β used, the fact that they also added platelet-derived growth factor-bb, or simply variation between cell types. FGF-2 and TGF-β3 supplementation during expansion failed to illicit a more positive response to dynamic compression than found in cells expanded under Norm conditions. Future work will examine other scaffold systems where cells adhere to the substrate. This may alter the response of MSCs to mechanical stimuli.

V. Conclusions

Dynamic compression in the absence of growth factors can augment sGAG accumulation by bone marrow MSCs in agarose hydrogel in comparison to unloaded controls; however this remains orders of magnitude lower than that induced due to TGF-β3 stimulation. Expansion in FGF-2 and TGF-β3 did not positively modulate chondrogenesis of MSCs in either loaded or unloaded culture.

Acknowledgment

Funding was provided by Science Foundation Ireland (07-RFP- ENMF142 and the President of Ireland Young Researcher Award: 08/YI5/B1336).

References

1. Johnstone, B. et al. (1998) In vitro chondrogenesis of bone marrow-derived mesenchymal progenitor cells. Exp Cell Res 238 (1), 265-272
2. Mackay, A.M. et al. (1998) Chondrogenic differentiation of cultured human mesenchymal stem cells from marrow. Tissue Eng 4 (4), 415-428
3. Yoo, J.U. et al. (1998) The chondrogenic potential of human bone-marrow-derived mesenchymal progenitor cells. J Bone Joint Surg Am 80 (12), 1745-1757
4. Kelly, D.J. and Jacobs, C.R. (2010) The role of mechanical signals in regulating chondrogenesis and osteogenesis of mesenchymal stem cells. Birth Defects Res C Embryo Today 90 (1), 75-85
5. Knothe Tate, M.L. et al. (2008) Mechanical modulation of osteochondroprogenitor cell fate. Int J Biochem Cell Biol 40 (12), 2720-2738
6. Angele, P. et al. (2003) Cyclic hydrostatic pressure enhances the chondrogenic phenotype of human mesenchymal progenitor cells differentiated in vitro. J Orthop Res 21 (3), 451-457
7. Huang, C.Y. et al. (2004) Effects of cyclic compressive loading on chondrogenesis of rabbit bone-marrow derived mesenchymal stem cells. Stem Cells 22 (3), 313-323
8. Mauck, R.L. et al. (2007) Regulation of cartilaginous ECM gene transcription by chondrocytes and MSCs in 3D culture in response to dynamic loading. Biomech Model Mechanobiol 6 (1-2), 113-125
9. Campbell, J.J. et al. (2006) Dynamic compressive strain influences chondrogenic gene expression in human mesenchymal stem cells. Biorheology 43 (3-4), 455-470
10. Huang, C.Y. et al. (2005) Temporal expression patterns and corresponding protein inductions of early responsive genes in rabbit bone marrow-derived mesenchymal stem cells under cyclic compressive loading. Stem Cells 23 (8), 1113-1121
11. Park, S.H. et al. (2006) An electromagnetic compressive force by cell exciter stimulates chondrogenic differentiation of bone marrow-derived mesenchymal stem cells. Tissue Eng 12 (11), 3107-3117
12. Terraciano, V. et al. (2007) Differential response of adult and embryonic mesenchymal progenitor cells to mechanical compression in hydrogels. Stem Cells 25 (11), 2730-2738
13. Huang, A.H. et al. (2010) Long-term dynamic loading improves the mechanical properties of chondrogenic mesenchymal stem cell-laden hydrogel. Eur Cell Mater 19, 72-85
14. Kisiday, J.D. et al. (2009) Dynamic compression stimulates proteoglycan synthesis by mesenchymal stem cells in the absence of chondrogenic cytokines. Tissue Eng Part A 15 (10), 2817-2824
15. Meyer, E.G. et al. (2010) Low oxygen tension is a more potent promoter of chondrogenic differentiation than dynamic compression. J Biomech (in press)
16. Ito, T. et al. (2008) FGF-2 increases osteogenic and chondrogenic differentiation potentials of human mesenchymal stem cells by inactivation of TGF-Î² signaling. Cytotechnology 56 (1), 1-7
17. Solchaga, L.A. et al. (2010) Fibroblast growth factor-2 enhances proliferation and delays loss of chondrogenic potential in human adult bone-marrow-derived mesenchymal stem cells. Tissue Engineering - Part A 16 (3), 1009-1019
18. Solchaga, L.A. et al. (2005) FGF-2 enhances the mitotic and chondrogenic potentials of human adult bone marrow-derived mesenchymal stem cells. Journal of Cellular Physiology 203 (2), 398-409
19. Stewart, A.A. et al. (2007) Effect of fibroblast growth factor-2 on equine mesenchymal stem cell monolayer expansion and chondrogenesis. American Journal of Veterinary Research 68 (9), 941-945
20. Jakob, M. et al. (2001) Specific growth factors during the expansion and redifferentiation of adult human articular chondrocytes enhance chondrogenesis and cartilaginous tissue formation in vitro. Journal of Cellular Biochemistry 81 (2), 368-377
21. Capito, R.M. and Spector, M. (2006) Effect of expansion medium on ex vivo gene transfer and chondrogenesis in type II collagen-glycosaminoglycan scaffolds in vitro. Osteoarthritis and Cartilage 14 (12), 1203-1213
22. Marsano, A. et al. (2007) Differential cartilaginous tissue formation by human synovial membrane, fat pad, meniscus cells and articular chondrocytes. Osteoarthritis Cartilage 15 (1), 48-58
23. Kelly, D.J. and Prendergast, P.J. (2005) Mechano-regulation of stem cell differentiation and tissue regeneration in osteochondral defects. J Biomech 38 (7), 1413-1422
24. Prendergast, P.J. et al. (1997) ESB Research Award 1996. Biophysical stimuli on cells during tissue differentiation at implant interfaces. J Biomech 30 (6), 539-548
25. Pelaez, D. et al. (2009) Cyclic compression maintains viability and induces chondrogenesis of human mesenchymal stem cells in fibrin gel scaffolds. Stem Cells and Development 18 (1), 93-102
26. Thorpe, S.D. et al. (2008) Dynamic compression can inhibit chondrogenesis of mesenchymal stem cells. Biochem Biophys Res Commun 377 (2), 458-462
27. Thorpe, S.D. et al. (2010) The Response of Bone Marrow-Derived Mesenchymal Stem Cells to Dynamic Compression Following TGF-β3 Induced Chondrogenic Differentiation. Ann Biomed Eng (in press)
28. Kim, Y.J. et al. (1988) Fluorometric assay of DNA in cartilage explants using Hoechst 33258. Anal Biochem 174 (1), 168-176
29. Kafienah, W. and Sims, T.J. (2004) Biochemical methods for the analysis of tissue-engineered cartilage. Methods Mol Biol 238, 217-230
30. Ignat'eva, N.Y. et al. (2007) Determination of hydroxyproline in tissues and the evaluation of the collagen content of the tissues. J Anal Chem 62 (1), 51-57

Corresponding author:

Author: Daniel J. Kelly
Institute: Trinity Centre for Bioengineering
School of Engineering
Trinity College
City: Dublin
Country: Ireland
Email: kellyd9@tcd.ie

Influences of Extracellular Matrix Properties and Flow Shear Stresses on Stem Cell Shape in a Three-Dimensional Dynamic Environment

B. Weyand, K. Reimers, and P.M. Vogt

Department of Plastic, Hand and Reconstructive Surgery, Hannover Medical School, Hannover, Germany

Abstract— **Collagen and ceramic matrices are extracellular scaffolds frequently used for bone tissue engineering. Human mesenchymal stem cells from adipose tissue with their unique properties for multipotent differentiation were cultured on a microporous collagen scaffold (Matriderm) and a macroporous ceramic scaffold (Sponceram) under static culture and in a dynamic flow environment in a laminar flow bioreactor. Both matrices differed in respect to cellular distribution after seeding which depended on pore size of the matrix. Cultivation under dynamic flow conditions influenced cellular morphology, collagen fiber alignment and extracellular matrix deposition compared to static culture. The flow rate had an effect on the amount of extracellular matrix formed by mesenchymal stem cells on the ceramic matrix. Further studies are necessary to reveal the ideal matrix and environmental culture conditions for bone tissue engineering.**

Keywords— **laminar flow, bioreactor, fluid shear stress, stem cell, bone tissue engineering.**

I. Introduction

The intercellular substance of bone tissue consists to 50% of minerals, to 25% of organic materials, here mainly collagen (90-95%) and to 25% of hydration water. Ceramic and collagen scaffolds are frequently used as biomaterials together with mesenchymal stem cells to imitate extracellular matrix and initiate osteogenesis for bone tissue engineering. Stem cell shape is influenced by extracellular matrix properties and external stresses (1). Recent studies have shown that exposure to fluid stress can induce osteogenic differentiation of mesenchymal stem cells (2,3). We examined a microporous collagen scaffold and a macroporous ceramic scaffold in respect to the influence of matrix stability, matrix porosity, matrix material properties and fluid shear stresses on stem cell shape of primary human mesenchymal stem cells inside a laminar flow bioreactor.

II. Material and methods

Stem cell isolation and culture: Human mesenchymal stem cells were isolated from abdominal fat of patients undergoing abdominoplasty after obtaining informed consent and approval from the Ethics committee of Hannover Medical School. Fat pads were dissected, digested in collagenase solution and separated by centrifugation according to standard protocols (4). Stem cells were plated on T150 culture flasks and cultured in DMEM-F12 medium (PAA Laboratories, U.S.) supplemented with 5% fetal calf serum, non-essential amino acids, sodium pyruvate and penicillin-streptomycin at 37°C and 5% CO_2. Multipotency of the isolated stem cells was verified by differentiation into the adipogenic, chondrogenic and osteogenic lineage and demonstration of common stem cell surface markers by FACS analysis.

Biomaterials: Sponceram discs (Zellwerk GmbH, Germany) made from zirconium dioxide with a medium pore size of 400-600µm were autoclaved and rinsed in PBS solution before use. Matriderm sterilization (Suwelack, Germany) made from a collagen-elastin matrix with a medium pore size between 20-150µm was obtained as an 1cm thick block and cylindrical discs of 10mm diameter were cut out by a blade after gas sterilization.

Cell-matrix seeding and cultivation: Stem cells of 2nd and 3rd passage were used for experiments. Briefly, cells were rinsed with PBS without magnesium and calcium addition and were detached from culture plates with 0,1% trypsin-EDTA solution. Cells were centrifuged at 300 rpm and suspended in standard culture medium. Cells were seeded onto Sponceram discs at a concentration of 2-6*10^6/disc and onto and into the Matriderm matrices by means of a syringe at a concentration of 4-10*10^6/cylinder. Controls were cultured in 6 well plates under static conditions in a standard incubator (37°C, 5% CO2).

Bioreactor cultivation: For three-dimensional dynamic culturing cell-seeded matrices were inserted within a laminar flow bioreactor (5,6,7). The bioreactor allows flow control through a differential pressure control system with a baseline set at 5 mbar and an integrated bypass system, which can release pressure built up during the cellular growth within the matrix pores. Cultivation was done within an incubator at 37°C, standard culture medium was supplemented with HEPES buffer solution at a concentration of 0.5mM in order to maintain pH balance. Perfusion was done via a roller pump (Ismatec, Germany) at a pump rate of 0.2 to 5ml/min which equivalates a flow velocity of 20 mm/sec to 500mm/sec. when corrected to the open diameter area. Culture period covered 3 days up to 2 months.

A. El Haj and D. Bader (Eds.): 8th International Conference on Cell & Stem Cell Engineering, IFMBE Proceedings 30, pp. 47–50, 2011.
www.springerlink.com

Analysis: Samples were analysed by reflected-light microscopy (Olympus, Germany) using Giemsa staining and life-dead-assay (Invitrogen, US). Matriderm was embedded in paraformaldehyde, processed into sections via a microtome and stained with Hematoxylin and Eosin and Alzarin Red staining. Cell morphology and extracellular matrix deposition was evaluated by raster electron microscopy (REM) (Zeiss, Oberkochen, Germany). For REM analysis, samples were fixated in 5% glutaraldehyde in cacodylate buffer solution and freeze-dried before being sputtered with gold labeling.

III. Results

Matrix porosity affects cell distribution: Microporous collagen matrices (Matriderm) demonstrated an inhomogenous cell distribution when cultured under static as well as dynamic flow conditions. Cross-sections showed cell clusters packed within the collagen fibrous network.

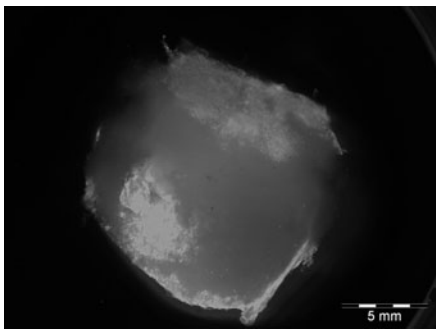

Fig. 1 Inhomogenous cell distribution within microporous collagen scaffold (Matriderm) cultured for 3days under static conditions (fluorescence viability staining)

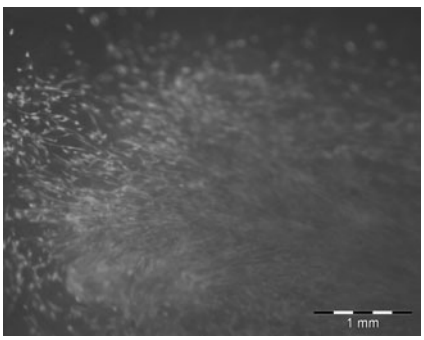

Fig. 2 Bioreactor culture of Matridem for 10 days shows cell alignment in flow direction but no homogenous cell distribution (fluorescence viability staining).

In contrast, macroporous ceramic scaffolds revealed a homogenous cell distribution within the matrix after seeding and cultivation under static conditions or low flow dynamic culture conditions. When using high flow rates in the bioreactor, some cell clustering was observed after a 10 day culture period.

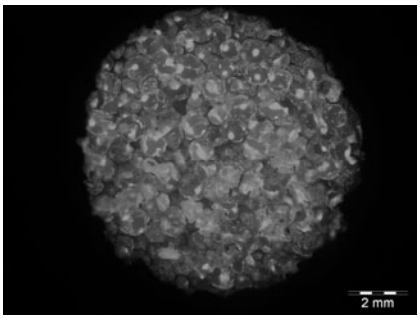

Fig. 3 Sponceram matrix seeded with stem cells and cultured for 3 days under static conditions (fluorescence viability staining)

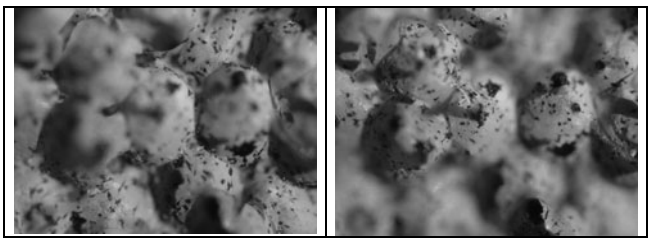

Fig. 4 Homogenous cell distribution in Sponceram matrix after a cultivation period of 10 days under low flow conditions (Giemsa staining)

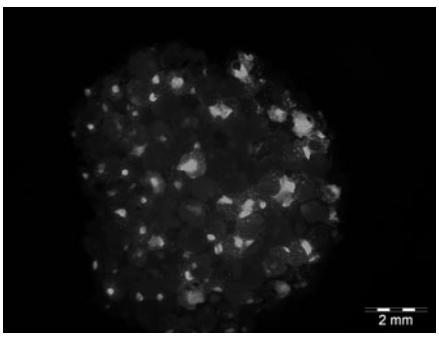

Fig. 5 High flow exposure within the bioreactor leads to cells clusters which are located within the pores after 10 days of culture (fluorescence viability staining)

Fluid shear stress affects collagen fiber organization along the fluid stream line when cultured in the bioreactor, but not under static culture conditions: Cross-sections of Matriderm scaffolds demonstrated alignment of cells within a fibrous network along the fluid stream line, whereas collagen scaffolds cultured under static culture condition showed a less organized matrix.

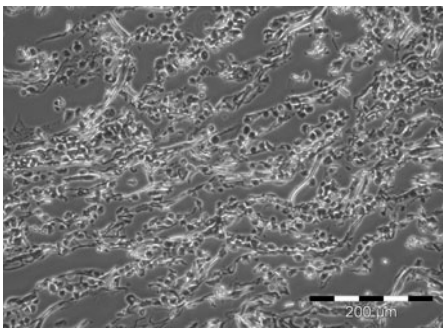

Fig. 6 Cell and collagen fiber alignment along flow direction in Matriderm cultured in the bioreactor for 2 months (Alzarin Red staining)

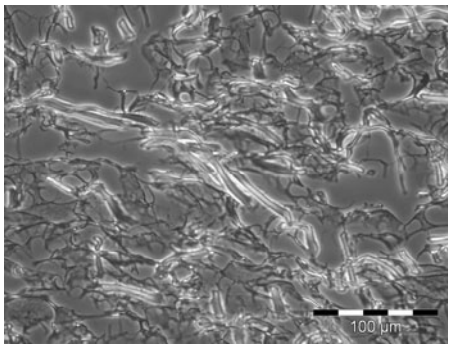

Fig. 7 Unorganized arrangement of collagen fibers in plain Matriderm without cells (Alzarin Red staining)

Cell morphology in macro-porous ceramic scaffolds differ between static and dynamic culture conditions: Morphology of stem cells cultured under static culture conditions showed long cell protrusions and extended cell bodies spanning between pore walls. Stem cell morphology differed from control fibroblast cultures under static conditions. Scaffolds cultured in the bioreactor showed a more flat cell body with radiating protrusions.

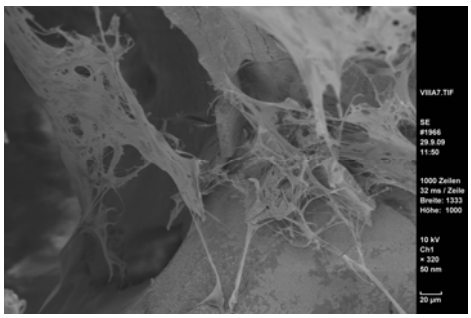

Fig. 8 Thin and dendritical shape of mesenchymal stem cells cultured on Sponceram under static culture conditions (REM)

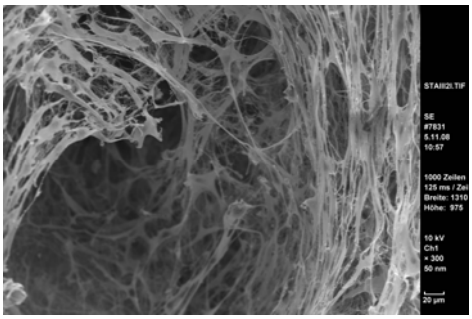

Fig. 9 Dense fibroblast morphology during static growth on Sponceram (REM)

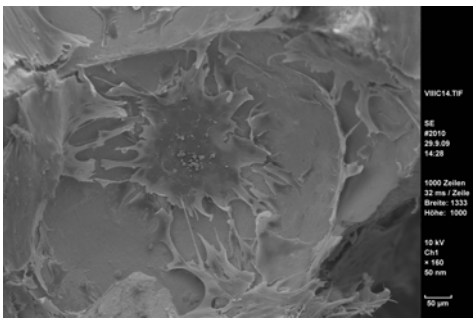

Fig. 10 Flat and star-like morphology of stem cells grown on Sponceram under dynamic flow exposure (REM)

Cell morphology and extracellular matrix formation depend on flow exposure and flow rate: Mesenchymal stem cells cultured onto macroporous ceramic scaffolds (Sponceram) formed extracellular matrix when cultured under dynamic flow conditions. The flow rate affects the amount of extracellular matrix (ECM) deposited by the cells, where the highest and densest amount of ECM was found under high flow rates.

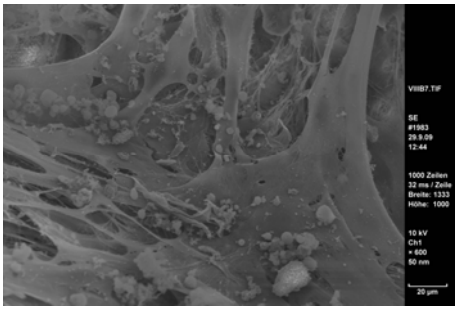

Fig. 11 ECM deposition by stem cells grown on Sponceram under low flow conditions cultured for 3 weeks in the bioreactor (REM)

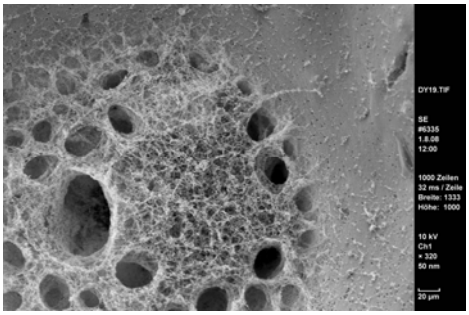

Fig. 12 Fibrous-like ECM formed after 3 weeks of stem cell cultivation on Sponceram under high flow condition in the bioreactor (REM)

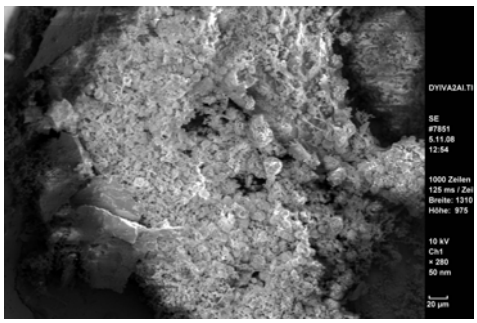

Fig. 13 Dense ECM deposition by stem cells on Sponceram after 6 weeks of high flow culture in the bioreactor (REM)

IV. Discussion

Extracellular matrix properties and external stresses can influence stem cell behaviour (1,7). Our study demonstrates that the two main components of bone extracellular matrix, mineral (here ceramic) and collagen, affect cell morphology, cell growth and cell differentiation diversely due to their unique properties. Recent studies have demonstrated that flow shear stress can induce osteogenic gene markers in mesenchymal stem cells and can induce osteogenic differentiation (2,8). Since high shear stresses can be detrimental to cells and can led to cell death, further studies have to reveal the control pathway of mechanical activation of gene expression within these cells in order to correlate cellular shape and extracellular matrix deposition to the functional state of the cells. Our results may add some information to learn about the optimal external and internal cellular forces required for ostegenic cell stimulation. The ideal biomaterial as well as the best culture environment for bone tissue engineering has still to be defined.

V. Conclusion

Cell shape of primary human adipogenous stem cells is affected by matrix architecture, matrix properties and externally applied flow shear stresses. Further evaluations such as gene expression studies are necessary in order to correlate differences of stem cell shape to their functional state.

Acknowledgment

The authors wish to thank Dr. Conny Kasper from the Leibniz University Hannover for matrix supplements.

This work was supported by a start-up grant (HILF) from Hannover Medical School (MHH).

Design and patent of the laminar flow reactor belongs to Biomimetics Technologies Inc, Toronto, Canada.

References

1. Ingber DE (2006) Mechanical control of tissue morphogenesis during embryonic development. Int J Dev Biol 50:255-266
2. McBride SH, Falls T, Knothe Tate ML (2008) Modulation of stem cell shape and fate B: mechanical modulation of stem cell shape and gene expression. Tissue Eng A 14(9):1573-1580
3. Bancroft GN, Sikavitsas VI, van den Dolder J et al (2002) Fluid flow increases mineralized matrix deposition in 3D perfusion culture of marrow stromal osteoblasts in a dose-dependent manner. Proc. Natl Acad Sci USA 99:12600- 12605
4. Kuhbier JW, Weyand B, Radtke C et al (2010) Isolation, characterization, differentiation, and application of adipose-derived stem cells. Adv Biochem Eng Biotechnol PMID:20091288
5. Israelowitz M et al (2007) United States Patent application 60838494/11, 895 645
6. Israelowitz M et al (2008) European Union Patent application 08011144.6/EP 08011144
7. Weyand B, Israelowitz M, von Schroeder HP et al: Fluid dynamics in bioreactor design. Considerations for the theoretical and practical approach. Adv Biochem Eng Biotechnol 112:251-268
8. Engler AJ, Sen S, Sweeney HL et al (2006) Matrix elasticity directs stem cell lineage specification. Cell 126(4):677-689

Author: Birgit Weyand
Institute: Department of Plastic Surgery, Hannover Medical School
Street: Carl-Neubergstr. 1, OE 6260
City: 30625 Hannover
Country: Germany
Email: weyand.birgit@mh-hannover.de

Cell-Matrix Interaction Study during Human Mesenchymal Stem Cells Differentiation

Haiyang Yu and Lay Poh Tan

School of Materials Science and Engineering, Nanyang Technological University, Singapore

Abstract— **Physically induced stem cells differentiation is gaining tremendous attention recently. Studies showed that matrix elasticity can induce human mesenchymal stem cells (hMSCs) differentiation [1]. In this work, we focused on how the cell-matrix interaction will affect hMSCs differentiation. First, the effect of matrix elasticity on hMSCs was explored, and it was found that besides the matrix compliance, selection of coating protein and concentration used play an important role in triggering the matrix elasticity effect on hMSCs differentiation. Collagen type I and human fibronectin could improve matrix compliance induced differentiation while gelatin did not have such effect. Secondly, we found that when the focal adhesion size and cytoskeleton development were controlled through micropatterning, the hMSCs differentiation was also affected.**

Keywords— **Matrix elasticity, mechanotransduction, hMSCs differentiation, micropatterning.**

I. Introduction

Recently, a lot of attention has been focused on stem cell differentiation induced by physical factors such as matrix elasticity and cell shape regulation [1, 2]. But in these studies, few of them are independent of induction factors. Moreover, the mechanisms underlying these effects have not been elucidated. For example, will different protein coating affect hMSCs differentiation in the same way? Is the differentiation due to the coating protein absorption variance on different materials, or cytoskeleton development, or focal adhesion structure, or FAK and Rho activation? All the questions are related to cell-matrix interactions, which cause cascade regulations in cells. Our study concentrating on cell-matrix interaction could contribute to some understanding to the differentiation mechanisms.

In this study, we proposed that besides matrix compliance, the type of coating protein and the concentration used will affect the matrix compliance induced differentiation. Poly-dimethylsiloxane (PDMS) of different crosslinking density was used to provide the matrix elasticity effect on hMSCs differentiation. Collagen, fibronectin, and gelatin were coated on the PDMS substrate to study the effect of protein type on hMSCs differentiation. Besides that, the role of focal adhesions in regulation of hMSCs differentiation was studied through micropatterning, combined with matrix compliance methods to explore how the substrate stiffness as well as focal adhesion interacts with hMSCs. All of the experiments were conducted in the absence of chemical induction factors. The novelty of this work is on the effectts of combining focal adhesion patterning with matrix compliance on stem cell differentiation. This interaction study may help to explain the role of focal adhesions in human stem cells differentiation, and to introduce matrix compliance study to optimize the micropatterning methods.

Acknowledgment

We would like to acknowledge Agency for Science, Technology and Research (A*STAR), Singapore (SERC Grant No: 072 101 0021) and Nanyang Technological University, Singapore, for financial support.

References

1. McBeath, R., et al., *Cell Shape, Cytoskeletal Tension, and RhoA Regulate Stem Cell Lineage Commitment.* Developmental Cell, 2004. **6**(4): p. 483-495.
2. Engler, A.J., et al., *Matrix elasticity directs stem cell lineage specification.* Cell, 2006. **126**(4): p. 677 - 689.

Address of the corresponding author:

Author: Lay Poh Tan
Institute: School of Materials Science and Engineering, Nanyang Technological University
Street: 50 Nanyang Avenue
City: Singapore
Country: Singapore
Email: LPTan@ntu.edu.sg

A. El Haj and D. Bader (Eds.): 8th International Conference on Cell & Stem Cell Engineering, IFMBE Proceedings 30, p. 51, 2011.
www.springerlink.com

Author Index

Keyword Index